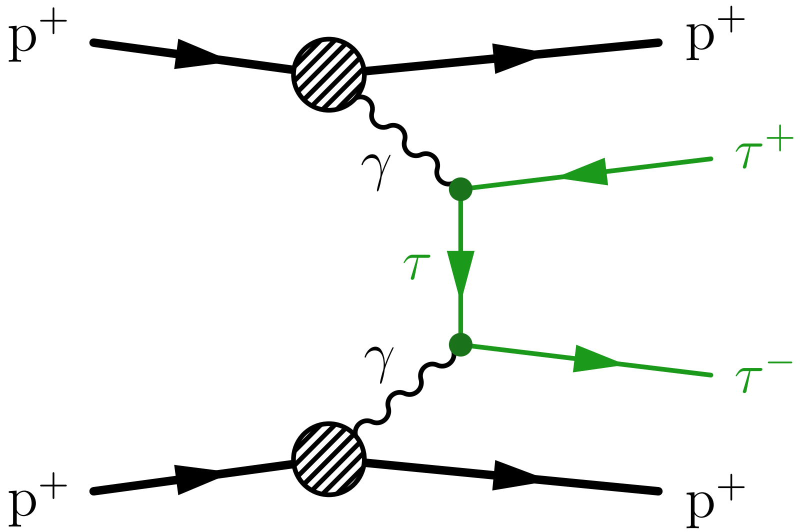

Measurement of the τ anomalous magnetic moment (g – 2) at CMS

Izaak Neutelings (CERN) on behalf of the CMS Collaboration

izaak.neutelings@cern.ch

18/07/2024, ICHEP

What is $g - 2$?

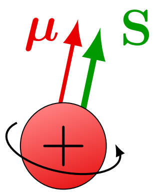

$$\boldsymbol{\mu} = g\frac{e}{2m}\mathbf{S} \longrightarrow \begin{cases} g = 1: \text{ classical} \\ g = 2: \text{ Dirac} \\ g \approx 2.002: \text{ QED} \end{cases}$$

- particles with spin **S** have a **magnetic moment $\boldsymbol{\mu}$**
- obtain quantum corrections with
  gyromagnetic factor / "g-factor" $\boldsymbol{g} \approx 2.002\ 32$ for spin ½

  ⇒ **anomalous magnetic moment** $\boldsymbol{a} = \frac{g-2}{2} \approx 0.001\ 16$

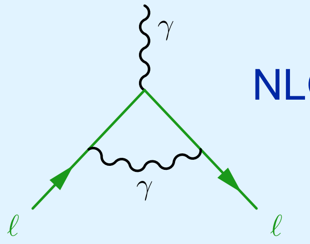

NLO correction (Schwinger)

$$a = \frac{\alpha}{2\pi} \approx 0.001\ 16$$

What is $g-2$?

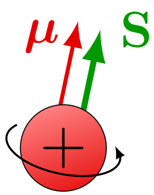

$$\mu = g\frac{e}{2m}\mathbf{S} \longrightarrow \begin{cases} g = 1: & \text{classical} \\ g = 2: & \text{Dirac} \\ g \approx 2.002: & \text{QED} \end{cases}$$

- particles with spin **S** have a **magnetic moment μ**
- obtain quantum corrections with gyromagnetic factor / "g-factor" $g \approx 2.002\ 32$ for spin ½

  $\Rightarrow$ **anomalous magnetic moment** $a = \frac{g-2}{2} \approx 0.001\ 16$
- measurements of **$(g-2)_e$** in Penning traps are the "most precise in physics"
- measurements of **$(g-2)_\mu$** in storage rings are in longstanding tension with theoretical computations

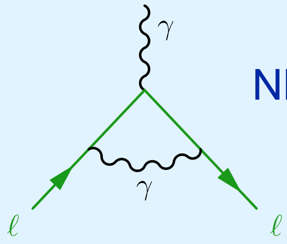

NLO correction (Schwinger)

$a = \frac{\alpha}{2\pi} \approx 0.001\ 16$

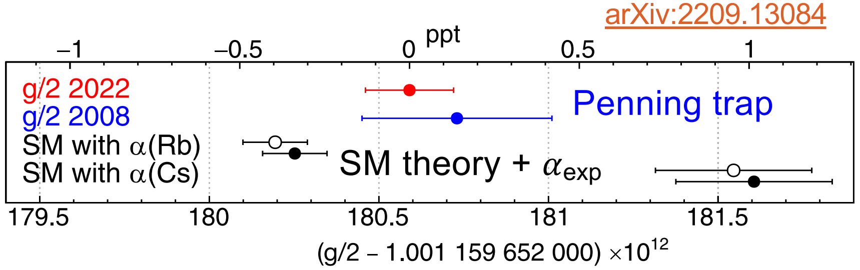

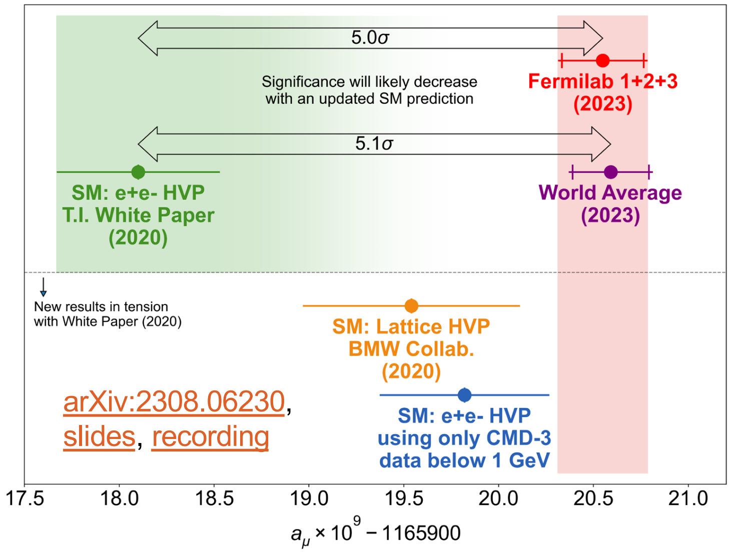

0.20 ppm !

BNL + FNAL

What is $g-2$?

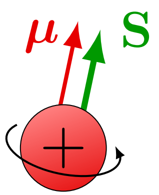

$$\boldsymbol{\mu} = g\frac{e}{2m}\mathbf{S} \longrightarrow \begin{cases} g = 1: \text{ classical} \\ g = 2: \text{ Dirac} \\ g \approx 2.002: \text{ QED} \end{cases}$$

- particles with spin **S** have a **magnetic moment $\boldsymbol{\mu}$**
- obtain quantum corrections with gyromagnetic factor / "g-factor" $\boldsymbol{g} \approx 2.002\,32$ for spin ½

  ⇒ **anomalous magnetic moment** $\boldsymbol{a} = \frac{g-2}{2} \approx 0.001\,16$

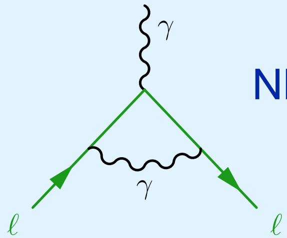

NLO correction (Schwinger)

$$a = \frac{\alpha}{2\pi} \approx 0.001\,16$$

- measurements of $(g-2)_e$ in Penning traps are the "most precise in physics"

arXiv:2209.13084

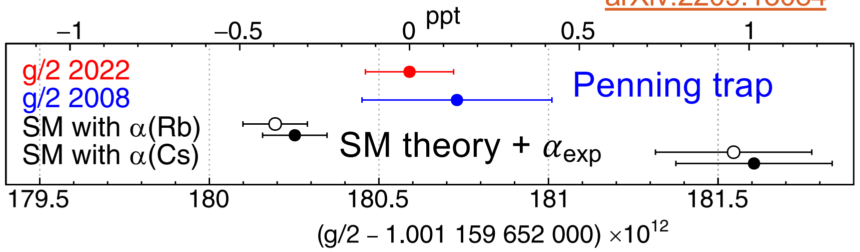

- measurements of $(g-2)_\mu$ in storage rings are in longstanding tension with theoretical computations
- constraints on $(g-2)_\tau$ in e^+e^- or PbPb collisions:
  - DELPHI@LEP: $-0.052 < a_\tau < 0.013$ (95% CL)
  - CMS HIN: $-0.088 < a_\tau < 0.056$ (68% CL)
  - ATLAS HIN: $-0.057 < a_\tau < 0.024$ (95% CL)

world's best since 2004

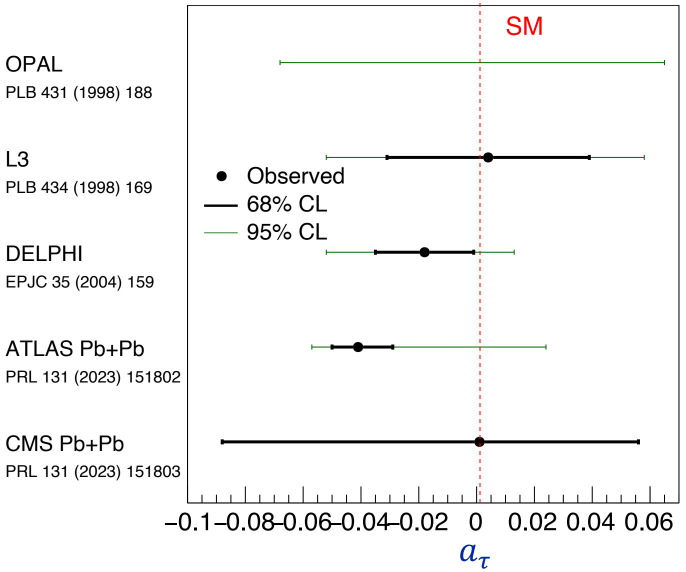

- many **BSMs** predict enhancement for $\boldsymbol{\tau}$ lepton

  e.g. Yukawa-like coupling: $\frac{m_\tau^2}{m_\mu^2} \approx 280$

  ⇒ probe for NP ?

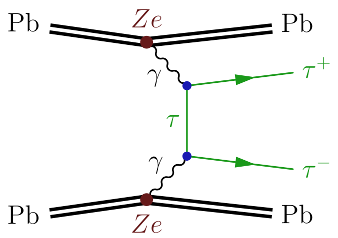

How can we measure tau g – 2 ?

- a_τ & electric dipole moment d_τ can be probed from $\boldsymbol{\gamma\tau\tau}$ **vertex**

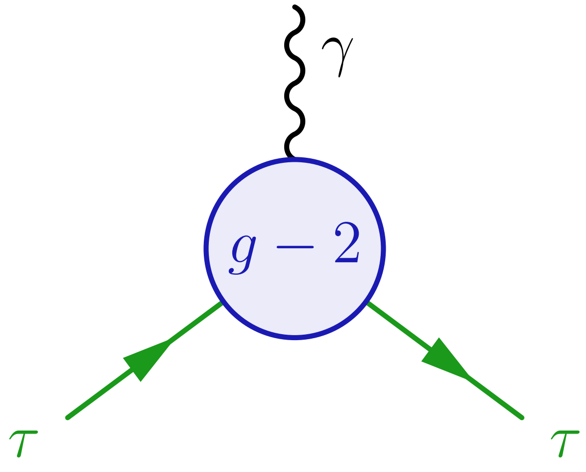

- FSR $\tau \to \tau\gamma$ contains 1 $\gamma\tau\tau$ vertices (LEP)

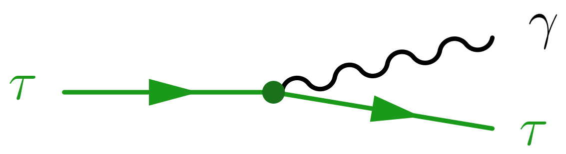

- $\gamma\gamma \to \tau\tau$ process contains 2 $\gamma\tau\tau$ vertices

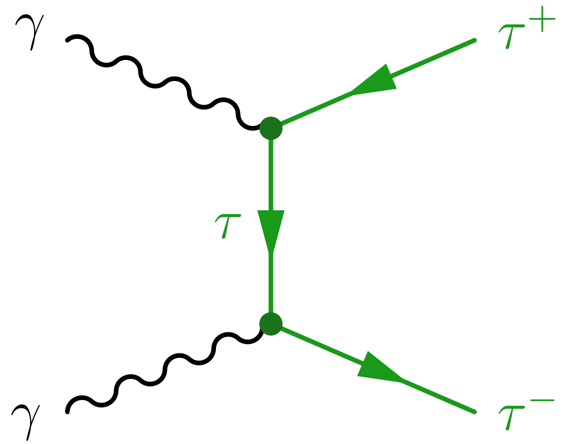

- contraints on electromagnetic moments a_τ & d_τ from *form factors* or *SMEFT*
- in the SM: $d_\tau \sim 10^{-37}$ ecm via CP violation in CKM, but could be much larger in BSMs

Photon-induced processes

- collide charged particles at high energies
  ⇒ intense electromagnetic fields
  ⇒ **photon-photon collisions**
- cross section $\sigma \propto Z^4$
  ⇒ PbPb collisions enhanced w.r.t. pp

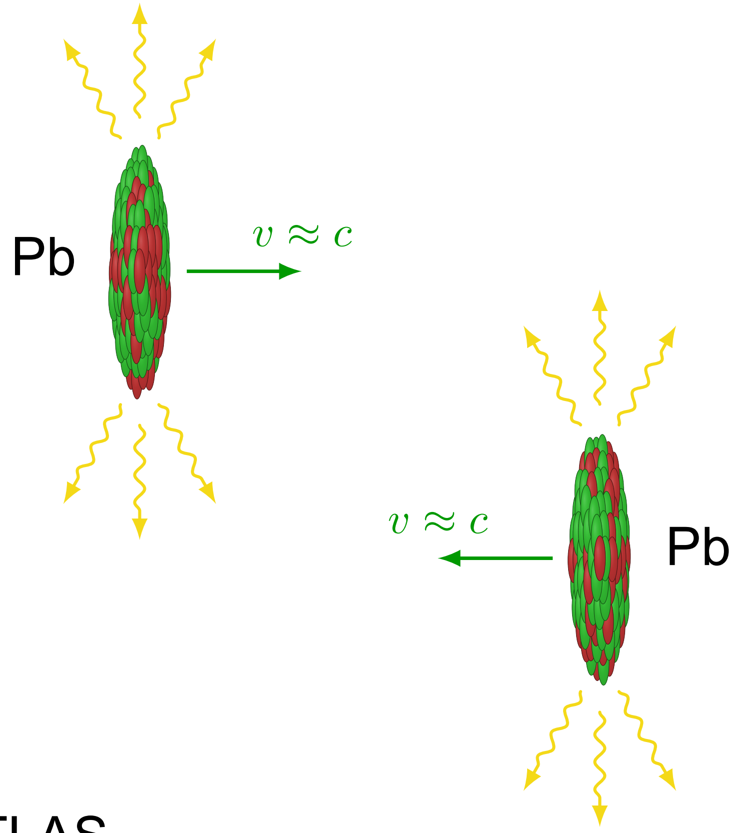

LEP: DELPHI, L3, ...

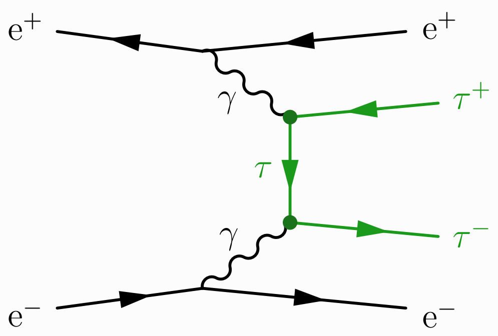

$e^+e^- \rightarrow e^+e^- \tau^+\tau^-$
(or $e^+e^- \rightarrow Z \rightarrow \tau\tau\gamma$)

LHC: CMS, ATLAS

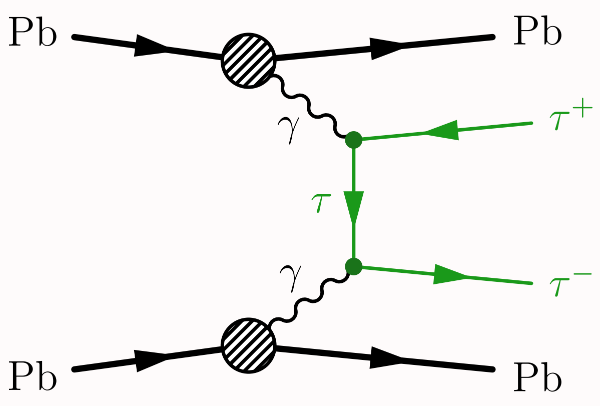

PbPb $\rightarrow$ PbPb $\tau^+\tau^-$

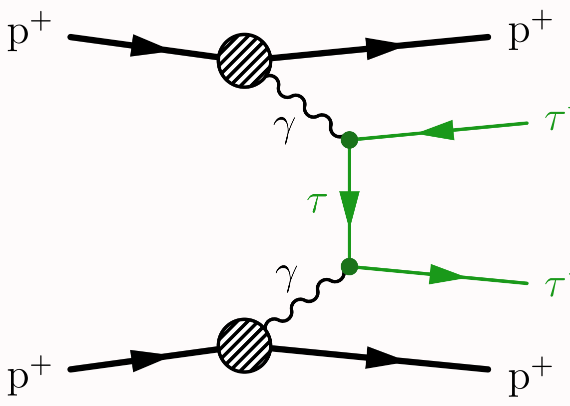

pp $\rightarrow$ pp $\tau^+\tau^-$

$\gamma\gamma \to \tau\tau$ in ultraperipheral PbPb collisions

- first observation of $\gamma\gamma \to \tau\tau$ in PbPb by CMS & ATLAS in 2022
- pros:
  - $\sigma \propto Z^4$ enhancement
  - use "ultraperipheral" collision events
  - clean channel: small backgrounds
- phase space $m_{\tau\tau} \lesssim 40$ GeV
- CMS:
  - 0.4 nb^{-1} collected in 2015
  - final state: $\mu\tau_h$ (3-prong τ_h)

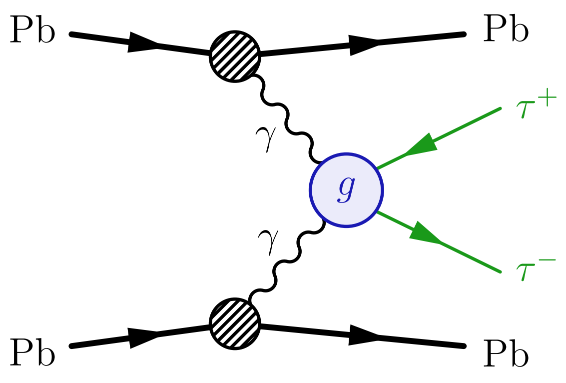

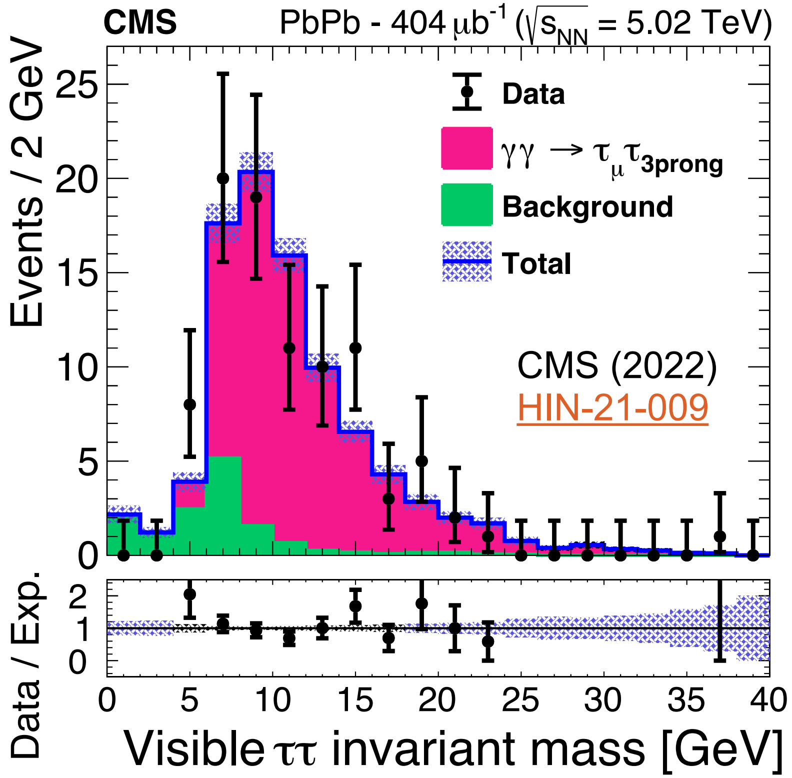

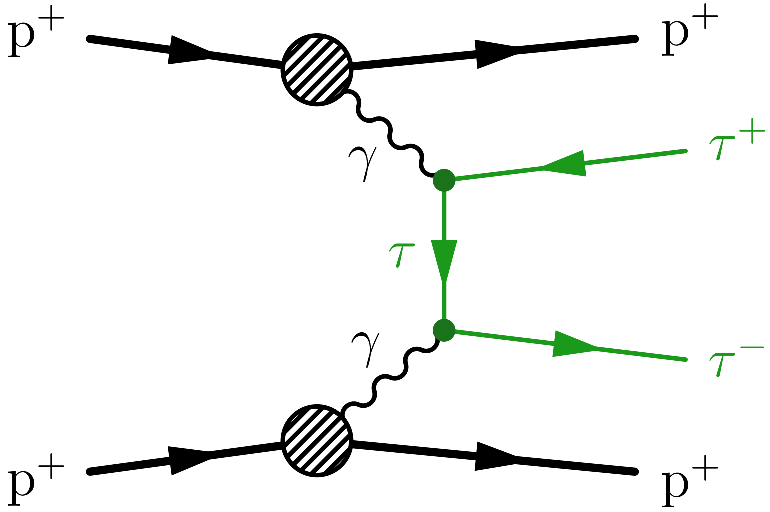

$\gamma\gamma \to \tau\tau$ in pp

CMS-SMP-23-005

$\gamma\gamma \to \tau\tau$ in pp collisions

- **cons**:
  - no $\sigma \propto Z^4$ enhancement
  - large background
  - high pileup
  - soft signal ⇒ low acceptance
- **pros** w.r.t. PbPb:
  - much larger data set: ~ O(10^8)
  - much more sensitive to a_τ modifications: expect large BSM enhancement at high τ p_T and $m_{\tau\tau}$

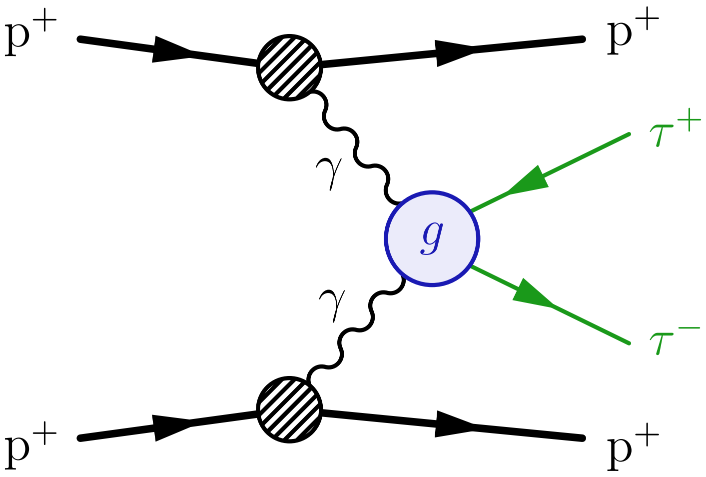

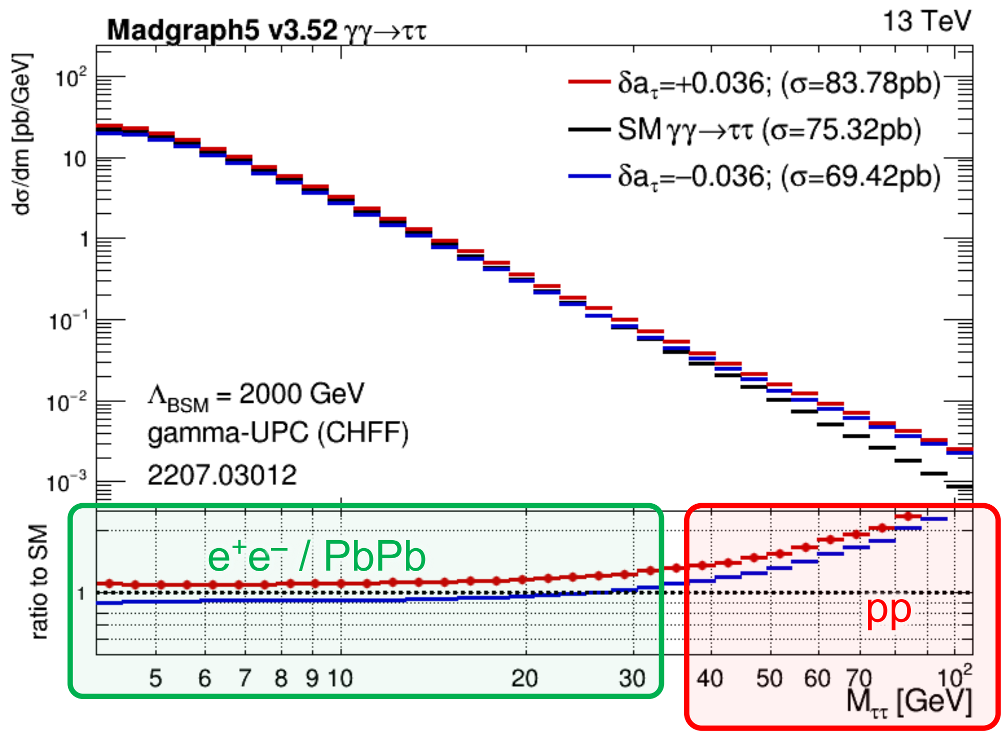

$\gamma\gamma \rightarrow \tau\tau$ signature

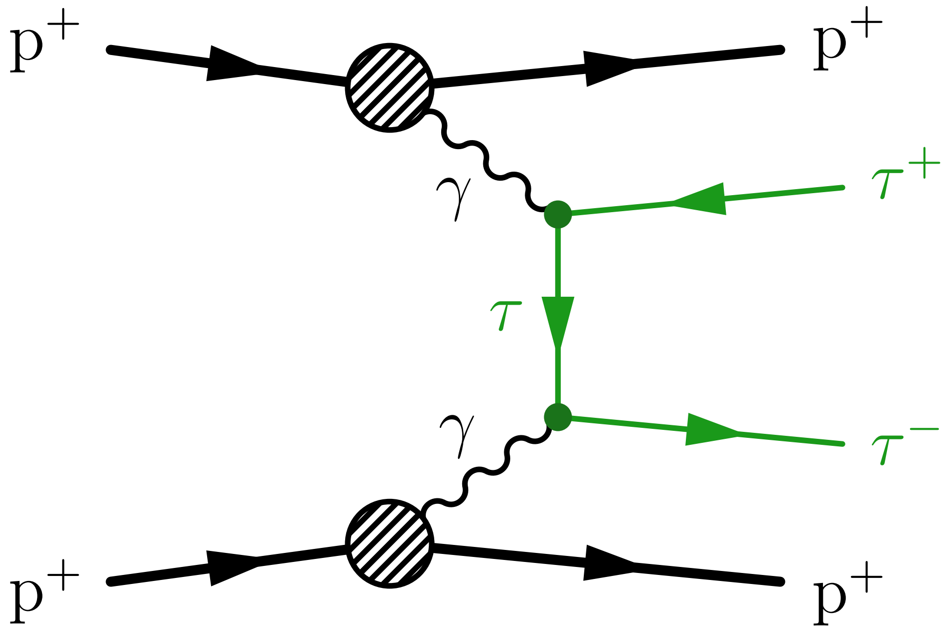

- **2 τ leptons**
  - opposite charge sign
  - back-to-back: $|\Delta\phi| \approx \pi$
  - τ decays:

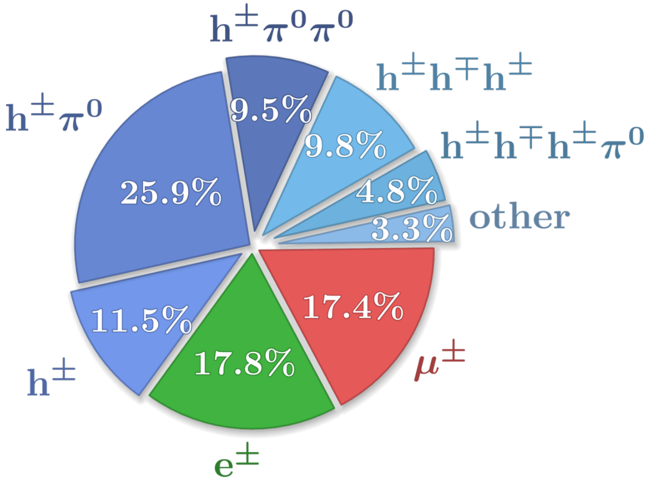

$\tau\tau$ decays:

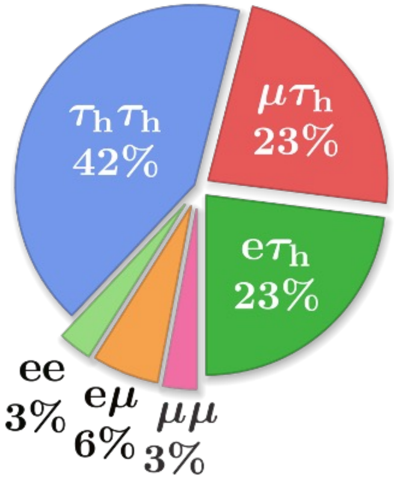

- **2 diffracted protons**
  - no hadronic activity close to $\tau\tau$ vertex

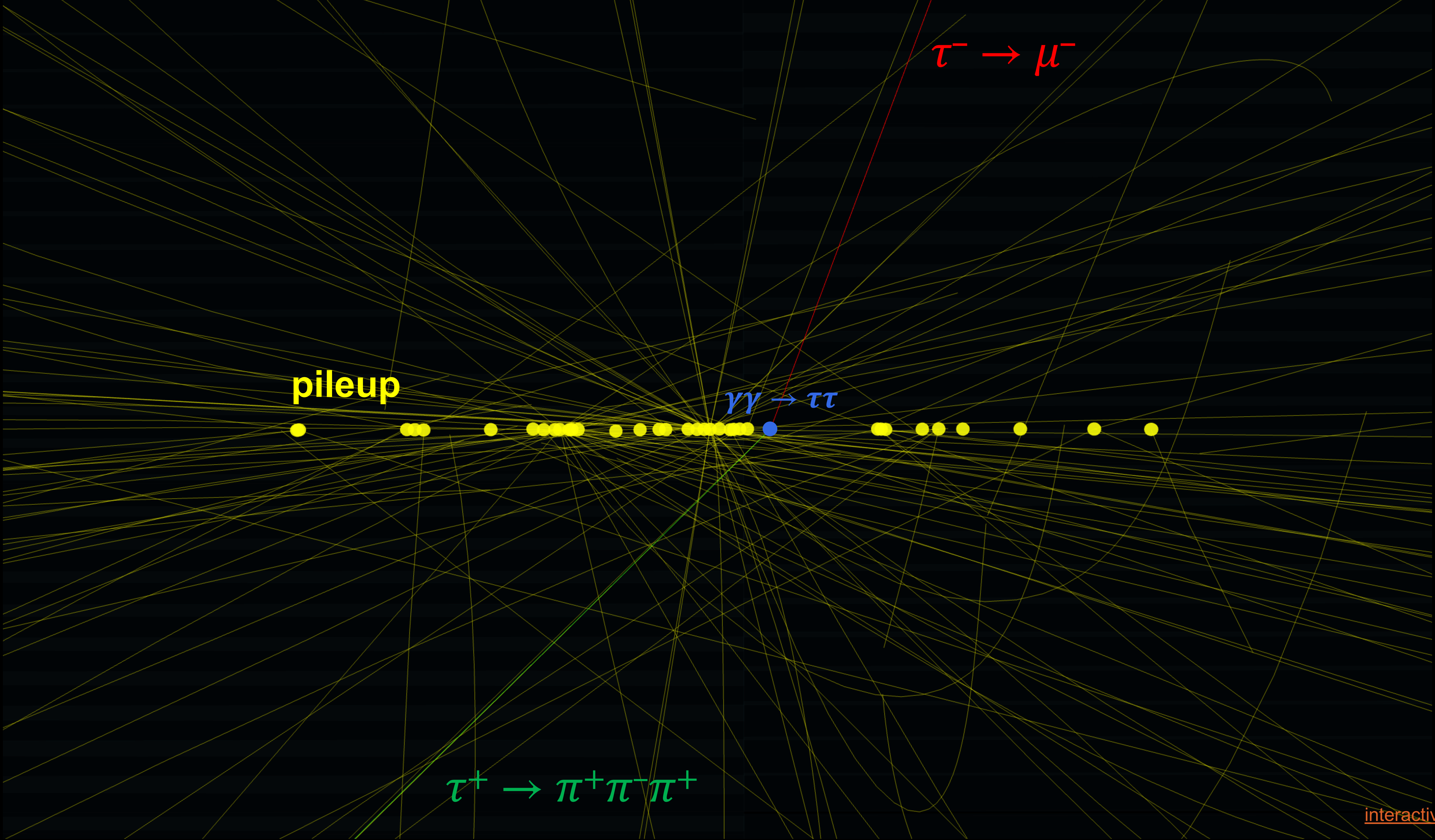

interactive

CMS Experiment at the LHC, CERN
Data recorded: 2018-May-01 13:53:45.602112 GMT
Run / Event / LS: 315512 / 65277407 / 69

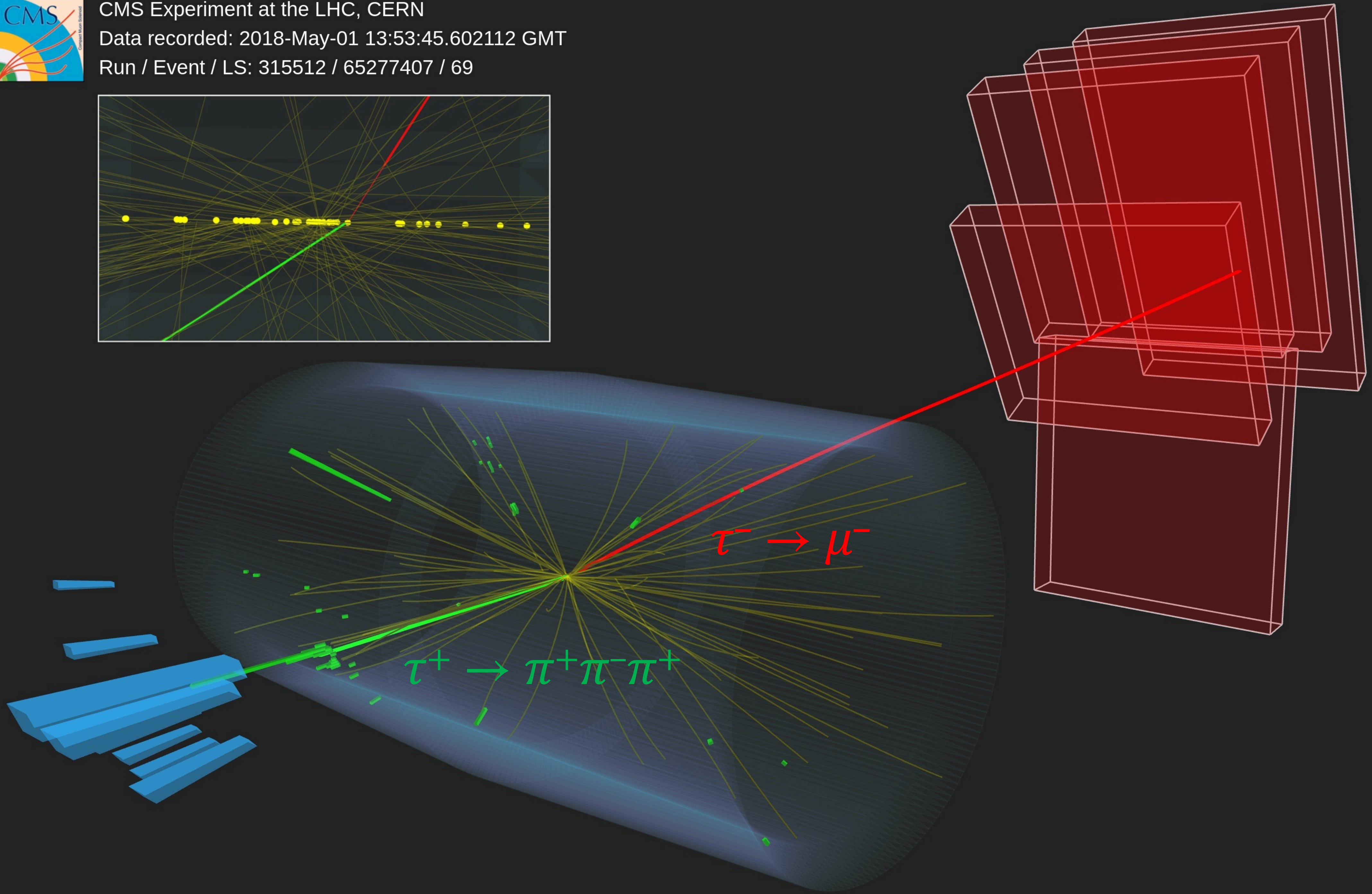

interactive

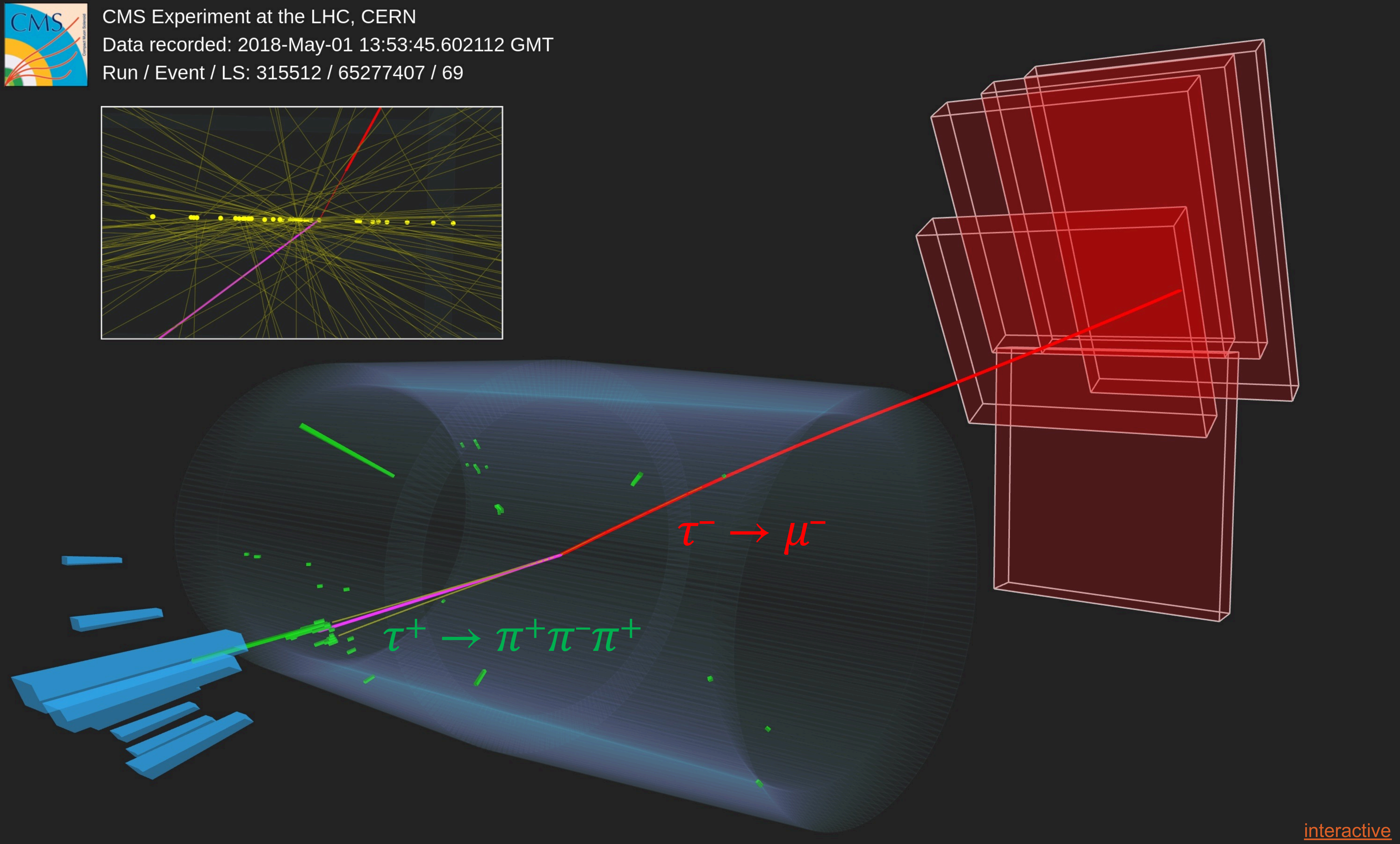
CMS Experiment at the LHC, CERN
Data recorded: 2018-May-01 13:53:45.602112 GMT
Run / Event / LS: 315512 / 65277407 / 69
$\tau^- \to \mu^-$
$\tau^+ \to \pi^+\pi^-\pi^+$
interactive

CMS-SMP-23-005

Strategy for $\gamma\gamma \rightarrow \tau\tau$ in pp

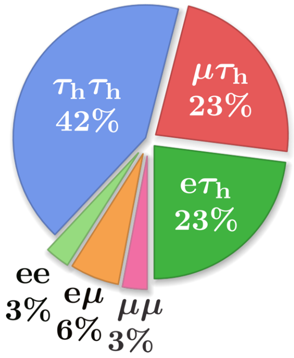

- select events with opposite-sign $\tau^+\tau^-$
  - combine 4 $\tau\tau$ final states: $e\mu$, $e\tau_h$, $\mu\tau_h$, $\tau_h\tau_h$
  - **exclusivity cuts**:
    - back-to-back: **acoplanarity** $A = 1 - \frac{|\Delta\phi|}{\pi} < 0.015$
    - low activity around $\tau\tau$ vertex: N_{tracks} **= 0 or 1** in 0.1 cm window

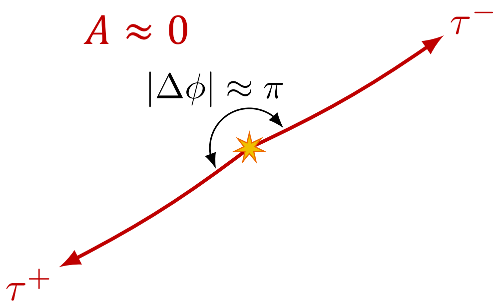

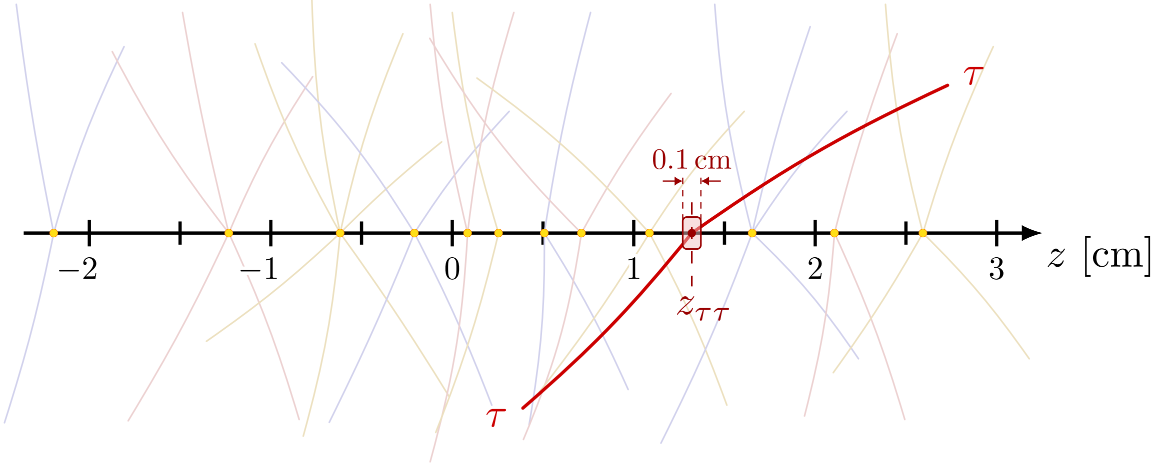

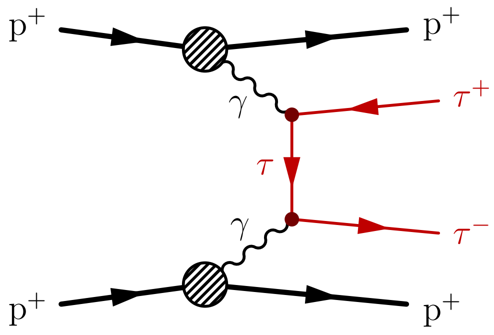

Strategy for $\gamma\gamma \to \tau\tau$ in pp

CMS-SMP-23-005

- select events with opposite-sign $\tau^+\tau^-$
  - combine 4 $\tau\tau$ final states: $e\mu$, $e\tau_h$, $\mu\tau_h$, $\tau_h\tau_h$
  - **exclusivity cuts**:
    - back-to-back: **acoplanarity** $A = 1 - \frac{|\Delta\phi|}{\pi} < 0.015$
    - low activity around $\tau\tau$ vertex: N_{tracks} **= 0 or 1** in 0.1 cm window

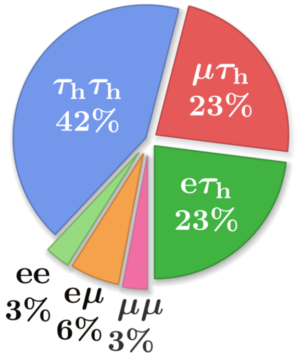

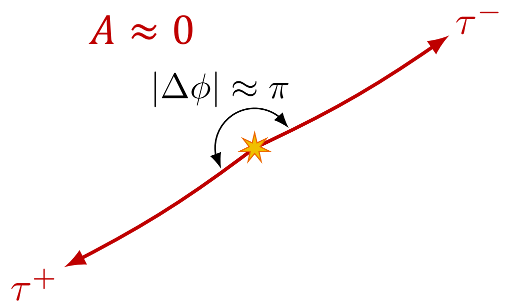

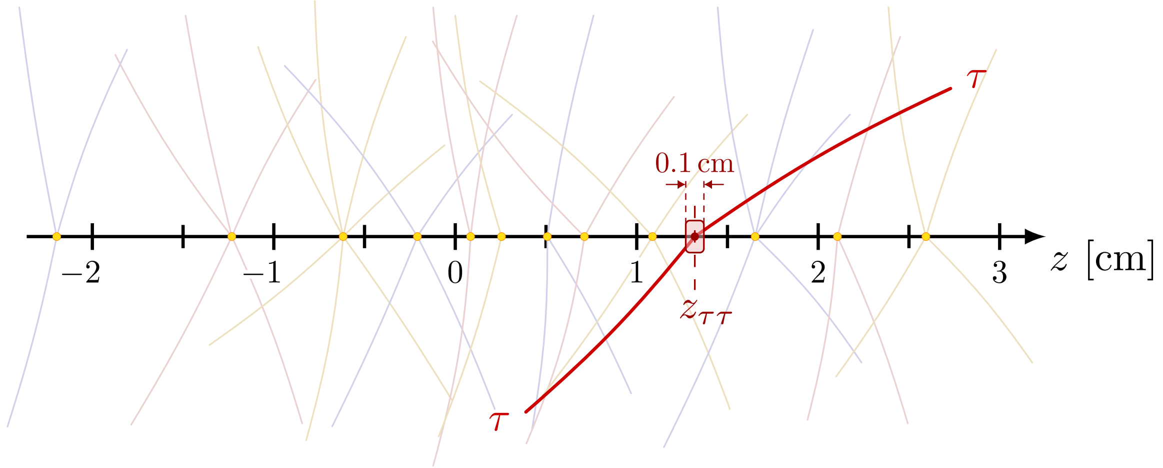

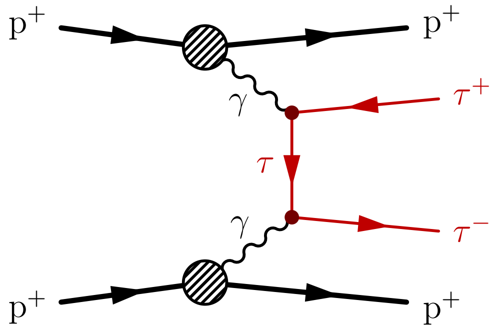

- measure corrections to simulation in $\mu\mu$ events ($Z \to \mu\mu$, $\gamma\gamma \to \mu\mu$)
- measure $\gamma\gamma \to \tau\tau$ from **observed** $m_{\tau\tau}^{\text{vis}}$ **shape & yield**:
  - sensitive to $m_{\tau\tau}^{\text{vis}} > 50$ GeV (above e⁺e⁻ & PbPb, $m_{\tau\tau} \lesssim 40$ GeV)
  - $m_{\tau\tau}^{\text{vis}} \lesssim 500$ GeV to ensure unitarity in signal samples

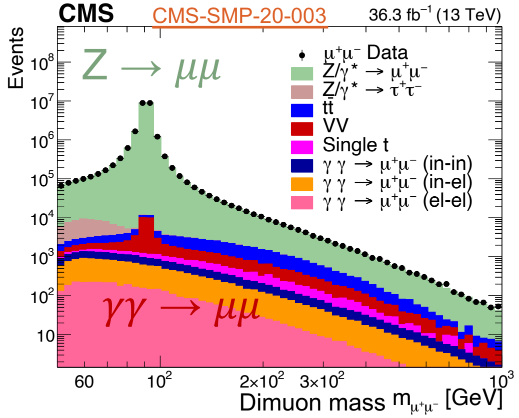

Track counting

applied to all simulation

beamspot has a gaussian profile

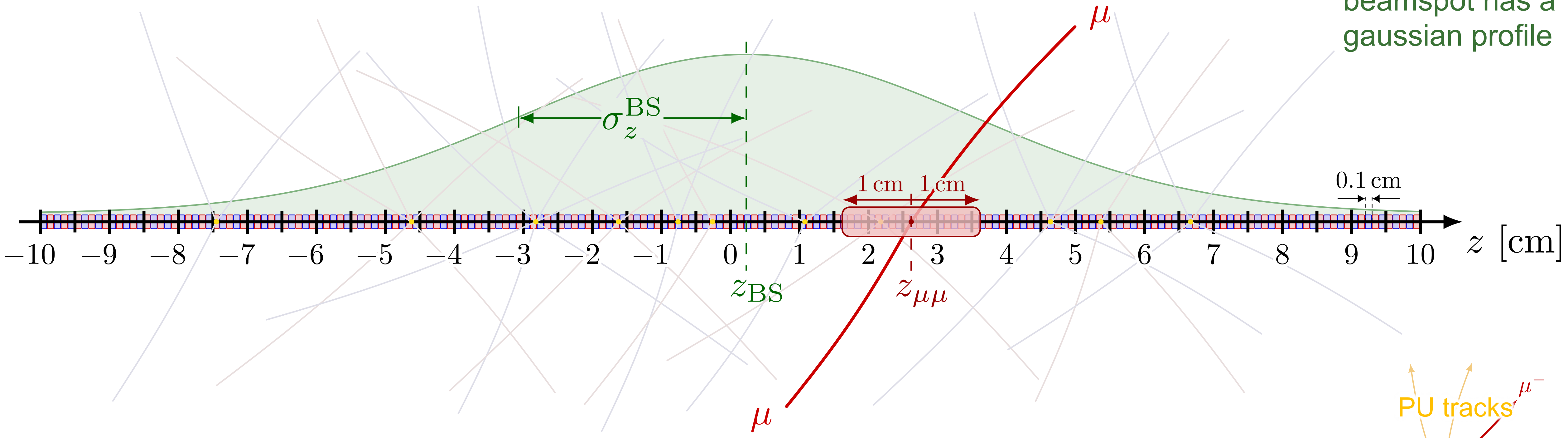

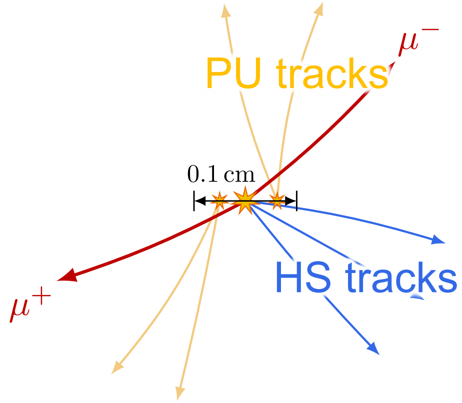

derive obs. / sim. corrections in Z $\rightarrow \mu\mu$ events at Z peak, $|m_{\mu\mu} - m_{\mathrm{Z}}| < 15$ GeV:

- **pileup tracks**: compare $N_{\mathrm{tracks}}^{\mathrm{PU}}$ distributions in 0.1 cm *z* windows (far away from $\mu\mu$ vertex)
- **hard scattering tracks**: compare $N_{\mathrm{tracks}}^{\mathrm{HS}}$ distributions in 0.1 cm *z* window around $\mu\mu$ vertex

Elastic rescaling

applied to photon-induced simulation ($\gamma\gamma \rightarrow \ell\ell$, WW)

- signal samples only include **elastic-elastic (ee)** process generated by gammaUPC
- **single-dissociative (sd)** and **double-dissociative (dd)** processes not included
  - have larger cross section
  - can have an exclusive signature

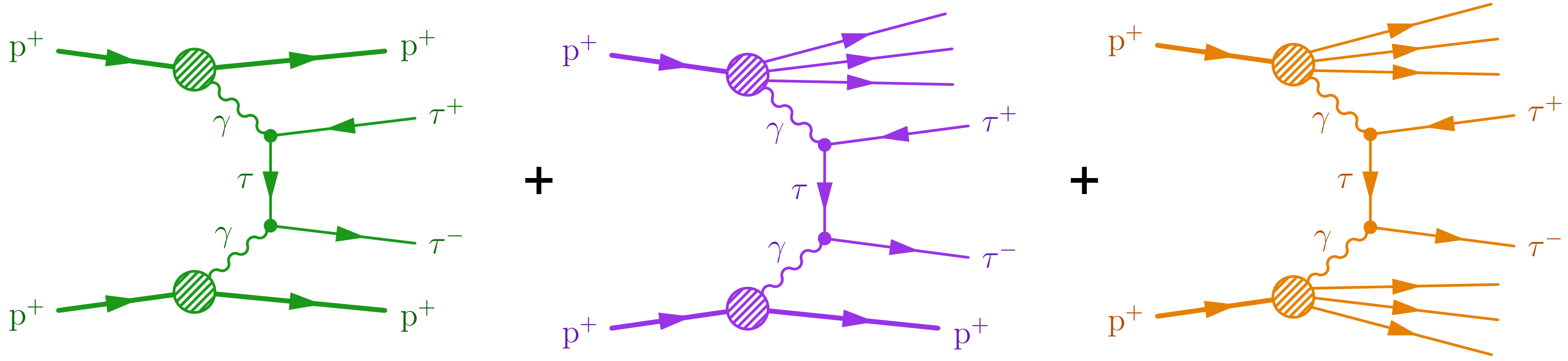

elastic-elastic (ee) single-dissociative (sd) double-dissociative (dd) *applied to photon-induced simulation ($\gamma\gamma \rightarrow \ell\ell$, WW)*

Elastic rescaling

- signal samples only include **elastic-elastic (ee)** process generated by gammaUPC
- **single-dissociative (sd)** and **double-dissociative (dd)** processes not included
  - have larger cross section
  - can have an exclusive signature
- estimate dissociative contributions (incl. higher-order corrections) by rescaling elastic-elastic $\gamma\gamma \rightarrow \mu\mu$ signal in $\mu\mu$ data

⇒ measure rescaling factor = $\dfrac{(\mathbf{ee}+\mathbf{sd}+\mathbf{dd})_{\text{obs}}}{(\mathbf{ee})_{\text{sim}}}$

SF ×

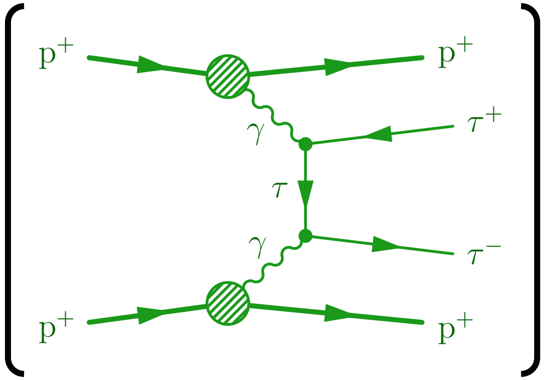

sim

elastic-elastic (ee)

=

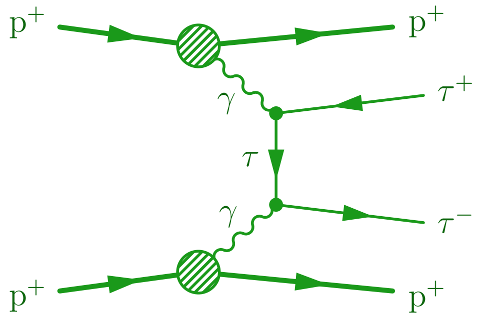

elastic-elastic (ee)

+

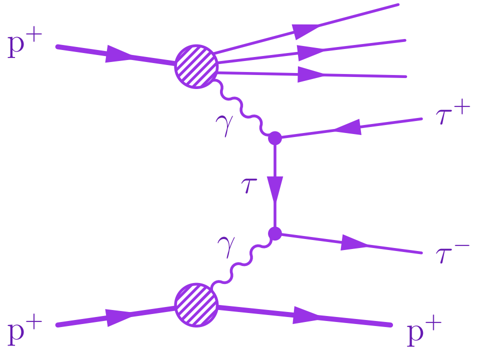

single-dissociative (sd)

+

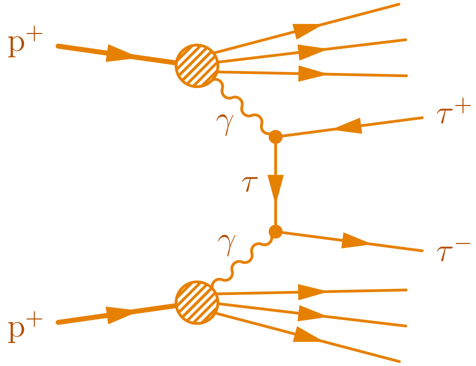

double-dissociative (dd)

Elastic rescaling

- rescaling factor measured in $m_{\mu\mu}$ distribution in dimuon events with A < 0.015 and N_{tracks} = 0 or 1
- **inclusive background** (mostly Drell–Yan)
  - estimated from data in $3 \leq N_{\text{tracks}} \leq 7$ region
  - normalized to Z peak
- **elastic $\gamma\gamma \rightarrow \mu\mu$/WW "signal"** (simulated)
  - contributes significantly $m_{\mu\mu}$ > 150 GeV
  - rescale to data to estimate nonelastic contribution

$$\text{rescaling factor} = \frac{(\text{ee}+\text{sd}+\text{dd})_{\text{obs}}}{(\text{ee})_{\text{sim}}} = \frac{\text{Obs.} - \text{Bkg.}}{\gamma\gamma \longrightarrow \mu\mu,\ \text{WW}}$$

applied to photon-induced simulation ($\gamma\gamma \rightarrow \ell\ell$, WW)

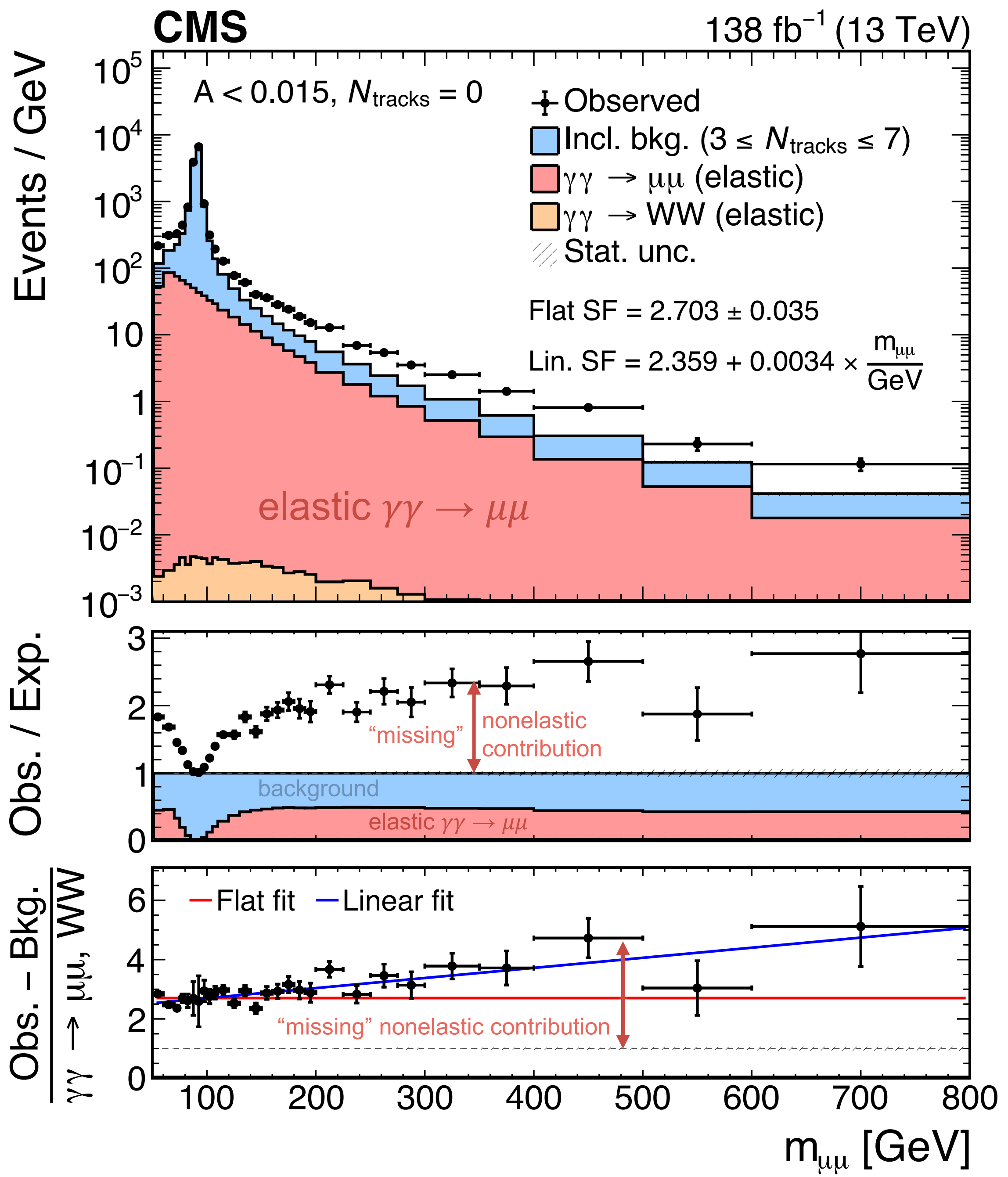

Elastic rescaling

- rescaling factor measured in $m_{\mu\mu}$ distribution in dimuon events with A < 0.015 and N_{tracks} = 0 or 1
- **inclusive background** (mostly Drell–Yan)
  - estimated from data in $3 \leq N_{\text{tracks}} \leq 7$ region
  - normalized to Z peak
- **elastic $\gamma\gamma \rightarrow \mu\mu$/WW "signal"** (simulated)
  - contributes significantly $m_{\mu\mu}$ > 150 GeV
  - rescale to data to estimate nonelastic contribution
- fits:
  - **linear fit** applied as nominal corrections to all elastic simulation ($\gamma\gamma \rightarrow$ ee, $\mu\mu$, $\tau\tau$, WW)
  - **flat fit (~2.7)** used to obtain uncertainty (conservative)

$$\text{rescaling factor} = \frac{(\mathrm{ee}+\mathrm{sd}+\mathrm{dd})_{\mathrm{obs}}}{(\mathrm{ee})_{\mathrm{sim}}} = \frac{\text{Obs.} - \text{Bkg.}}{\gamma\gamma \longrightarrow \mu\mu, \text{WW}}$$

applied to photon-induced simulation ($\gamma\gamma \rightarrow \ell\ell$, WW)

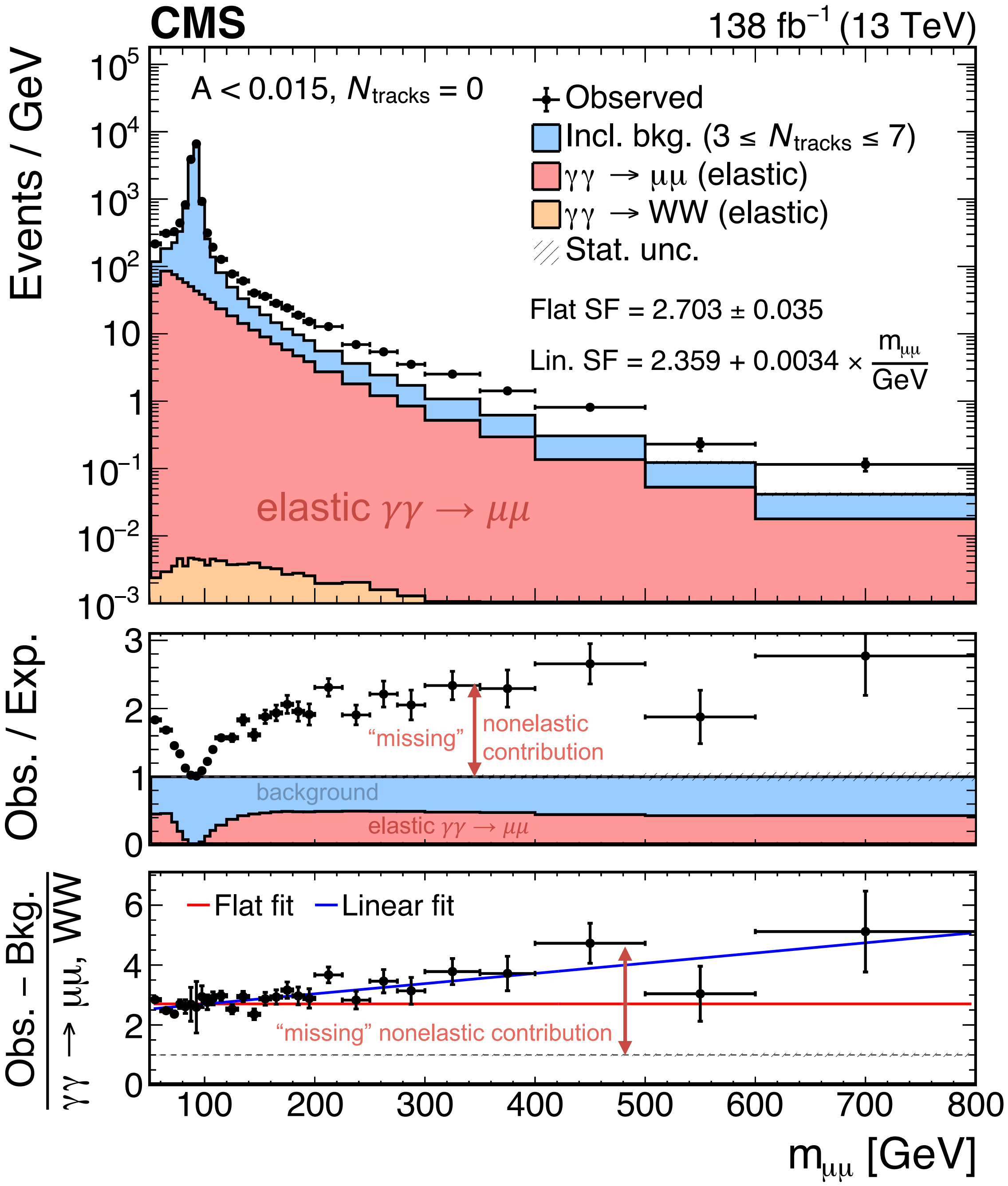

$\gamma\gamma \rightarrow \tau\tau$ RESULTS

CMS-SMP-23-005

SR with N_{tracks} = 0

- after maximum-likelihood fit to observed data
- assuming SM a_τ & d_τ
- signal clearly visible in high $m_{vis}(\tau\tau)$ bins

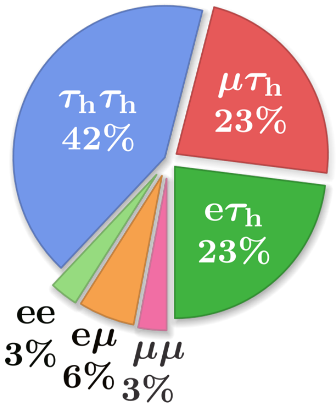

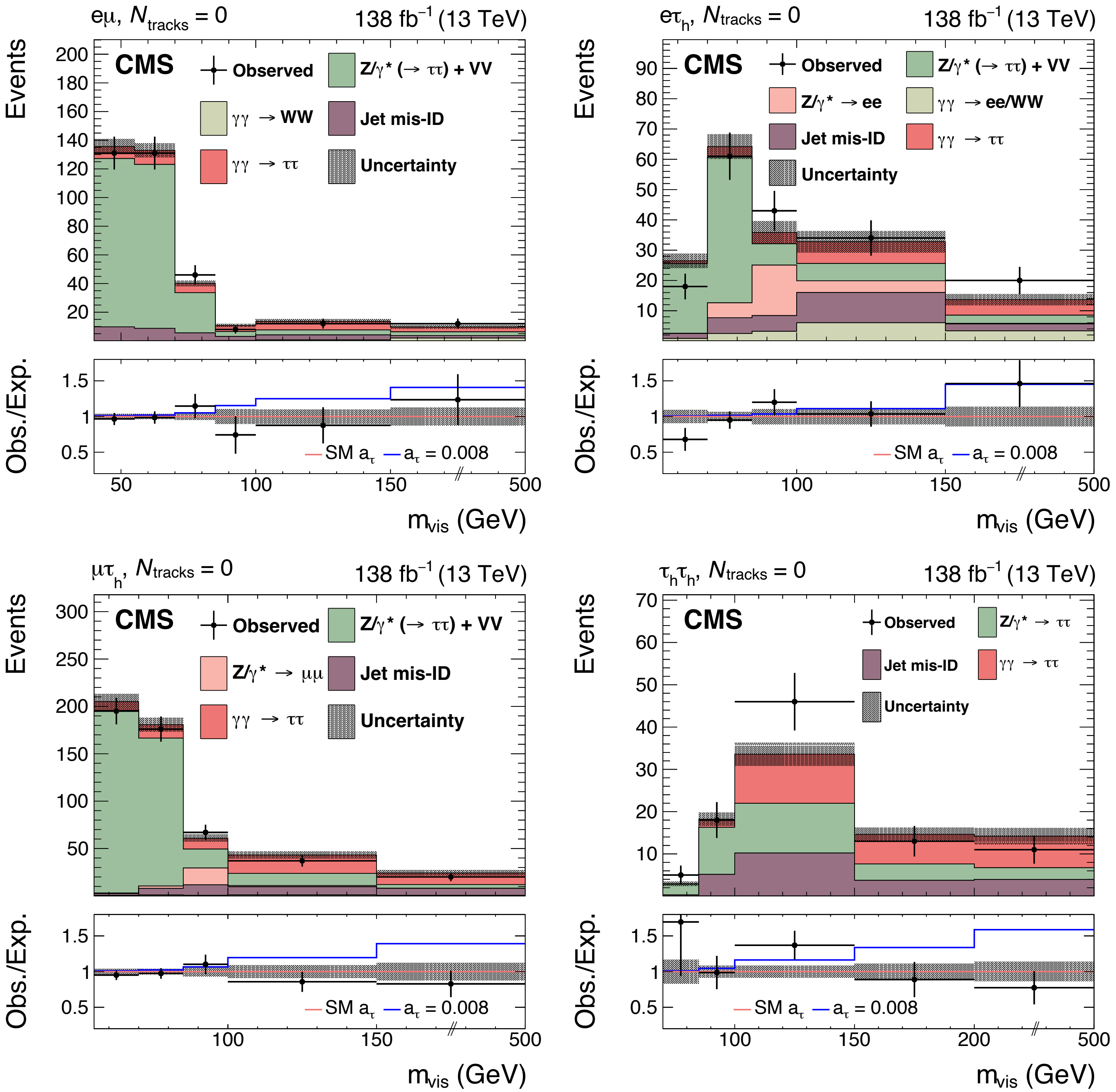

SR with N_{tracks} = 1

- after maximum-likelihood fit to observed data
- assuming SM a_τ & d_τ
- lower signal efficiency, but
  - still adds sensitivity
  - allows for validation of background modeling

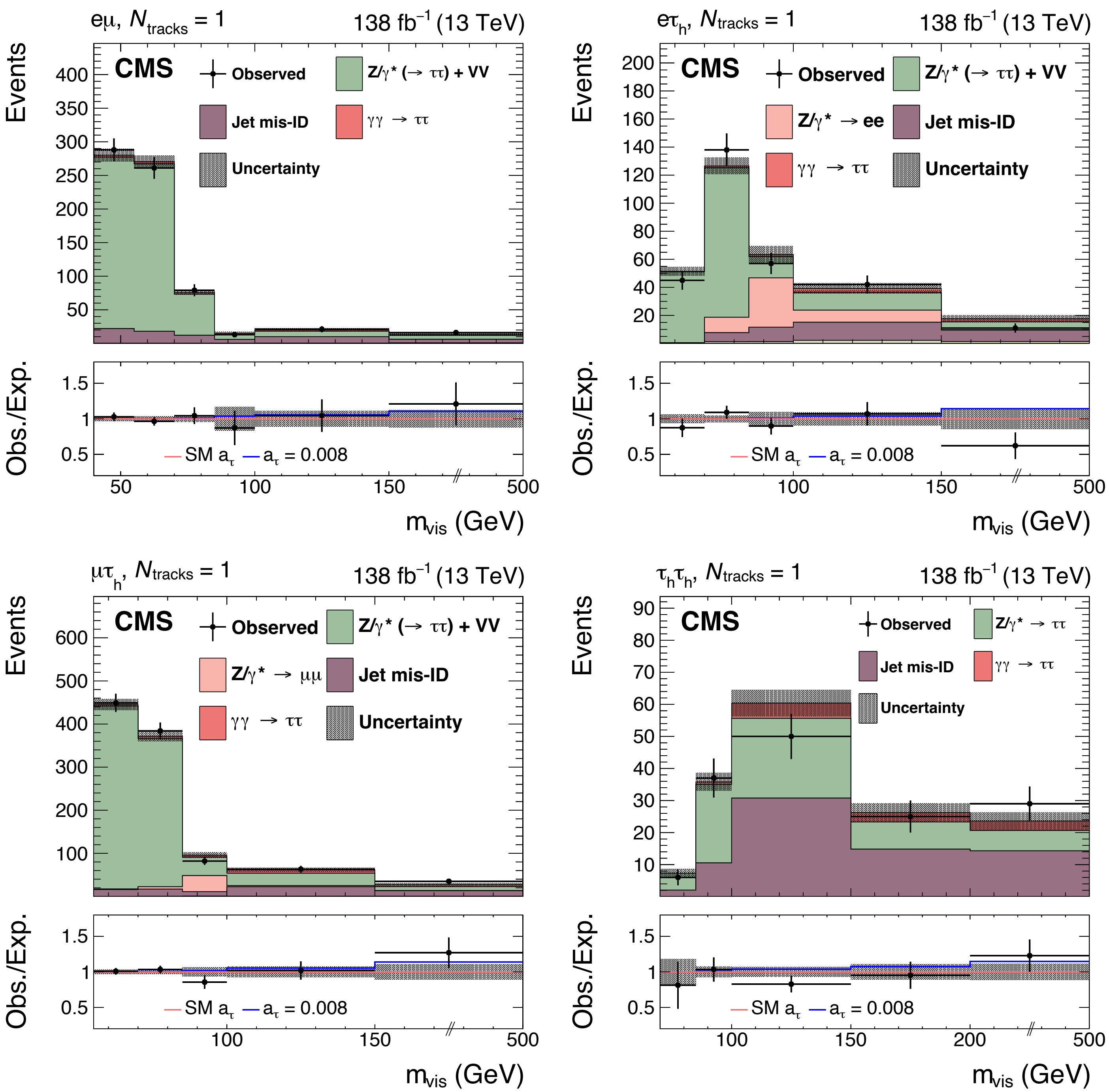

N_{tracks} distributions

- same selections as SR, but
  - allowing $N_{\text{track}} < 10$
  - **$m_{\text{vis}} > 100$ GeV**
- combination of
  - all 4 $\tau\tau$ channels
  - all 3 data-taking years
- very nice modeling of N_{track} !
- signal clearly visible

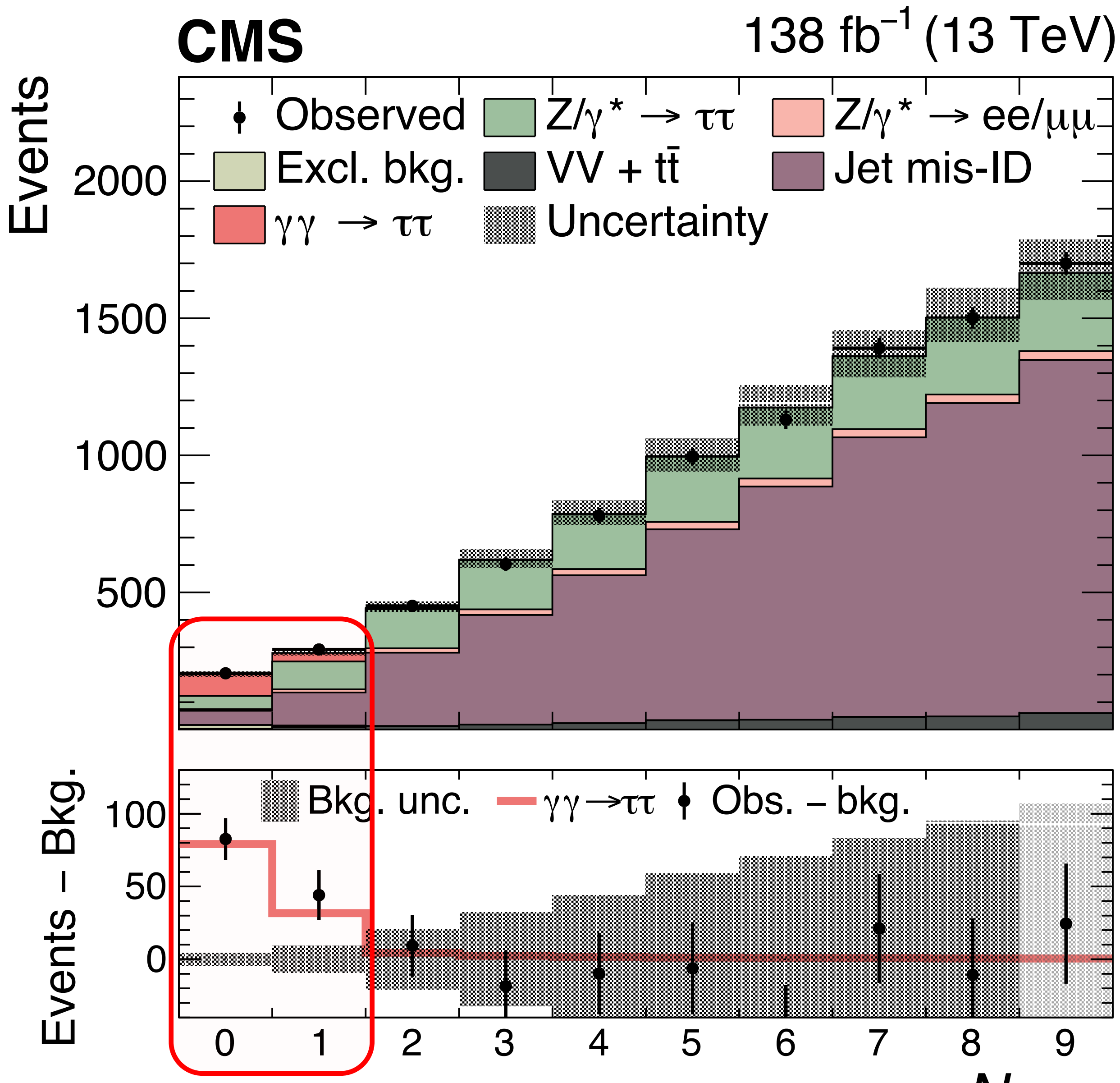

SR with $m_{\text{vis}} > 100$ GeV

First observation of $\gamma\gamma \to \tau\tau$ in pp collisions !

- combined observed significance of **5.3σ** (6.5σ expected) assuming SM a_τ

  ⇒ *first* observation of $\gamma\gamma \to \tau\tau$ in pp !

- combined **signal strength**

  $r = 0.75 +0.21 -0.18$

  w.r.t. gammaUPC elastic prediction

  × rescaling measured in $\mu\mu$ data

- dominant systematic uncertainties:
  - elastic rescaling to $\gamma\gamma \to \tau\tau$
  - $N_{\text{tracks}}^{\text{HS}}$ corrections to Drell–Yan

$\tau\tau$ channel	Observed	Expected
$e\mu$	2.3σ	3.2σ
$e\tau_h$	3.0σ	2.1σ
$\mu\tau_h$	2.1σ	3.9σ
$\tau_h\tau_h$	3.4σ	3.9σ
Combined	5.3σ	6.5σ

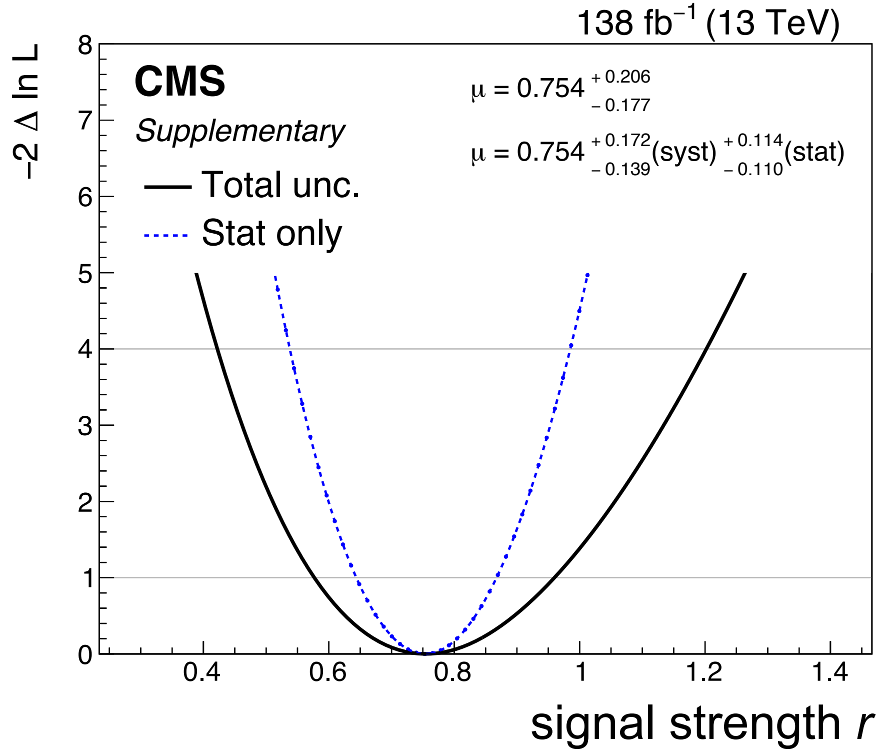

CONSTRAINTS ON a_τ & d_τ

CMS-SMP-23-005

EFT interpretation to contrain a_τ

- previous analyses used form factors (DELPHI, ATLAS, CMS), but SMP-23-005 uses an SMEFT approach (equivalent for $q^2 \to 0$)
- deviations of δa_τ & δd_τ from the SM can be parametrized in terms of a BSM Lagrangian with dim-6 operators with NP scale Λ:

$$\mathcal{L}_{\mathrm{BSM}} = \bar{L}_\tau \sigma^{\mu\nu} \tau_R H \left[\frac{C_{\tau B}}{\Lambda^2} B_{\mu\nu} + \frac{C_{\tau W}}{\Lambda^2} W_{\mu\nu} \right]$$

- contributions to a_τ & d_τ are linearly dependent on the *complex* Wilson coefficients:

$$\delta a_\tau = \frac{2 m_\tau}{e} \frac{\sqrt{2} v}{\Lambda^2} \mathrm{Re}[\cos\theta_W\, C_{\tau B} - \sin\theta_W\, C_{\tau W}]$$

$$\delta d_\tau = \frac{\sqrt{2} v}{\Lambda^2} \mathrm{Im}[\cos\theta_W\, C_{\tau B} - \sin\theta_W\, C_{\tau W}]$$

- scan a_τ & d_τ values in $\gamma\gamma \to \tau\tau$ signal samples by scanning $C_{\tau B}$ and $C_{\tau W}$ in matrix element reweighting
  $\Rightarrow$ causes variations in the cross section and $m_{\tau\tau}$ distribution

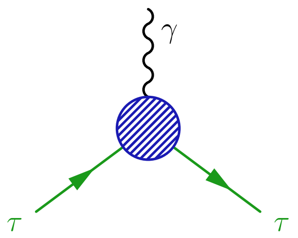

$a_\tau^{\mathrm{SM}} \approx 0.001\,177$

$a_\tau = \frac{g-2}{2} = a_\tau^{\mathrm{SM}} + \delta a_\tau$

CP violation in CKM:
$d_\tau^{\mathrm{SM}} \approx 10^{-37}$ ecm

some BSMs predict:
$d_\tau \approx 10^{-19}$ ecm

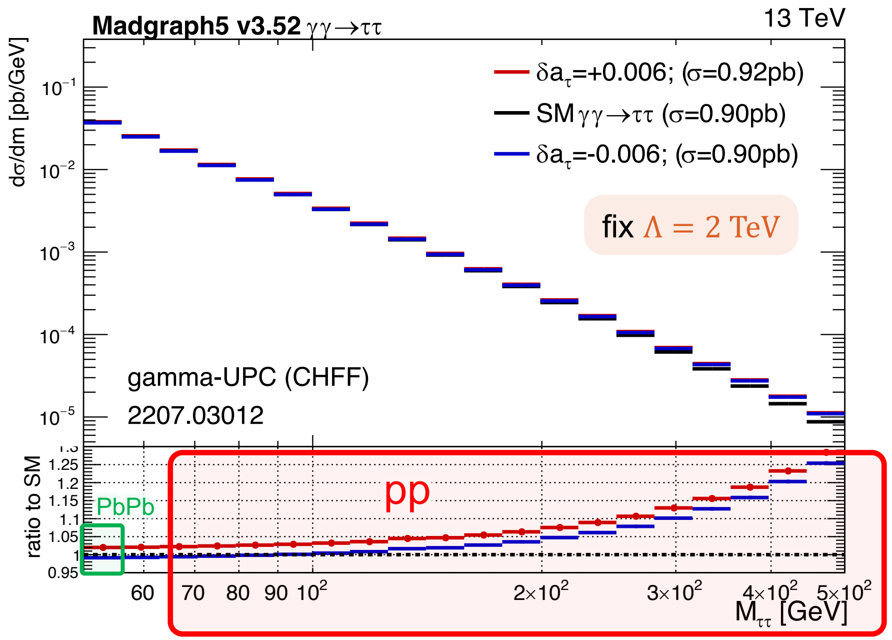

How BSM in a_τ affects $\gamma\gamma \to \tau\tau$

- at $m_{\tau\tau}$ > 100 GeV:
  – cross section grows with $m_{\tau\tau}$
  – same direction for $\delta a_\tau > 0$ & $\delta a_\tau < 0$
- constrain a_τ by measuring the **yield** *and* $\mathbf{m_{\tau\tau}}$ distribution of $\gamma\gamma \to \tau\tau$
- pp data looks at $m_{\tau\tau}$ > 50 GeV
  ⇒ better sensitivity than PbPb !

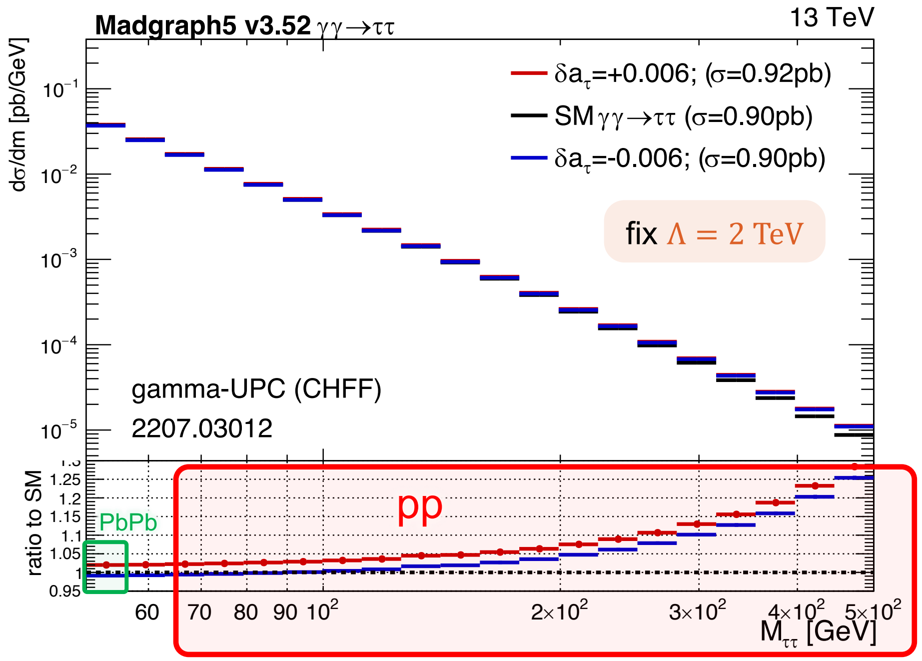

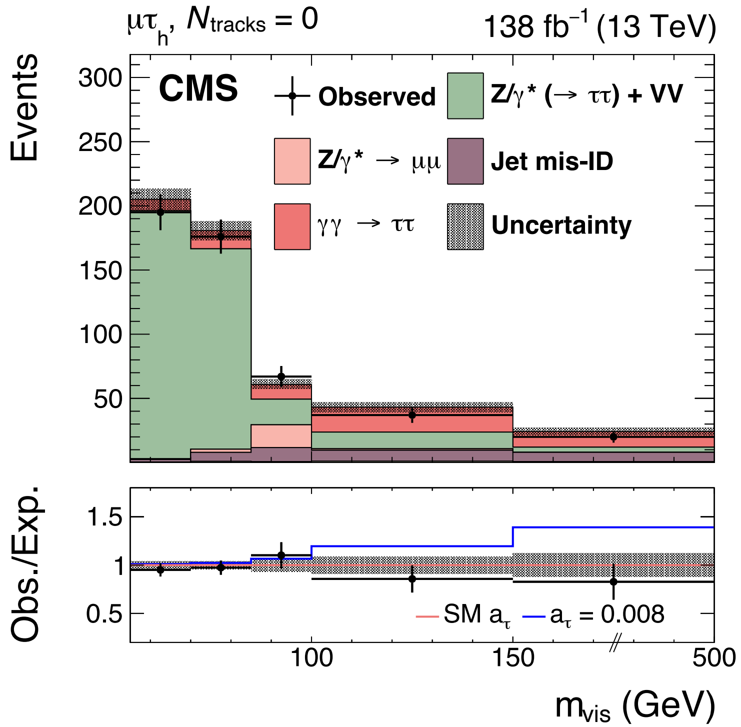

differences increase with $m_{\tau\tau}$

Constraints on a_τ

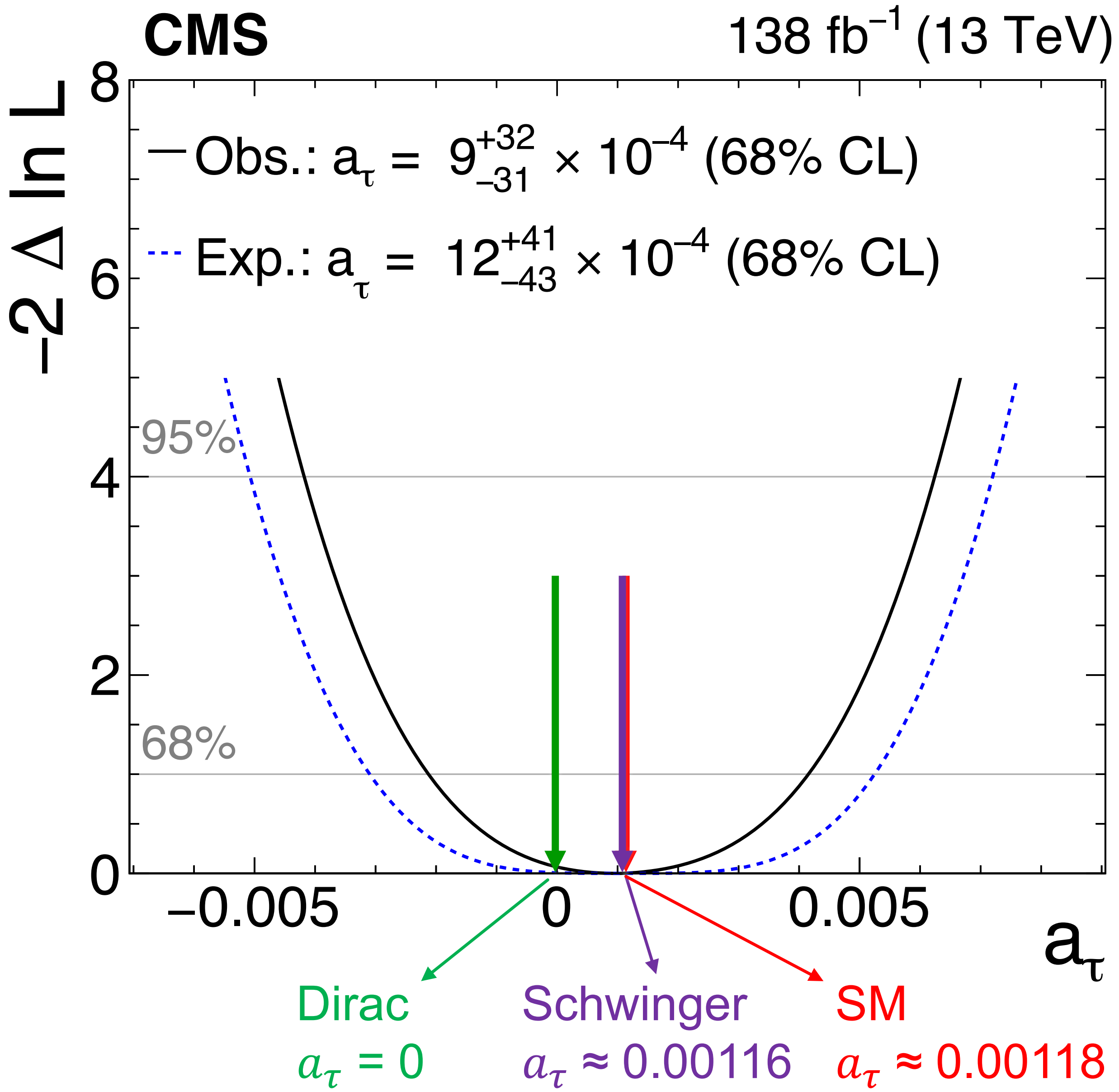

- fit all $m_{\tau\tau}$ distributions
- scan likelihood over a_τ
- small $\gamma\gamma \to \tau\tau$ deficit observed
  $\Rightarrow$ tighter contraint than expected
- but compatible with the SM

Schwinger: $a_\tau = 0.001\,161\,4$

SM: $a_\tau = 0.001\,177\,21(5)$

our result: $a_\tau = 0.0009\,(32)$

$\Rightarrow$ uncertainty ~3 × Schwinger !

Constraints on a_τ

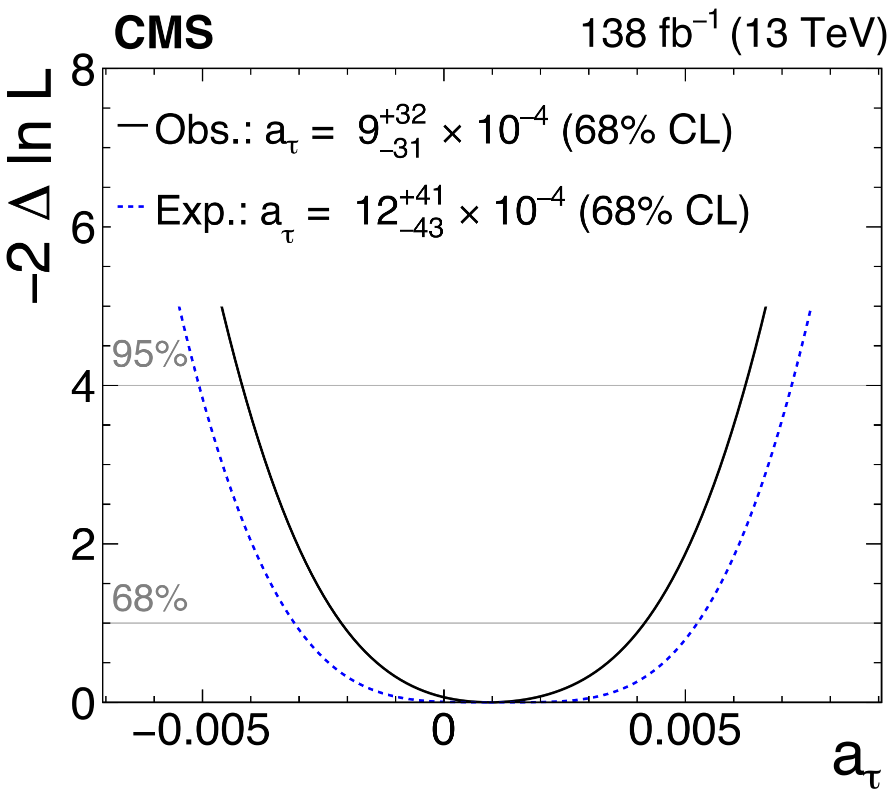

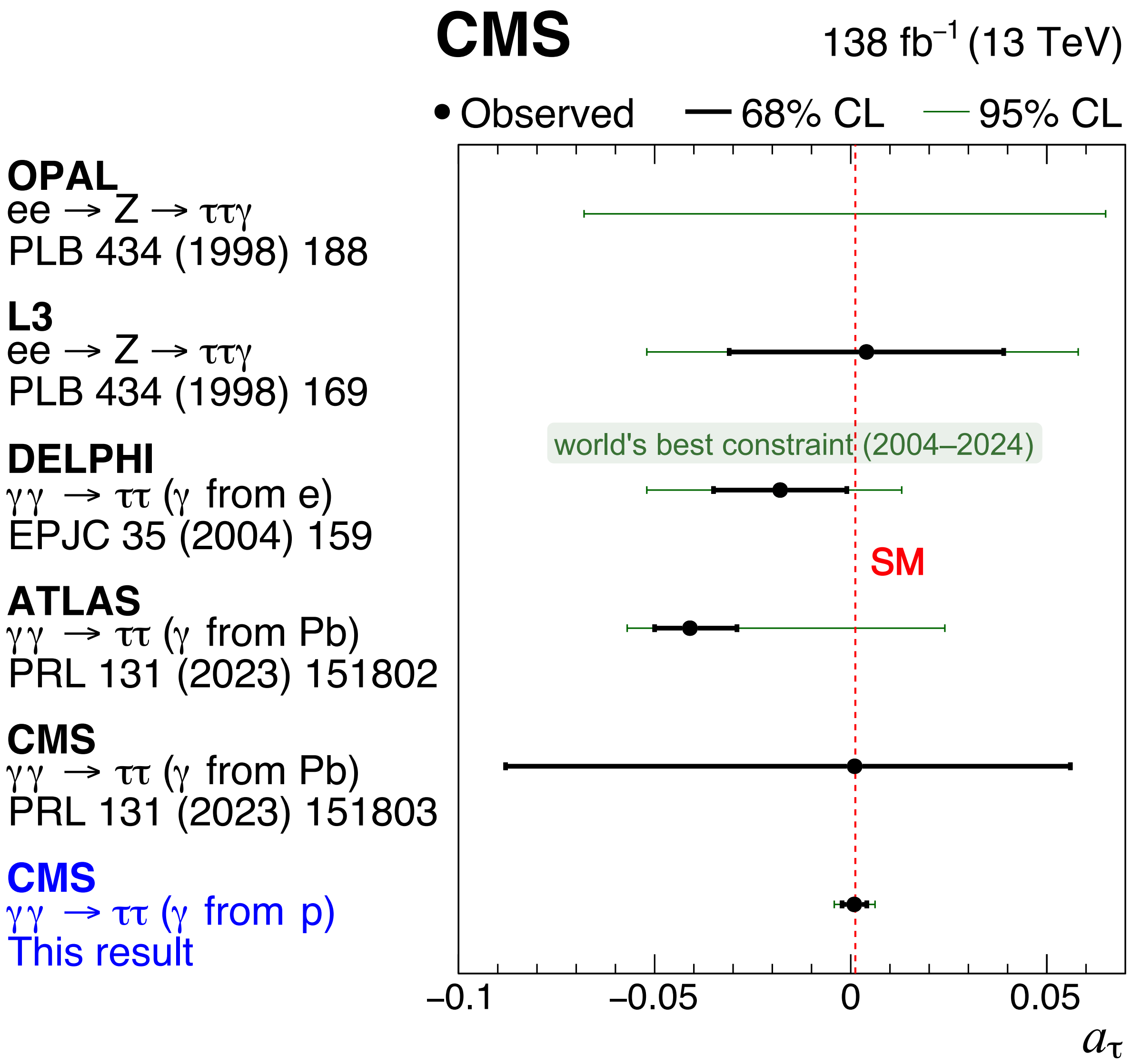

- SM: $a_\tau = 0.001\ 177\ 21(5)$
- DELPHI: $a_\tau = -0.018 \pm 0.017$
- ATLAS: $a_\tau = -0.041 +0.012 -0.009$
- CMS HIN: $a_\tau = 0.001 +0.055 -0.089$
- our result: $a_\tau = 0.0009 +0.0032 -0.0031$

~2.7x above SM, >5x better than LEP !

Constraints on d_τ

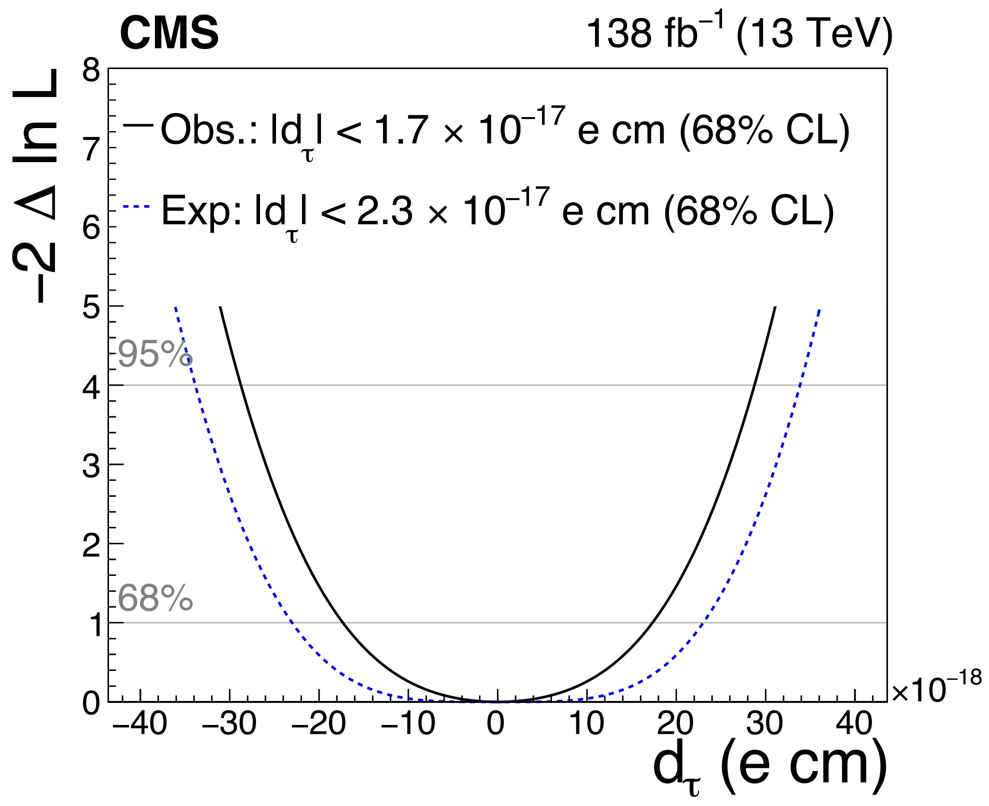

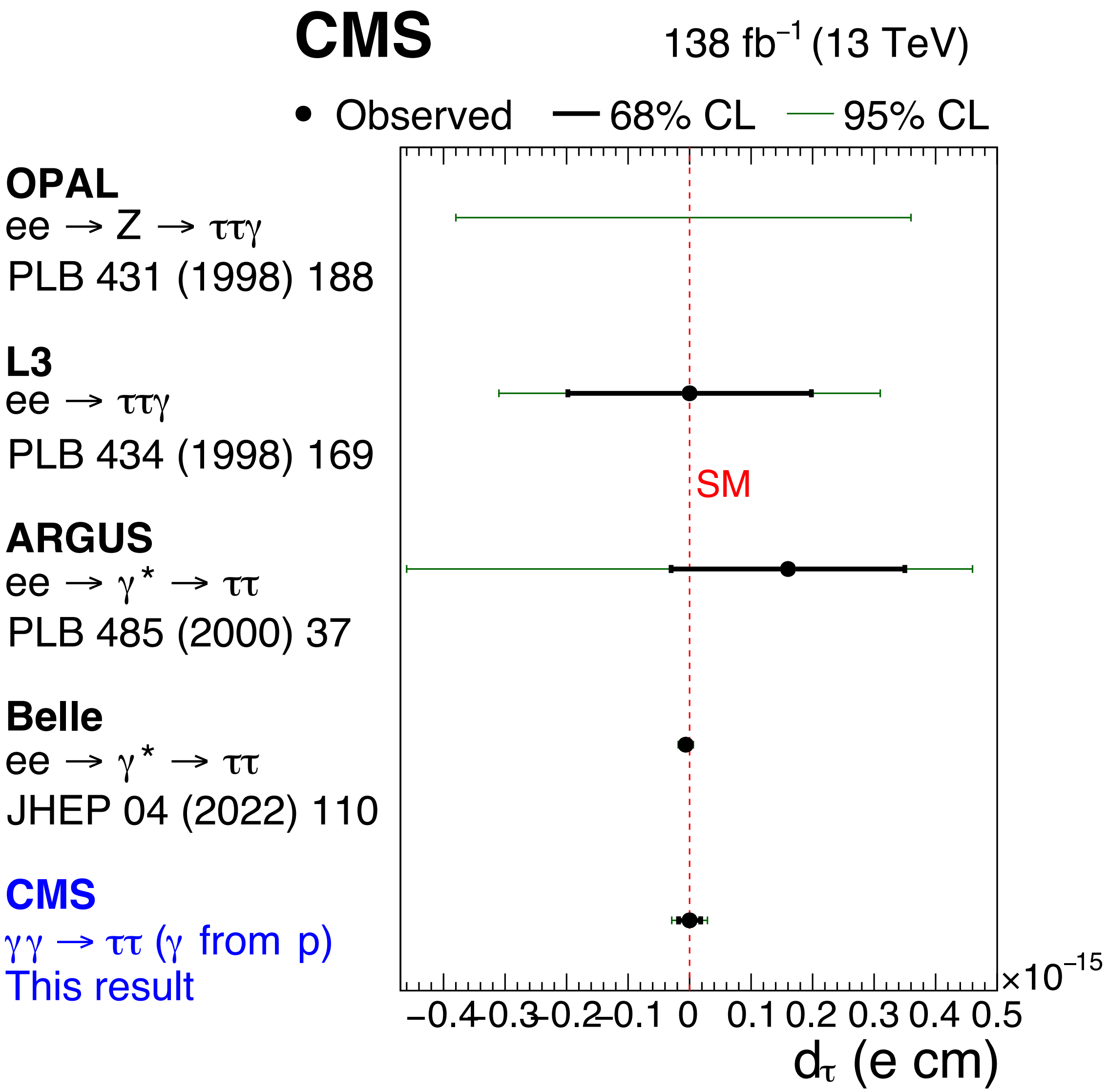

- SM: $d_\tau \sim 10^{-37}$ ecm (due to CPV in CKM)
- Belle: $-1.85 < d_\tau < 0.61 \times 10^{-17}$ ecm (95%)
- our result: $-1.70 < d_\tau < 1.70 \times 10^{-17}$ ecm (68%)

approaching Belle !

Constraints on Wilson coefficients

$a_\tau = a_\tau^{\mathrm{SM}} + \delta a_\tau = \frac{g-2}{2}$

$d_\tau = d_\tau^{\mathrm{SM}} + \delta d_\tau$

recast results to make exclusion of $C_{\tau B}/\Lambda^2$ vs. $C_{\tau W}/\Lambda^2$:

$$\delta a_\tau = \frac{2m_\tau}{e}\frac{\sqrt{2}v}{\Lambda^2}\mathbf{Re}[\cos\theta_W\, C_{\tau B} - \sin\theta_W\, C_{\tau W}]$$

$$\delta d_\tau = \frac{\sqrt{2}v}{\Lambda^2}\mathbf{Im}[\cos\theta_W\, C_{\tau B} - \sin\theta_W\, C_{\tau W}]$$

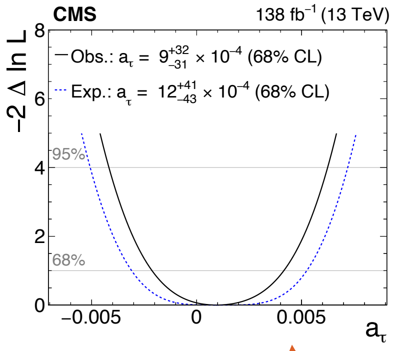

real part:

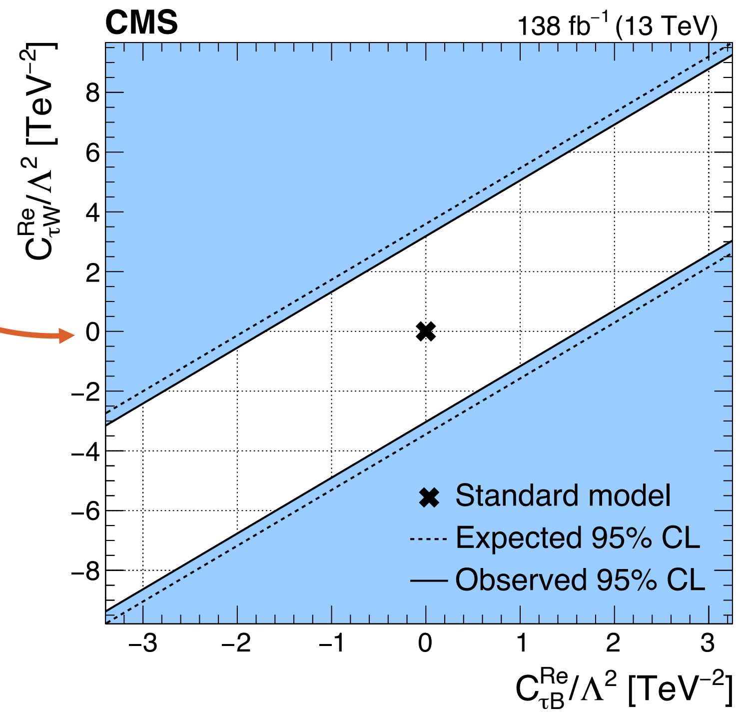

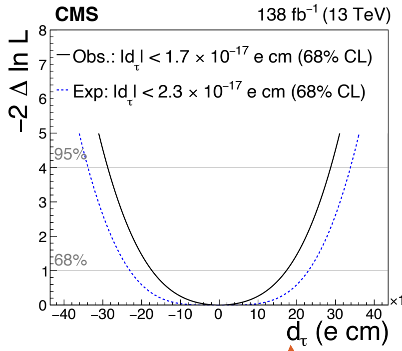

imaginary part:

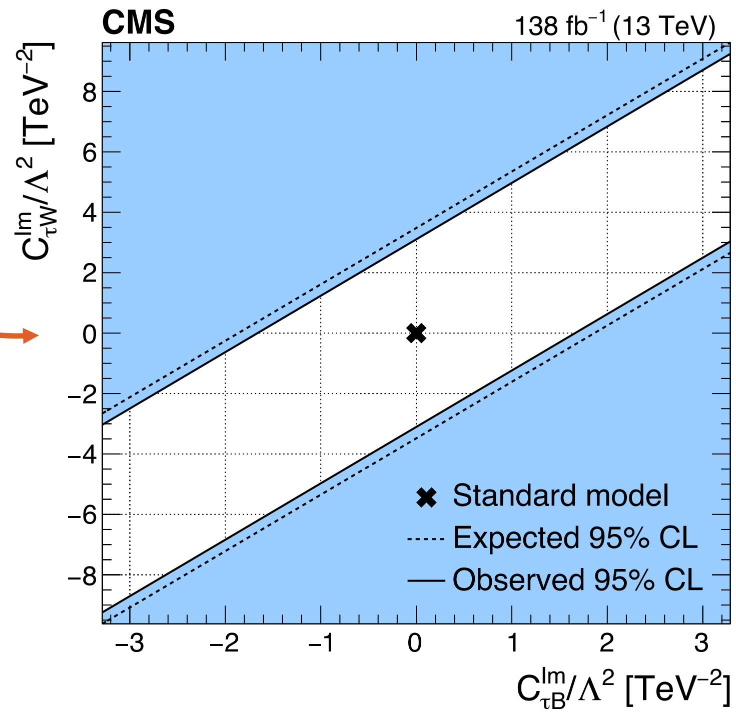

SUMMARY

Summary

- $(g-2)_\tau$ has a strong potential to probe new physics
- ATLAS & CMS have put limits on a_τ using PbPb data
  - enjoying from $\sigma \propto Z^4$ and clean signal
  - sensitive to $m_{\tau\tau} < 40$ GeV
- new results in **pp** by CMS [SMP-23-005]:
  - using exclusivity cuts on **acoplanarity** & N_{tracks}
  - fitting shape and yield in $m_{\tau\tau} > 50$ GeV
  - full Run-2 UL data analyzed in 4 $\tau\tau$ final states
  - first observation of $\gamma\gamma \to \tau\tau$ process in pp (5.3σ)
  - puts strongs constraints on
    - $a_\tau = 0.0009^{+0.0032}_{-0.0031}$: > 5x better than LEP
      $\Rightarrow g_\tau = 2.0018^{+0.0064}_{-0.0062}$, i.e. 0.3% precision ! ☺
    - $|d_\tau| < 1.7 \times 10^{-17}$ ecm (68%): same order as Belle

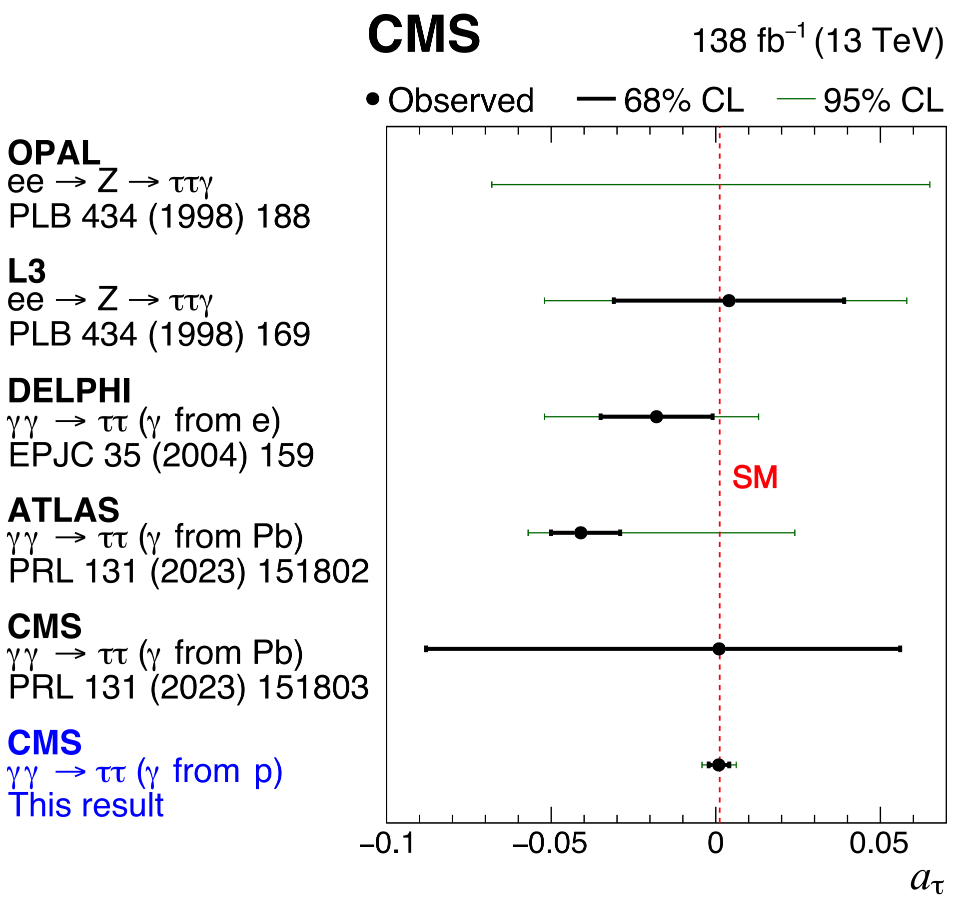

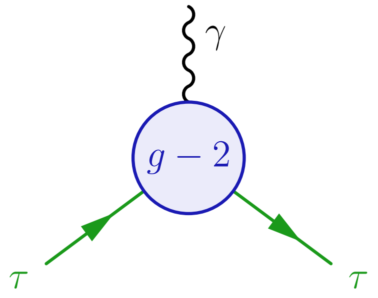

References

Theory & phenomenology

- gammaUPC (2022) arXiv:2207.03012
- Beresford, Liu (2020) arXiv:1908.05180
- Dynal et al. (2020) arXiv:2002.05503
- Haisch et al. (2023) arXiv:2307.14133
- Beresford et al (2024) arXiv:2403.06336

Experiment

- a_e Penning Trap (2023) arXiv:2209.13084
- a_μ FNAL (2023) arXiv:2308.06230
- a_τ DELPHI (2004) arXiv:hep-ex/0406010
- d_τ Belle (2022) arXiv:2108.11543
- $\gamma\gamma \to$ WW ATLAS (2021) arXiv:2010.04019
- $\gamma\gamma \to$ ee ATLAS (2023) arXiv:2207.12781
- $\gamma\gamma \to$ tt CMS (2023) arXiv:23w10.11231

$(g-2)_\tau$ with UPC PbPb ($m_{\tau\tau}$ < 50 GeV):

- a_τ CMS (2022) HIN-21-009
- a_τ ATLAS (2022) STDM-2019-19

$(g-2)_\tau$ with pp (50 < $m_{\tau\tau}$ < 500 GeV):

- a_τ CMS (2024) SMP-23-005
  - talks: LHC seminar, Moriond, UZH
  - press: CMS, CERN, Courier

BACK UP

Bigger picture

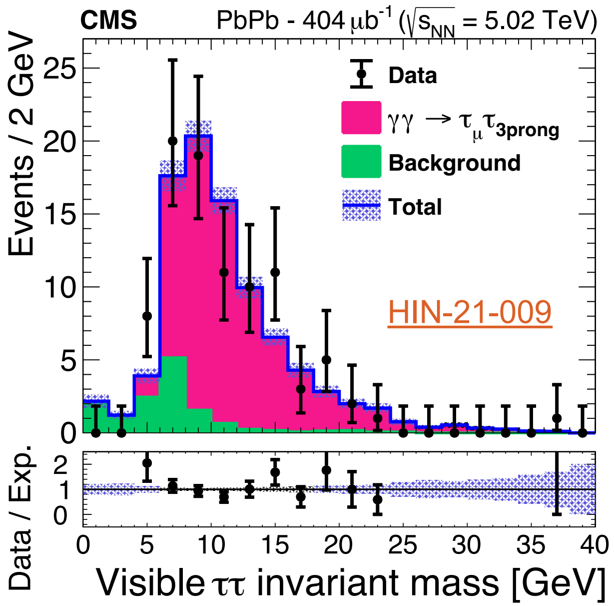

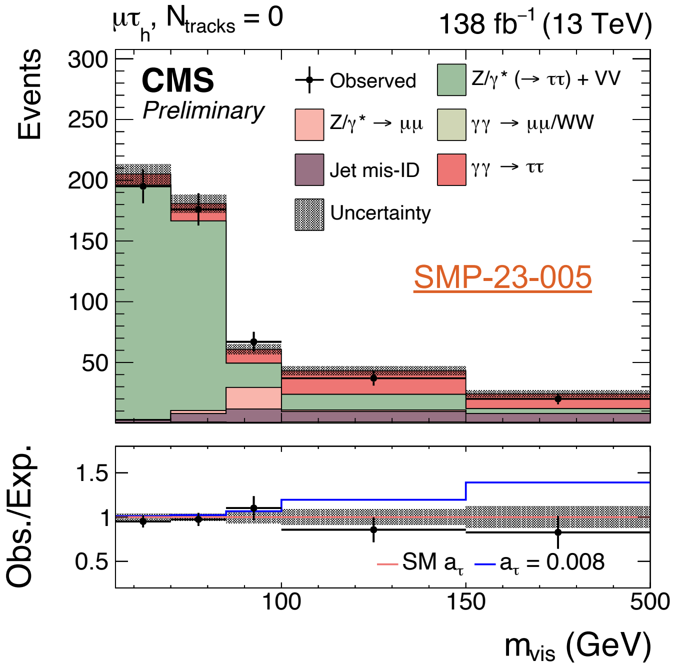

Precision Proton Spectrometer

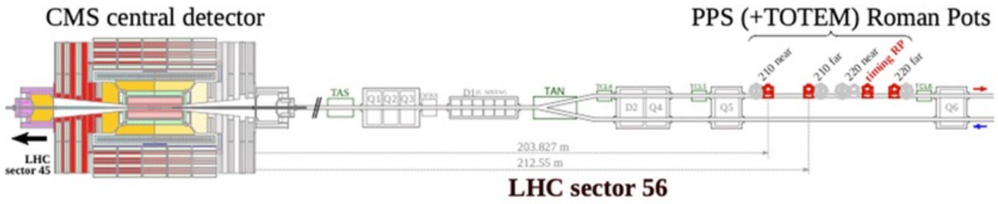

ultra-peripheral PbPb | pp with track counting | pp with forward proton tagging

0 GeV | 50 GeV | 350 GeV | 2 TeV

Object reconstruction & selection

- **e**: MVA WP80, p_T > 15 GeV, $|\eta|$ < 2.5
- $\boldsymbol{\mu}$: medium ID, medium isolation, p_T > 10 GeV, $|\eta|$ < 2.4
- $\boldsymbol{\tau_h}$: HPS, p_T > 30 GeV, $|\eta|$ < 2.3, DeepTau v2p1 (VSe, VSmu, VSjet), four decay modes:

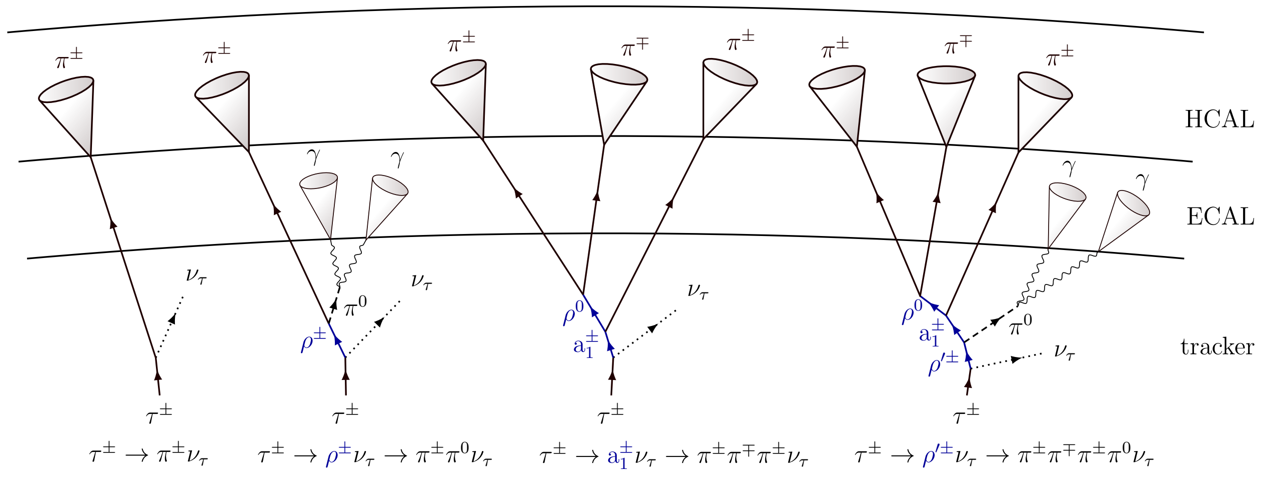

- **MET**: PFMET reconstruction
- **tracks**: charged PFCandidate collection in miniAOD, p_T > 0.5 GeV, $|\eta|$ < 2.5

Inclusive pre-selections

CMS-SMP-23-005

	$e\mu$	$e\tau_h$	$\mu\tau_h$	$\tau_h\tau_h$	$\mu\mu$
p_T^e (GeV)	$> 15/24$	$> 25 - 33$	—	—	—
$\|\eta^e\|$	< 2.5	$< 2.1 - 2.5$	—	—	—
p_T^μ (GeV)	$> 24/15$	—	$> 21 - 29$	—	$> 26 - 29/10$
$\|\eta^\mu\|$	< 2.4	—	$< 2.1 - 2.4$	—	
$p_T^{\tau_h}$ (GeV)	—	$> 30 - 35$	$> 30 - 32$	> 40	—
$\|\eta^{\tau_h}\|$	—	$< 2.1 - 2.3$	$< 2.1 - 2.3$	< 2.1	—
$m_{\mu\mu}$ (GeV)	—	—	—	—	> 50
OS	yes	yes	yes	yes	yes
$\|d_z(\ell, \ell')\|$ (cm)	< 0.1	< 0.1	< 0.1	< 0.1	< 0.1
$\Delta R(\ell, \ell')$	> 0.5	> 0.5	> 0.5	> 0.5	> 0.5
$m_T(e/\mu, \vec{p}_T^{miss})$ (GeV)	—	< 75	< 75	—	—

Exclusivity cuts

define **signal regions** based on exclusivity cuts

- **acoplanarity** $A = 1 - \frac{|\Delta\phi|}{\pi}$
  - **A < 0.015**: >95% signal efficiency, and <30% Drell–Yan efficiency
- N_{tracks}: count tracks with in 0.1 cm window around $\tau\tau$ vertex
  - $\tau\tau$ vertex reconstructed as $z_{\tau\tau} = \frac{1}{2}\left(z_{\tau_1} + z_{\tau_2}\right)$
  - two categories: N_{tracks} **= 0 or 1**: ≈75% signal efficiency, and reduces backgrounds (like Drell–Yan) by ~10^3

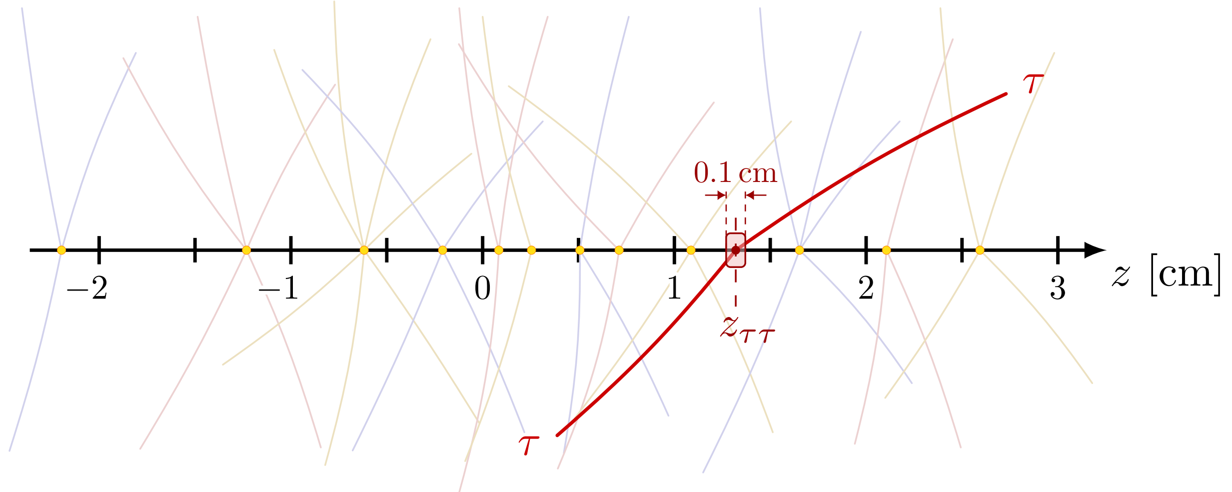

signal:

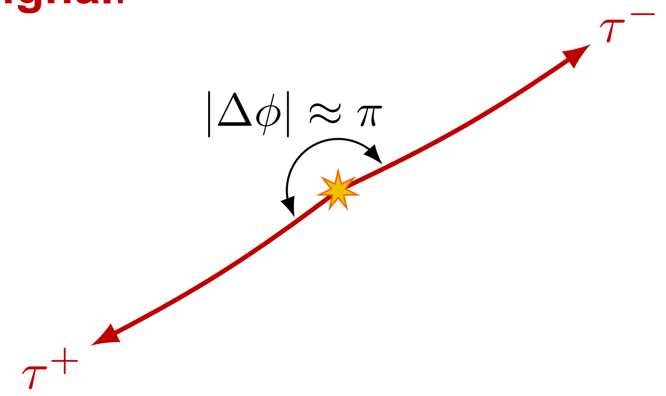

Drell–Yan background:

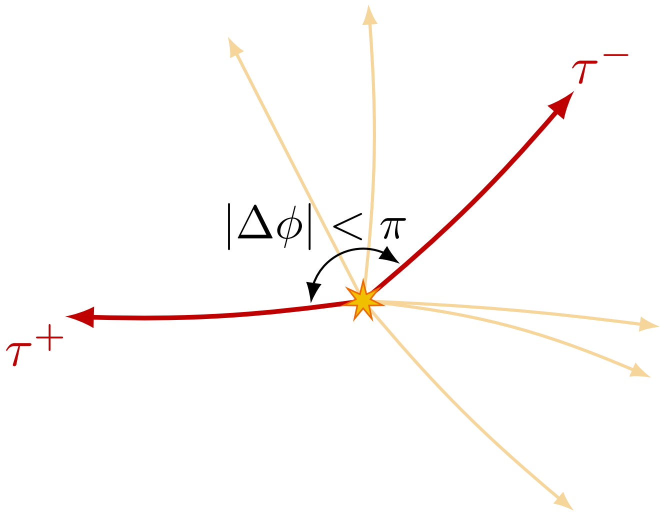

CORRECTIONS

CMS-SMP-23-005

Corrections to simulation

modeling of observed data is not perfect

⇒ derive corrections in pure **dimuon ($\mu\mu$)** sample

1. **acoplanarity** in **Drell–Yan**
2. **pileup tracks**: $N_{\text{tracks}}^{\text{PU}}$ in all simulation
3. **hard scattering tracks**: $N_{\text{tracks}}^{\text{HS}}$ in **Drell–Yan**
4. **nonelastic contributions** of $\gamma\gamma \rightarrow \ell\ell$ simulation

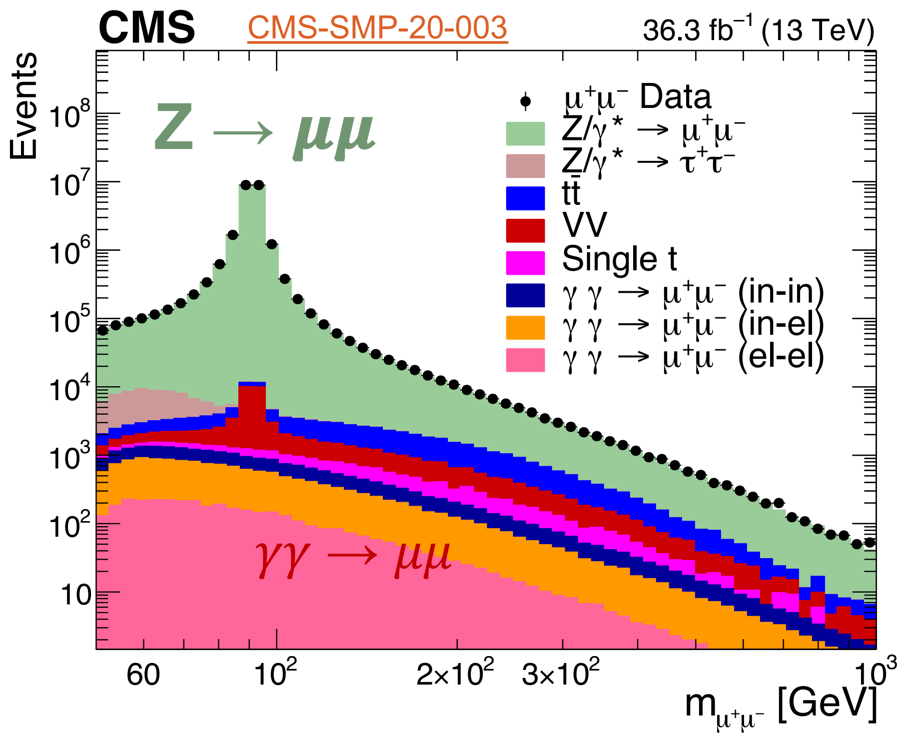

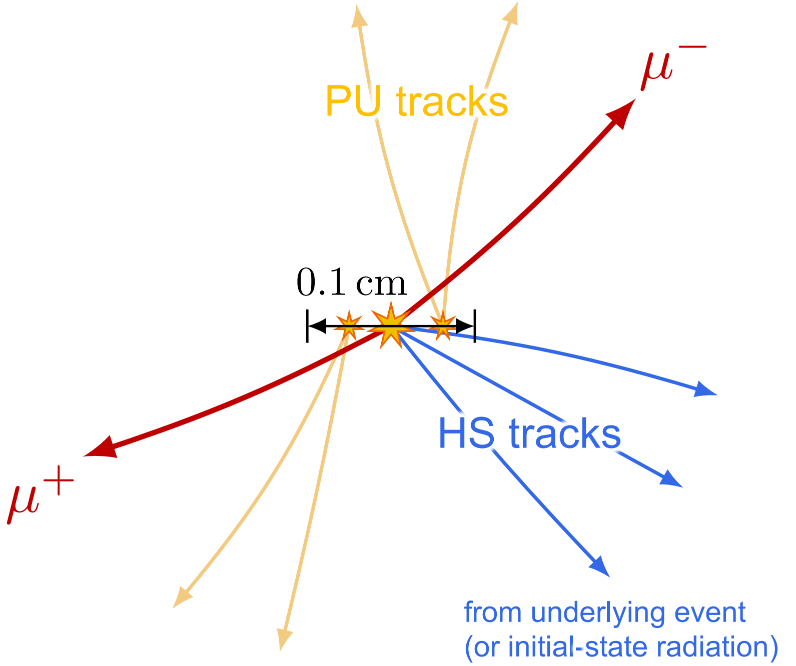

1. Acoplanarity corrections

- Drell–Yan generated by aMC@NLO does not describe well
  - Z boson p_T
  - acoplanarity A
- measure corrections in pure $Z/\gamma^* \to \mu\mu$ sample
- apply correction as a function of
  - acoplanarity A
  - leading and subleading muon p_T

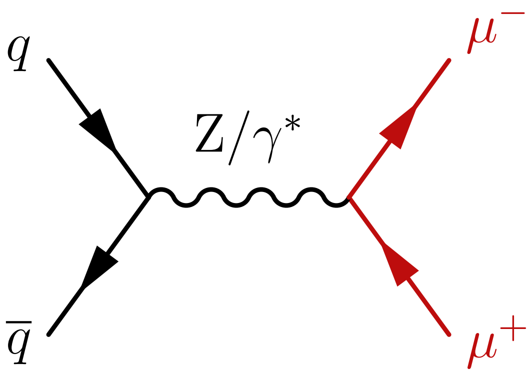

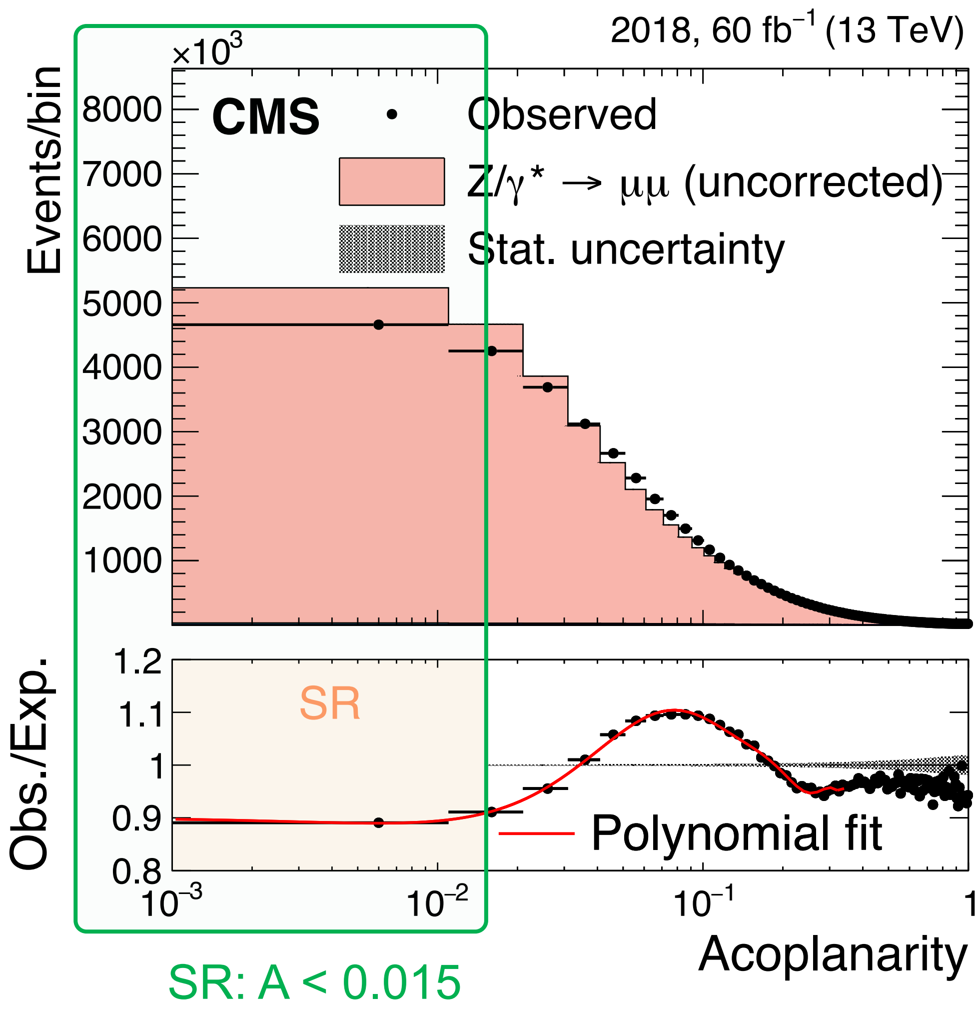

2. $N_{\text{tracks}}^{\text{PU}}$ corrections

applied to all simulation

gaussian
= beamspot profile

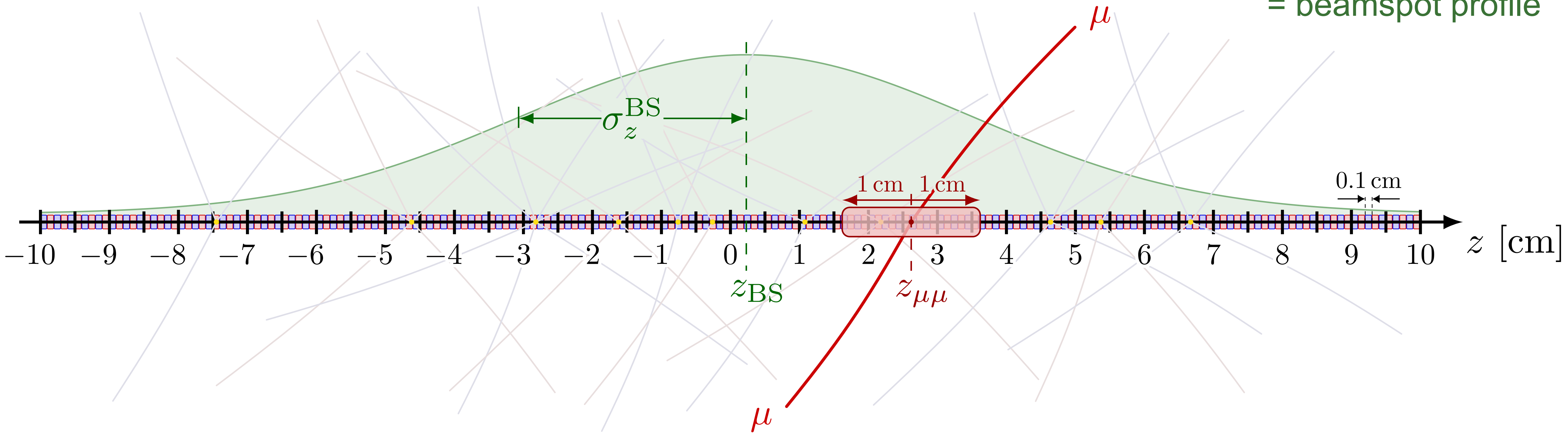

- use Z → $\mu\mu$ events at Z peak, $|m_{\mu\mu} - m_{\text{Z}}| < 15\ \text{GeV}$
- count number of PU tracks in small *z* windows (far away from $\mu\mu$ vertex)
- derive correction from obs. / sim. ratio as a function of ***z*** and N_{tracks}

2. $N_{\mathrm{tracks}}^{\mathrm{PU}}$ corrections

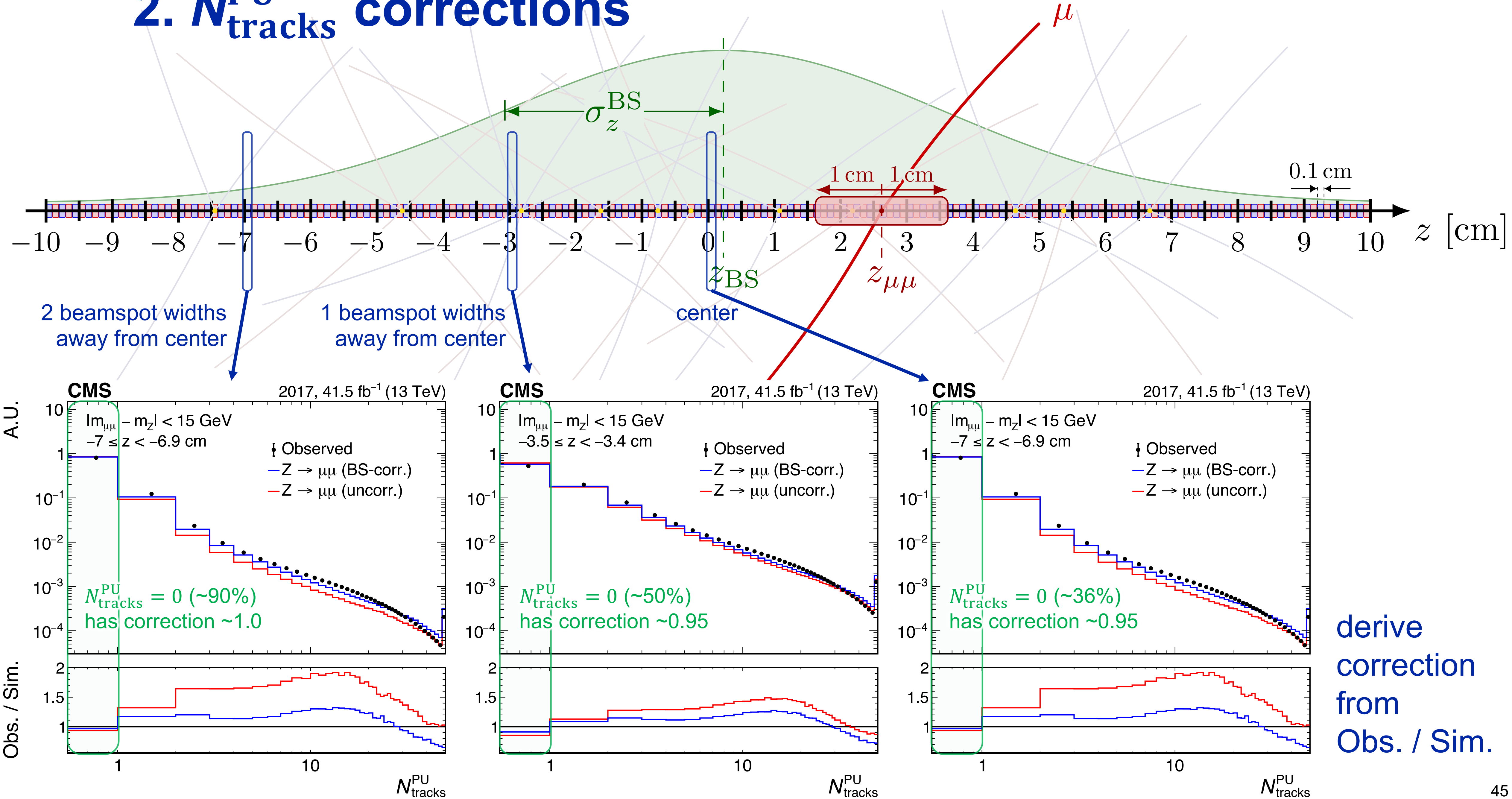

derive correction from Obs. / Sim.

3. $N_{\text{tracks}}^{\text{HS}}$ correction

- use $Z \to \mu\mu$ events at Z peak
- count N_{tracks} in signal window (0.1 cm) around $\mu\mu$ vertex
- separate Drell–Yan into bins of $N_{\text{tracks}}^{\text{HS}}$ by gen-matching reco tracks

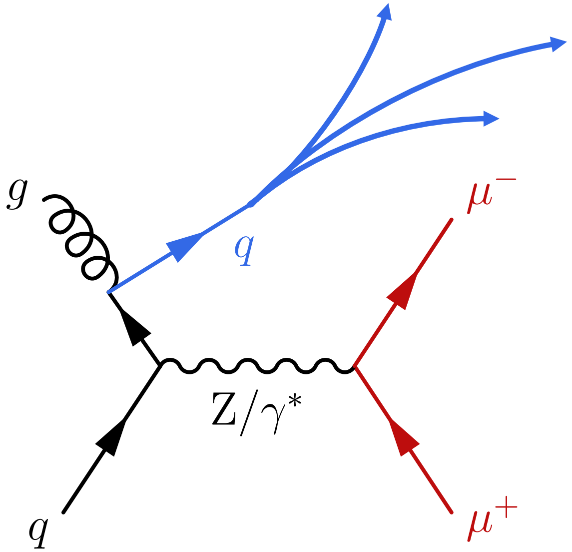

Drell-Yan ($Z/\gamma^* \to \mu\mu$)
with initial-state radiation

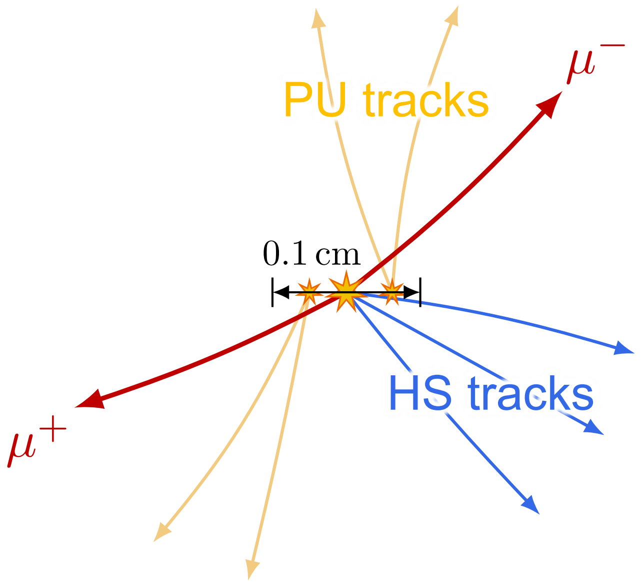

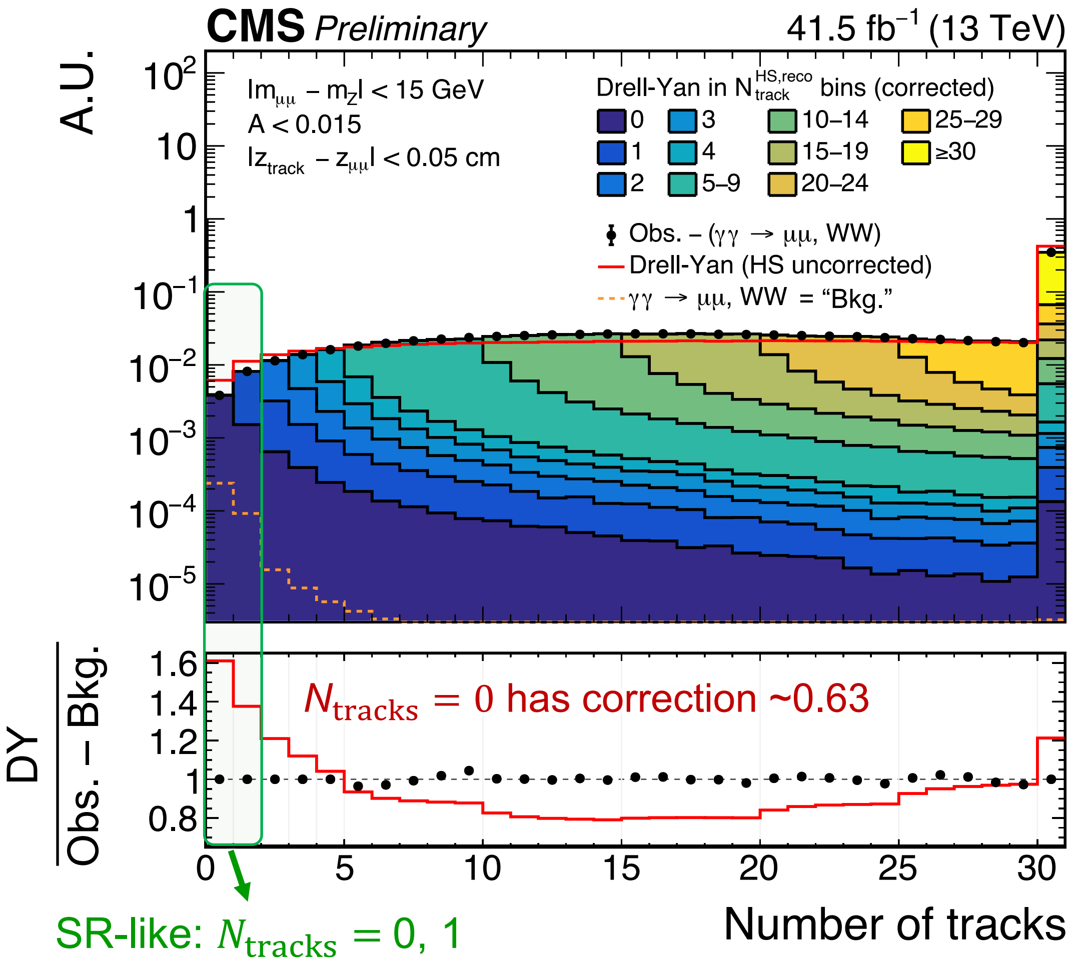

$N_{\text{tracks}} = N_{\text{tracks}}^{\text{HS}} + N_{\text{tracks}}^{\text{PU}}$

in signal window (0.1 cm)

After corrections

1. acoplanarity in **Drell–Yan**
2. pileup tracks: $N_{\text{tracks}}^{\text{PU}}$ in all simulation
3. hard scattering tracks: $N_{\text{tracks}}^{\text{HS}}$ in **Drell–Yan**

simulation describes observed data well after these corrections !

- $m_{\text{vis}}(\tau\tau)$ < 100 GeV (low signal efficiency)
- in all $\tau\tau$ final states

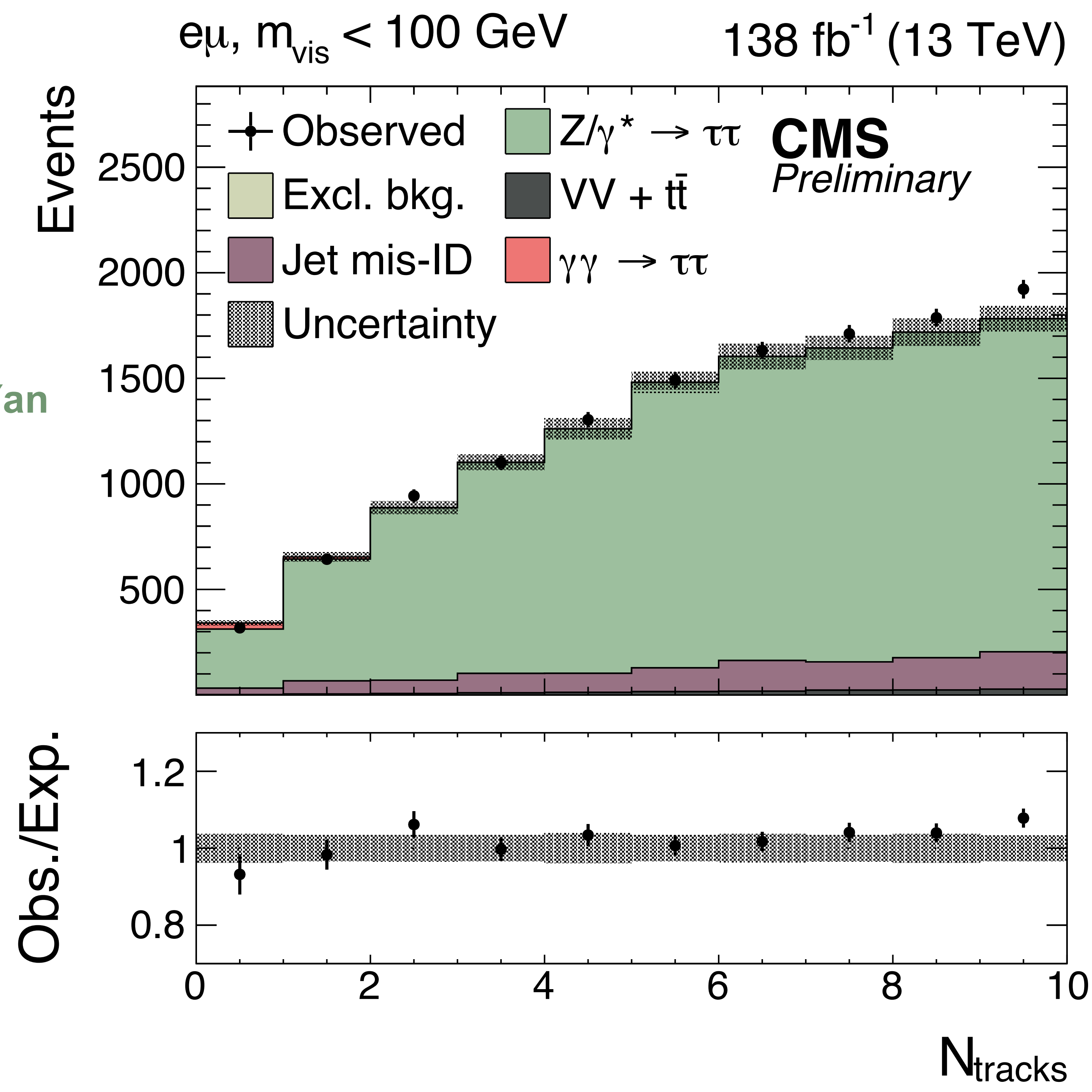

4. Elastic rescaling

- signal samples only include **elastic-elastic (ee)** process generated by gammaUPC
- **single-dissociative (sd)** and **double-dissociative (dd)** processes not included
  - have larger cross section
  - can have an exclusive signature
- estimate dissociative contributions (incl. higher-order corrections) by rescaling elastic-elastic $\gamma\gamma \rightarrow \mu\mu$ signal in $\mu\mu$ data

$\Rightarrow$ measure rescaling factor = $\dfrac{(\mathbf{ee}+\mathbf{sd}+\mathbf{dd})_{\mathrm{obs}}}{(\mathbf{ee})_{\mathrm{sim}}}$

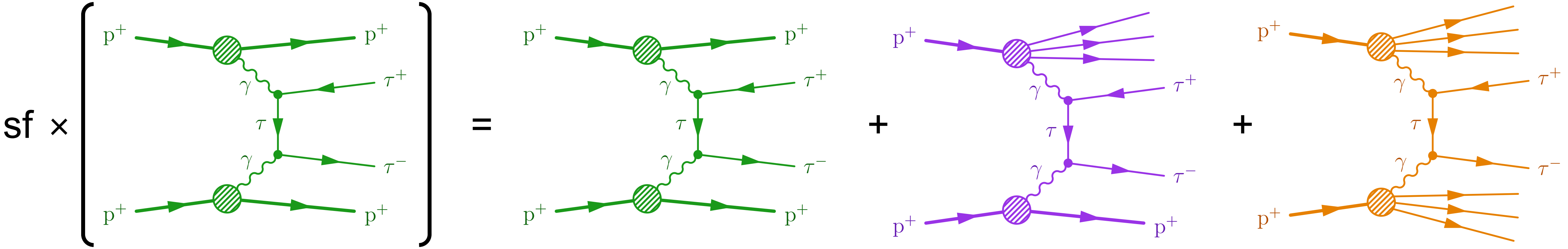

elastic-elastic (ee) elastic-elastic (ee) single-dissociative (sd) double-dissociative (dd)

4. Elastic rescaling

- rescaling factor measured in $m_{\mu\mu}$ distribution in dimuon events with A < 0.015 and N_{tracks} = 0 or 1
- **inclusive background** (mostly Drell–Yan)
  - estimated from data in $3 \leq N_{\text{tracks}} \leq 7$ region
  - normalized to Z peak
- **elastic $\gamma\gamma \to \mu\mu$/WW "signal"**
  - contributes significantly $m_{\mu\mu}$ > 150 GeV
  - rescale to data to estimate nonelastic contribution
- fits:
  - **linear fit** applied as nominal corrections to all elastic simulation ($\gamma\gamma \to$ ee, $\mu\mu$, $\tau\tau$, WW)
  - **flat fit (~2.7)** used to obtain uncertainty (conservative)

$$\text{rescaling factor} = \frac{(\mathbf{ee}+\mathbf{sd}+\mathbf{dd})_{\text{obs}}}{(\mathbf{ee})_{\text{sim}}} = \frac{\text{Obs.} - \text{Bkg.}}{\gamma\gamma \longrightarrow \mu\mu, \text{WW}}$$

applied to photon-induced simulation ($\gamma\gamma \to \ell\ell$, WW)

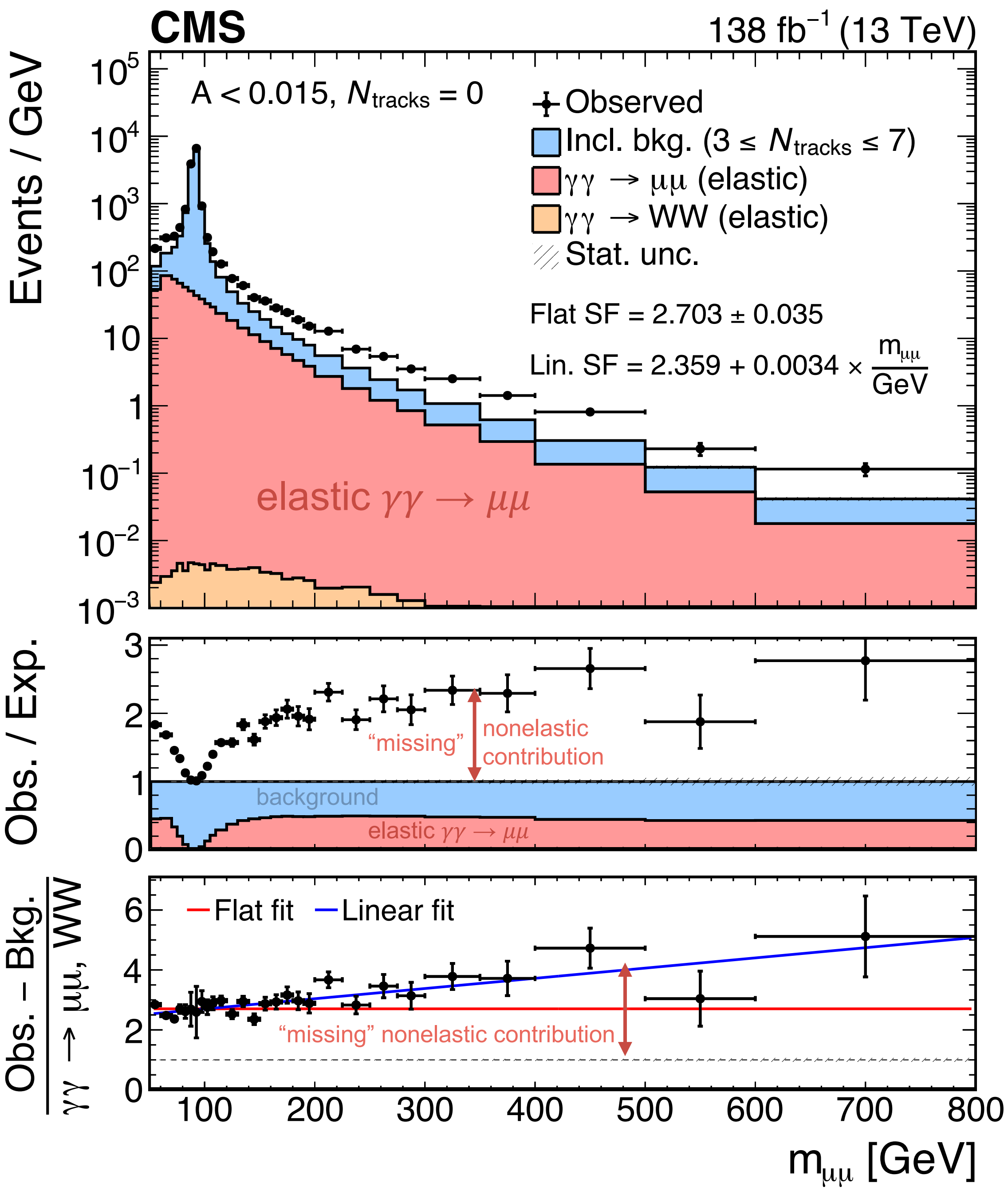

4. Elastic rescaling

applied to photon-induced simulation ($\gamma\gamma \rightarrow \ell\ell$, WW)

measured rescaling factor consistent with prediction by **SuperChic** generator within uncertainties!

- Measured: SF = 2.359 + 0.0032 × $\frac{m_{\mu\mu}}{\text{GeV}}$
- SuperChic: SF = 2.243 + 0.0026 × $\frac{m_{\mu\mu}}{\text{GeV}}$

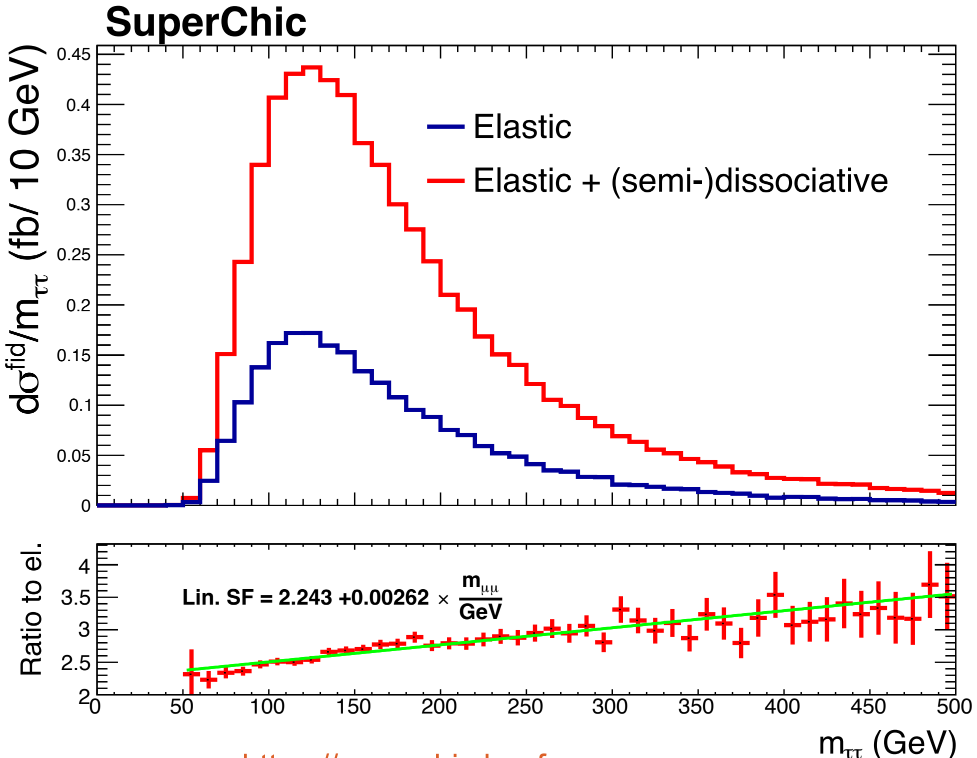

https://superchic.hepforge.org

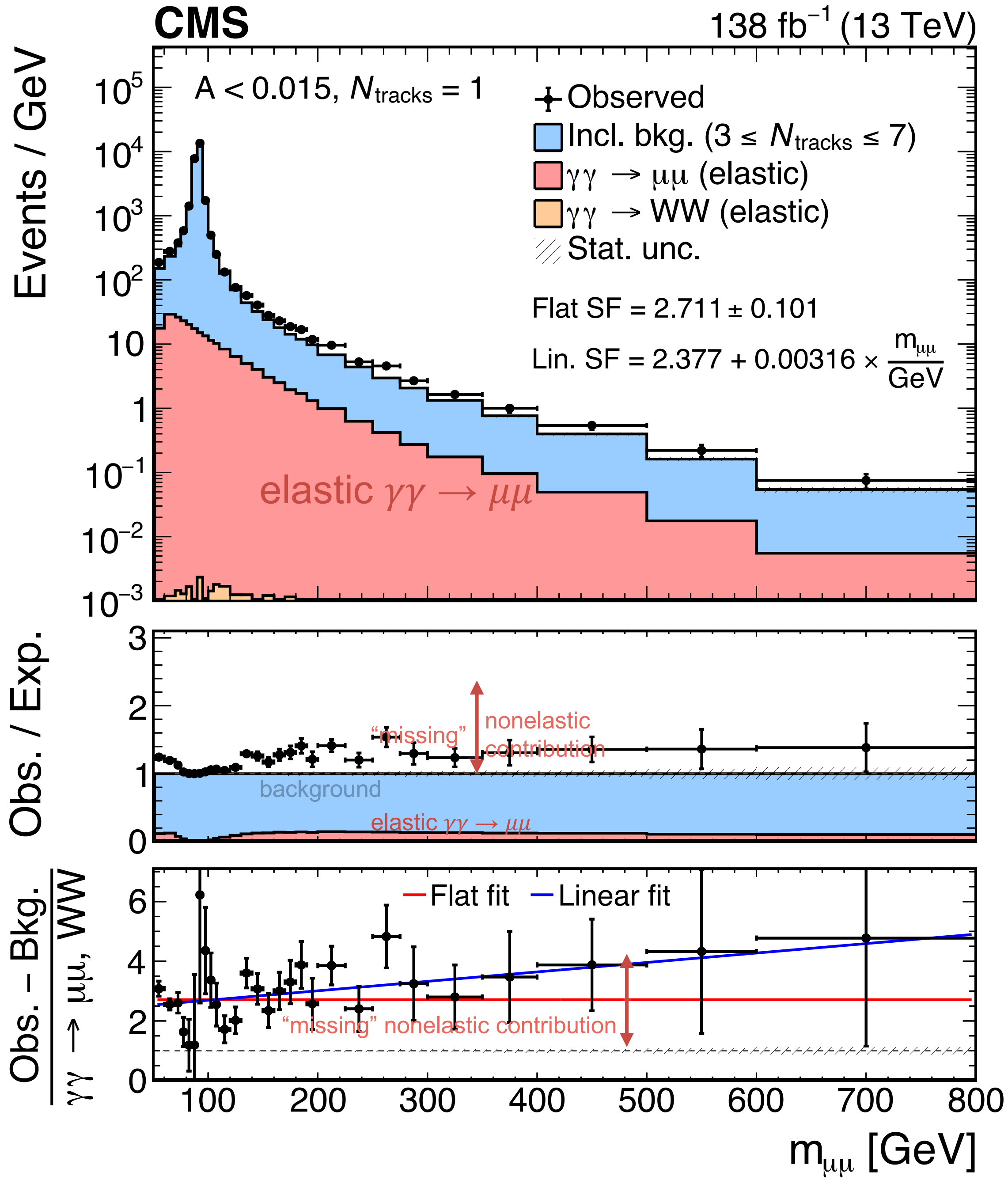

Beamspot smearing to pileup tracks

applied to all simulation

- **simulated events** have a *fixed* beamspot *z* position and width for a given era
- **in data**, beamspot *z* position and width are *run-dependent*
- to each simulated event, randomly assign a BS position $z_{\mathrm{data}}^{\mathrm{BS}}$ & a BS width $\sigma_{\mathrm{data}}^{\mathrm{BS}}$ by sampling the BS distributions in data
- correct *z* position of the pileup tracks
  - smear: $z^{\mathrm{corr}} = z_{\mathrm{MC}}^{\mathrm{BS}} + \frac{\sigma_{\mathrm{MC}}^{\mathrm{BS}}}{\sigma_{\mathrm{data}}^{\mathrm{BS}}}(z - z_{\mathrm{MC}}^{\mathrm{BS}})$
  - shift: $z^{\mathrm{corr}} = z + \left(z_{\mathrm{data}}^{\mathrm{BS}} - z_{\mathrm{MC}}^{\mathrm{BS}}\right)$

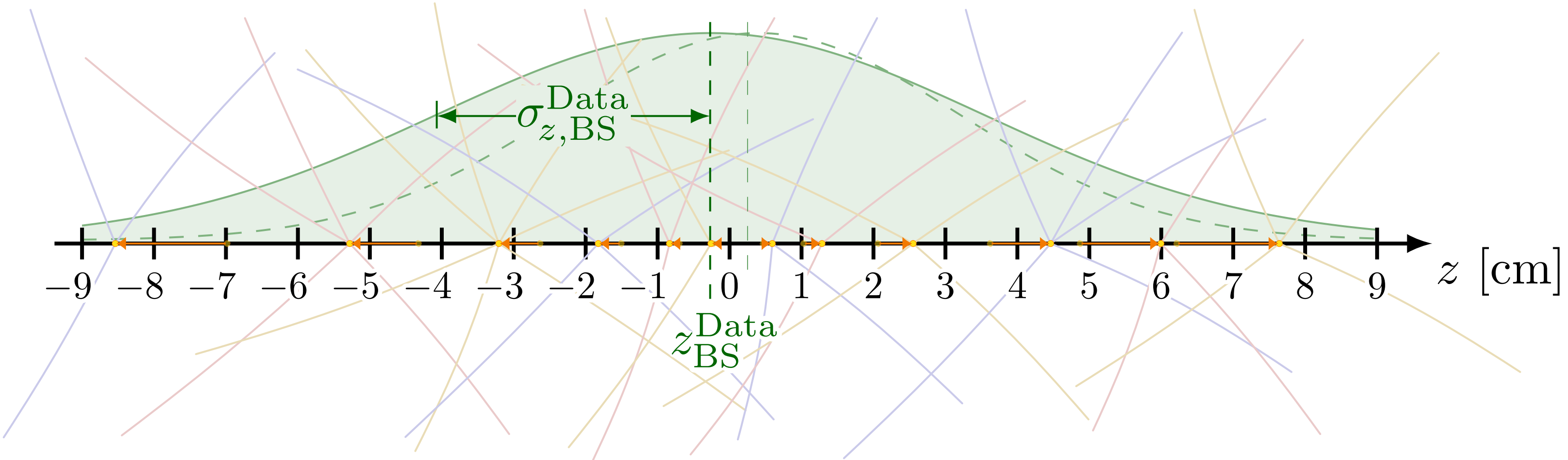

BACKGROUND ESTIMATION

CMS-SMP-23-005

Backgrounds to $\gamma\gamma \to \tau\tau$ search

- **MC simulation**
  - Drell–Yan ($Z/\gamma^* \to \ell\ell$): dominant at low mass
  - exclusive $\gamma\gamma \to$ ee, $\mu\mu$, WW production
  - inclusive WW production (small)
- **data-driven**: misidentified hadronic jets
  - $j \to \tau_h$: $e\tau_h$, $\mu\tau_h$ & $\tau_h\tau_h$ channels
  - $j \to e/\mu$: $e\mu$ channels

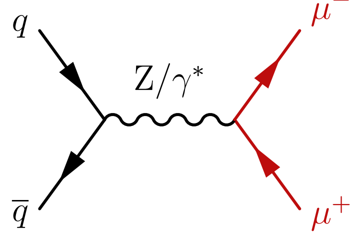

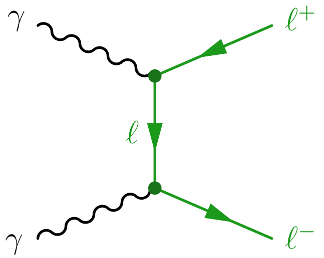

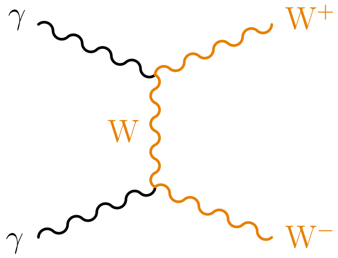

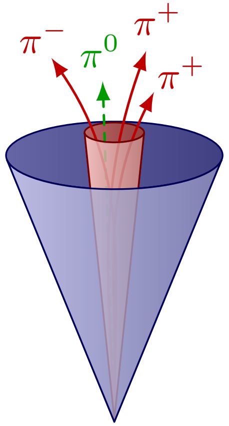

hadronic τ_h jet

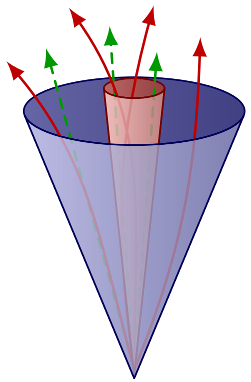

hadronic quark/gluon jet

$j \to \tau_h$ mis-ID background estimation

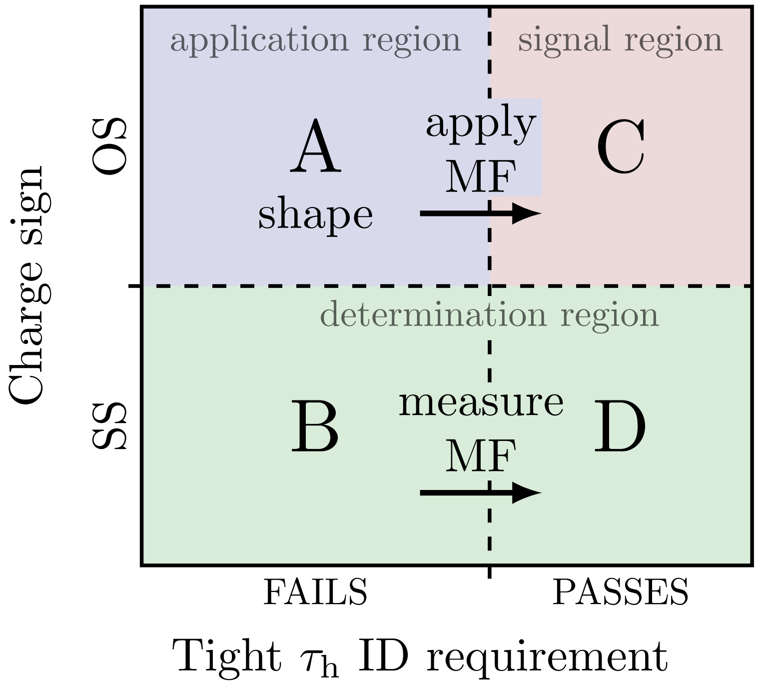

- background from $j \to \tau_h$ mis-IDs mostly include **QCD multijet** and **W + jets** events
- estimated in a **data-driven** way
- measure **"mis-ID rate" (MF)** in several CRs

$$\text{MF} = \frac{N(j \to \tau_h \text{ passes } \textbf{tight}\ \tau_h \text{ ID requirement})}{N(j \to \tau_h \text{ fails } \textbf{tight}\text{, but passes } \textbf{looser}\ \tau_h \text{ ID requirement})}$$

- as a function of τ_h p_T & decay mode

Corrections to $j \to \tau_h$ MF in $e\tau_h$ & $\mu\tau_h$

jet is 4 times more likely to pass the tight τ_h ID criteria if there is no other track at the vertex

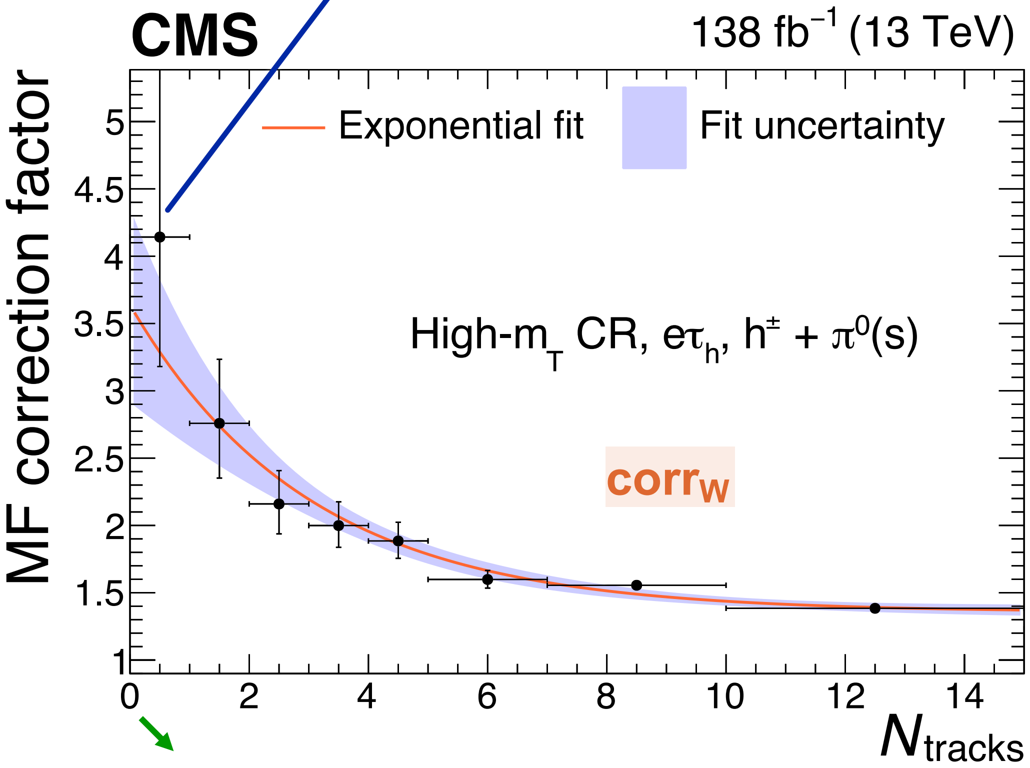

SR-like: $N_{\text{tracks}} = 0, 1$

- MFs & corrections measured in separate CRs:
  - W + jets: m_T > 75 GeV
  - QCD: SS, m_T < 75 GeV
- fewer tracks lead to more isolated τ_h
  ⇒ higher fake rates
  ⇒ apply corrections as a function of N_{tracks}
- total fake rate "$j \to \tau_h$ misidentification factors":

$$\mathrm{MF} = f_\mathrm{W}(m_\mathrm{vis}, m_\mathrm{T}) \times \mathrm{MF_W}(p_\mathrm{T}^{\tau_h}, \mathrm{DM}^{\tau_h}) \times \mathrm{corr_W}(N_\mathrm{tracks}, \mathrm{DM}^{\tau_h})$$
$$+ \Big(1 - f_\mathrm{W}(m_\mathrm{vis}, m_\mathrm{T})\Big) \times \mathrm{MF_{QCD}}(p_\mathrm{T}^{\tau_h}, \mathrm{DM}^{\tau_h}) \times \mathrm{corr_{QCD}}(N_\mathrm{tracks}, \mathrm{DM}^{\tau_h})$$

RESULTS

CMS-SMP-23-005

Systematics

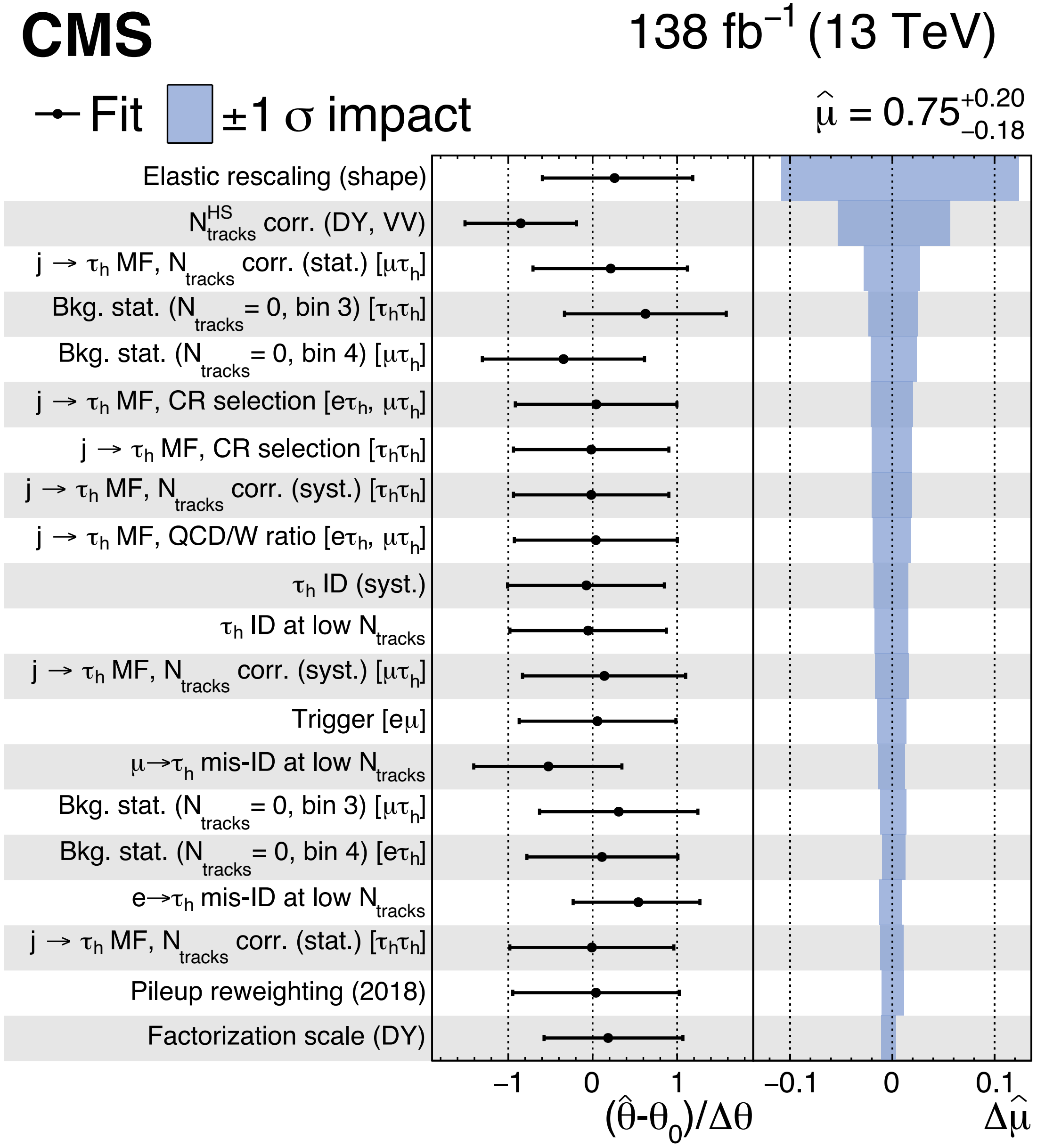

Uncertainty	Process	Magnitude
Luminosity	All simulations	1.6%
DY cross section	DY	2%
Inclusive diboson cross section	WW, WZ, ZZ	5%
e ID, iso, trigger	All simulations	up to 2%
e ID low-N_{tracks} correction	All simulations	1%
μ ID, iso, trigger	All simulations	<2%
τ_h ID	All simulations	1–5%
τ_h trigger	All simulations	up to 5%
$e \to \tau_h$ mis-ID	$Z/\gamma* \to$ ee and $\gamma\gamma \to$ ee	<10%
$\mu \to \tau_h$ ID	$Z/\gamma* \to \mu\mu$ and $\gamma\gamma \to \mu\mu$	<10%
τ_h energy scale	All simulations	<1.2%
$e \to \tau_h$ energy scale	$Z/\gamma* \to$ ee and $\gamma\gamma \to$ ee	<5%
$\mu \to \tau_h$ energy scale	$Z/\gamma* \to \mu\mu$ and $\gamma\gamma \to \mu\mu$	<1%
τ_h ID low-N_{tracks} correction	All simulations	2.1%
e ID low-N_{tracks} correction	All simulations	2.0%
$e \to \tau_h$ ID low-N_{tracks} correction	$Z/\gamma* \to$ ee and $\gamma\gamma \to$ ee	22%
$\mu \to \tau_h$ ID low-N_{tracks} correction	$Z/\gamma* \to \mu\mu$ and $\gamma\gamma \to \mu\mu$	15%
$N^{\text{PU}}_{\text{tracks}}$ reweighting	All simulations	2%
$N^{\text{HS}}_{\text{tracks}}$ reweighting	DY and inclusive VV	1.5–6.5%
Acoplanarity correction	DY	5%
DY extrapolation from $N_{\text{tracks}} < 10$	DY simulation	1.4–2.0%
μ_R, μ_f	DY simulation	Shape
PDF	DY simulation	Shape
jet$\to \tau_h$ MF, extrapolation with $p_T^{\tau_h}$	jet$\to \tau_h$ mis-ID bkg.	<50%
jet$\to \tau_h$ MF, N_{tracks} extrapolation (stat.)	jet$\to \tau_h$ mis-ID bkg.	6–18%
jet$\to \tau_h$ MF, inversion of CR selection	jet$\to \tau_h$ mis-ID bkg.	<10%
jet$\to \tau_h$ MF, x^{QCD} fraction	jet$\to \tau_h$ mis-ID bkg.	9%
jet$\to \tau_h$ MF, N_{tracks} extrapolation (syst.)	jet$\to \tau_h$ mis-ID bkg.	<10%
jet$\to$ e/μ OS-to-SS (stat.)	jet$\to$ e/μ mis-ID bkg.	<20%
jet$\to$ e/μ OS-to-SS (syst.)	jet$\to$ e/μ mis-ID bkg.	10%
jet$\to$ e/μ OS-to-SS N_{tracks} extrapolation	jet$\to$ e/μ mis-ID bkg.	8%
Elastic rescaling (stat.)	$\gamma\gamma \to \tau\tau/\mu\mu$/ee, WW	1.3–3.7%
Elastic rescaling (syst., shape)	$\gamma\gamma \to \tau\tau/\mu\mu$/ee, WW	Mass-dependent
Limited statistics	All processes	Bin-dependent
Pileup reweighting	All simulations	Event-dependent

Leading systematics

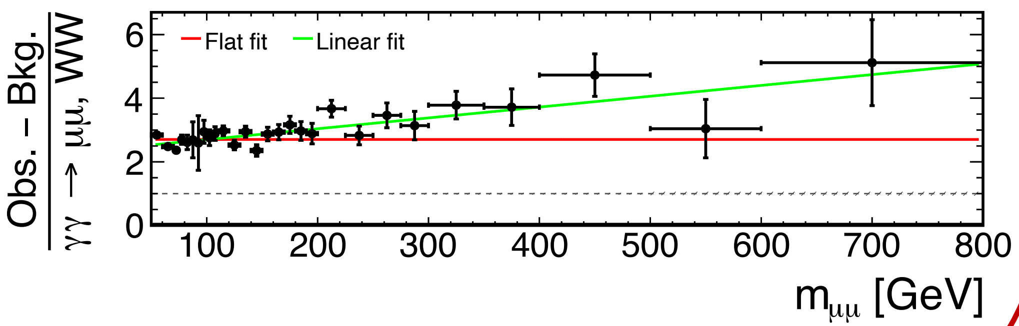

rescaling of elastic simulation ($\gamma\gamma \to \ell\ell$, WW)

- use linear fit to estimate uncertainty
- dominant systematic

$N^{\mathrm{HS}}_{\mathrm{tracks}}$ correction in Drell–Yan
(~6.5% in N_{tracks} = 0)

N_{tracks} extrapolation to $j \to \tau_h$ mis-ID rate
(up to ~20%)

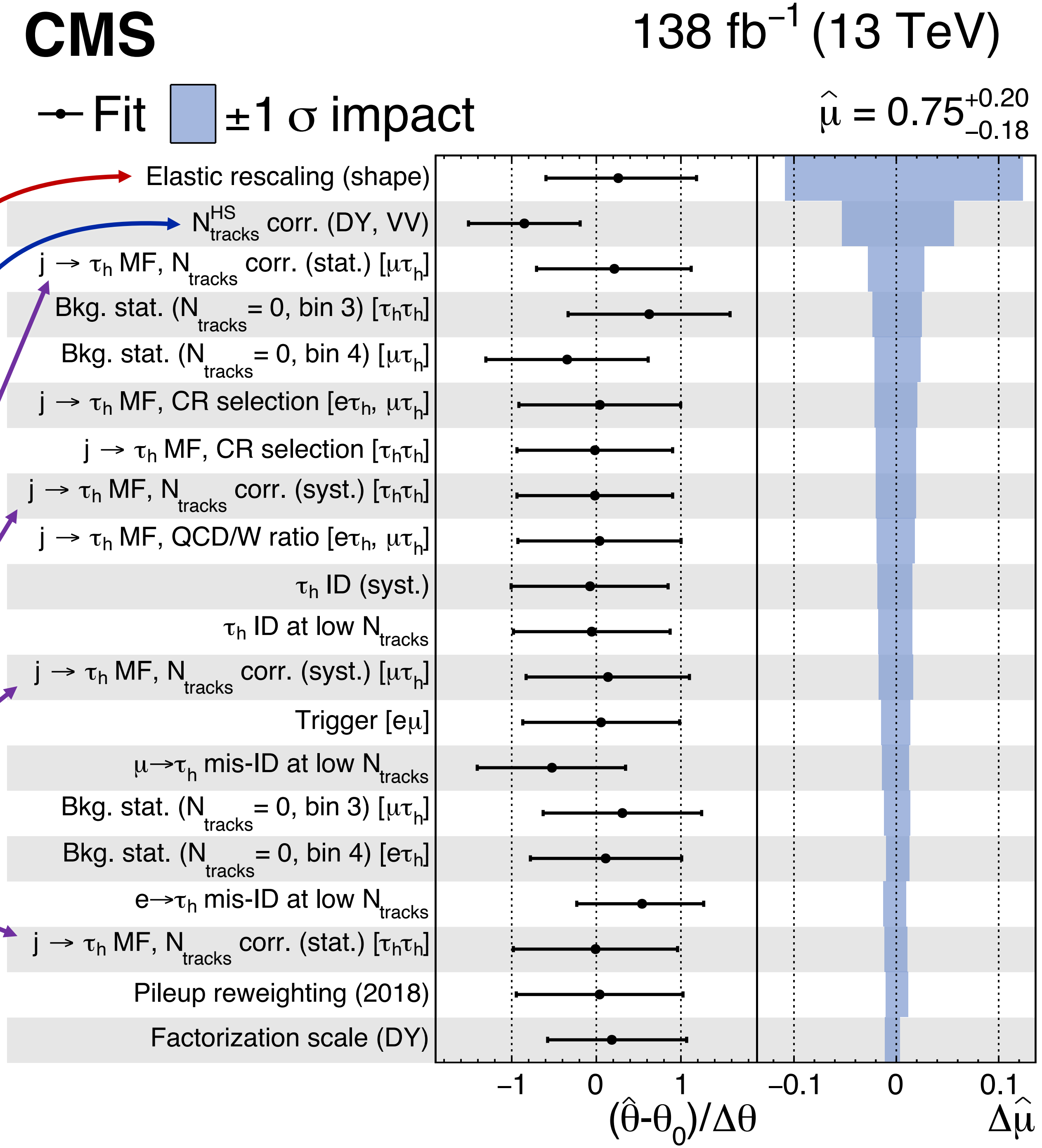

NLL breakdown by stat. & syst.

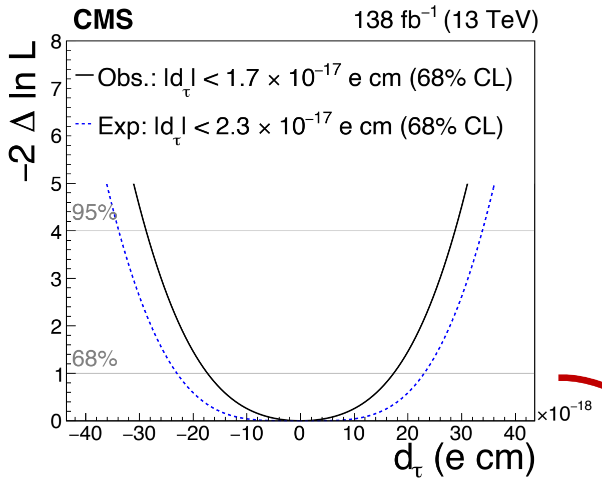

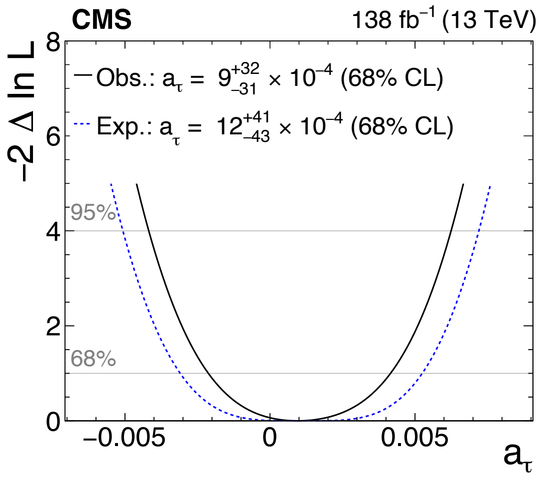

measurements mostly statistically limited !

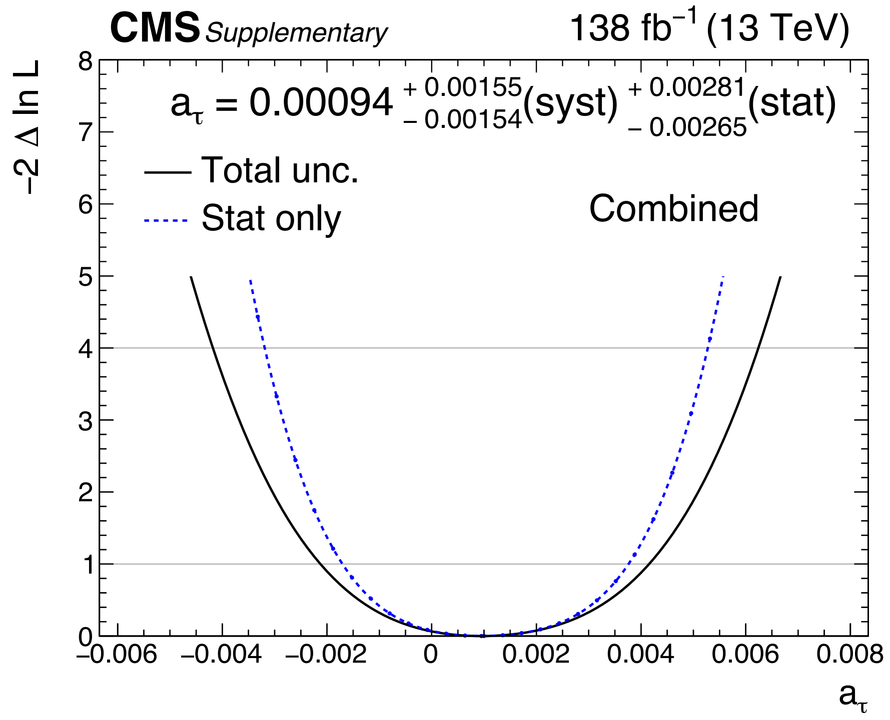

breakdowns of likelihood profiles into **stat.** & **syst.** components

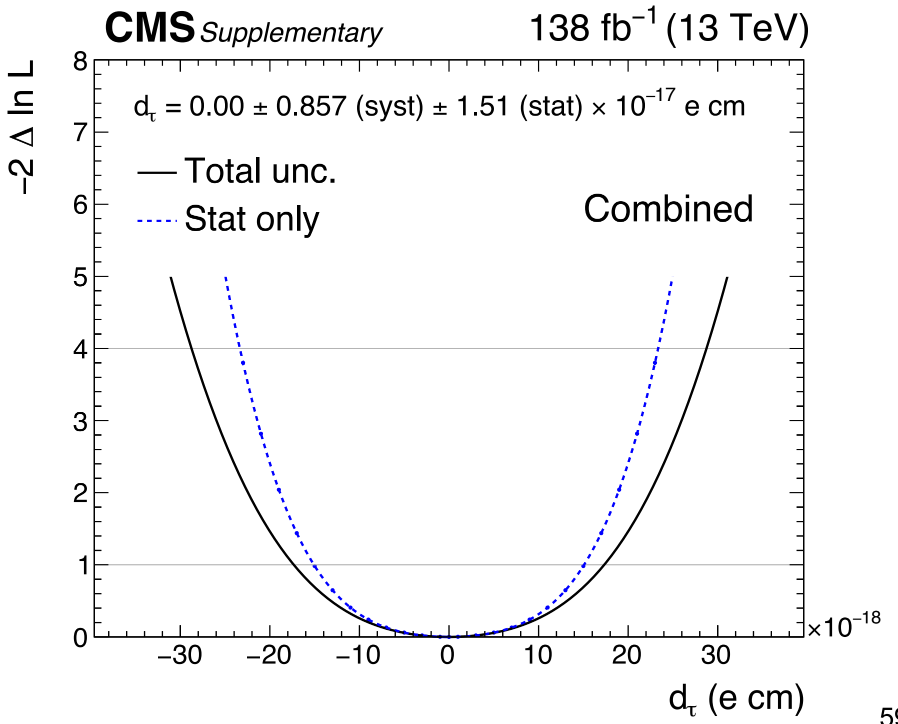

Form factors vs. EFTs

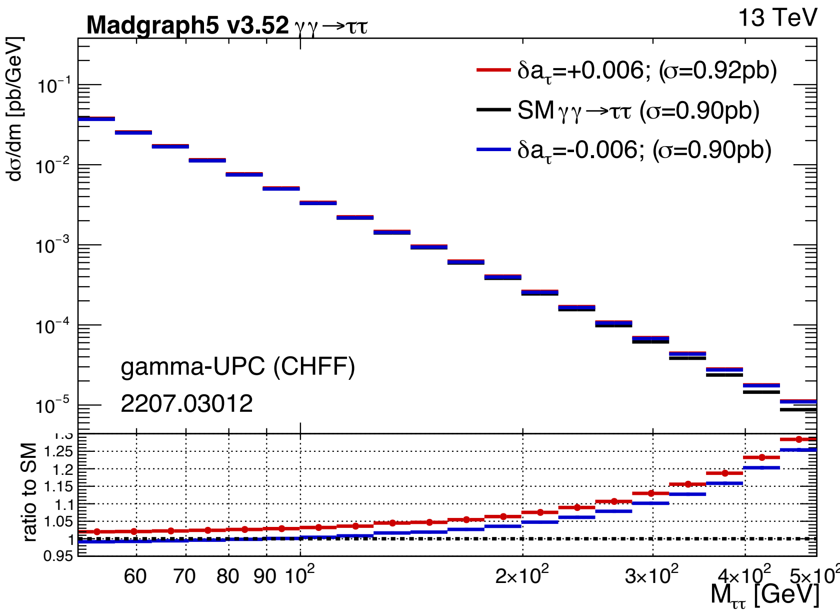

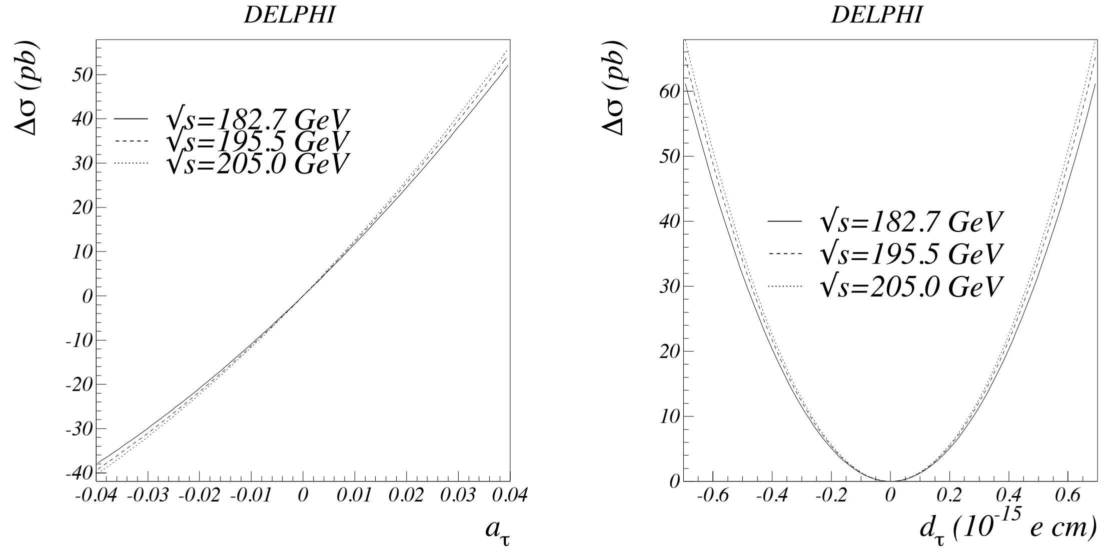

Figure 7: Total cross-section change as a function of anomalous magnetic moment and as a function of electric dipole moment.

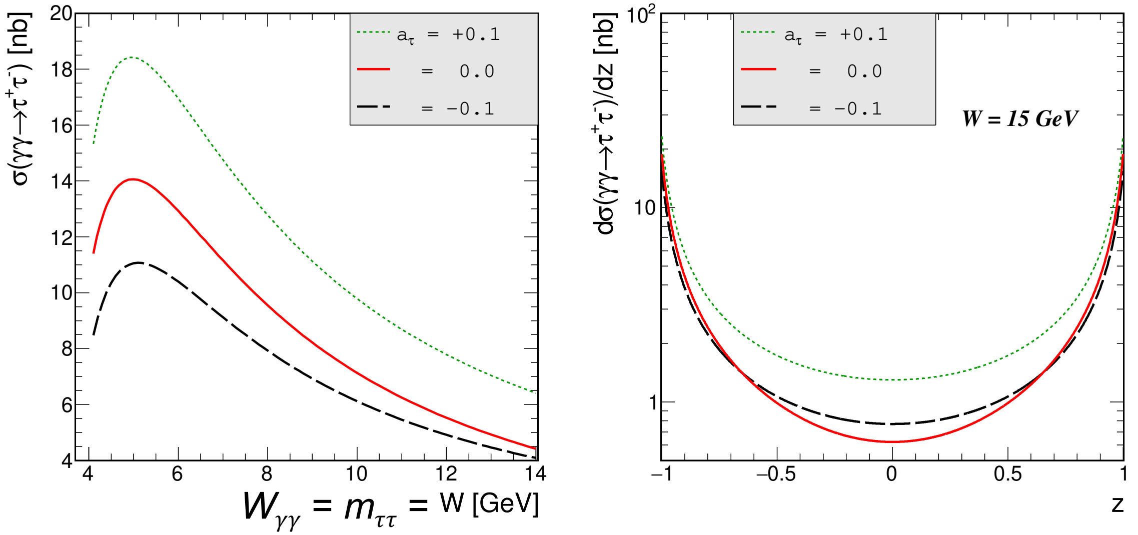

FIG. 1. Elementary cross section for $\gamma\gamma \to \tau^+\tau^-$ process as a function of $W_{\gamma\gamma} = m_{\tau\tau}$ (left) and as a function of $z = \cos\theta$ for $W_{\gamma\gamma} = 15$ GeV (right).

DELPHI (2004) arXiv:hep-ex/0406010

Dynal et al. (2020) arXiv:2002.05503

a_τ comparisons

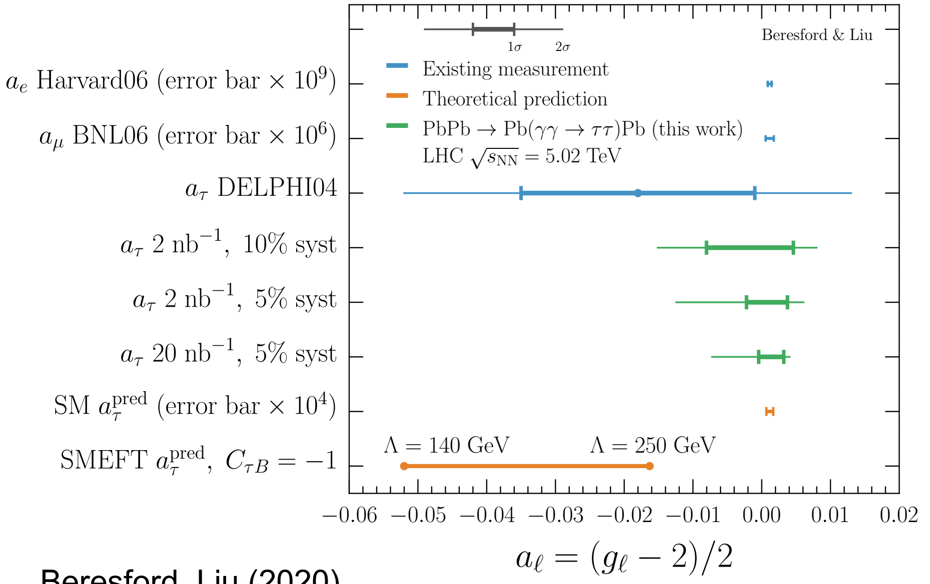

Beresford, Liu (2020)
arXiv:1908.05180

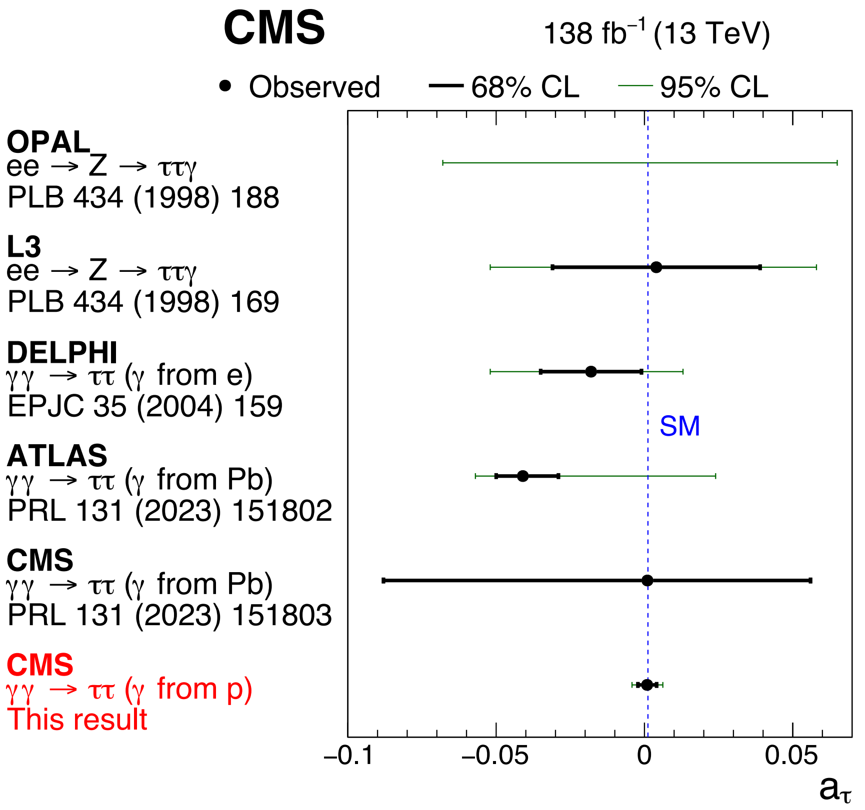

ATLAS (2022) STDM-2019-19

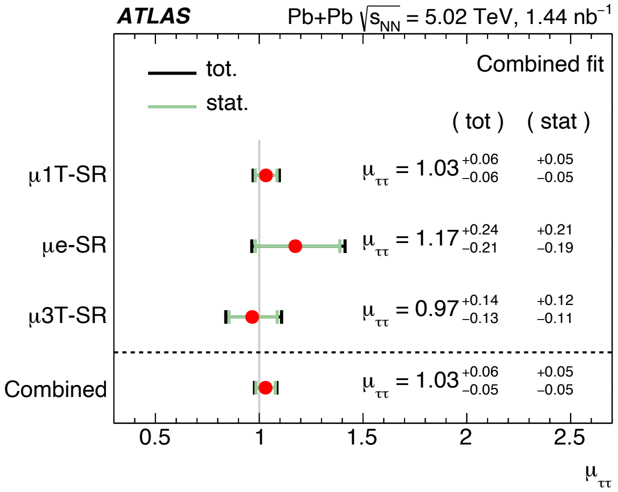

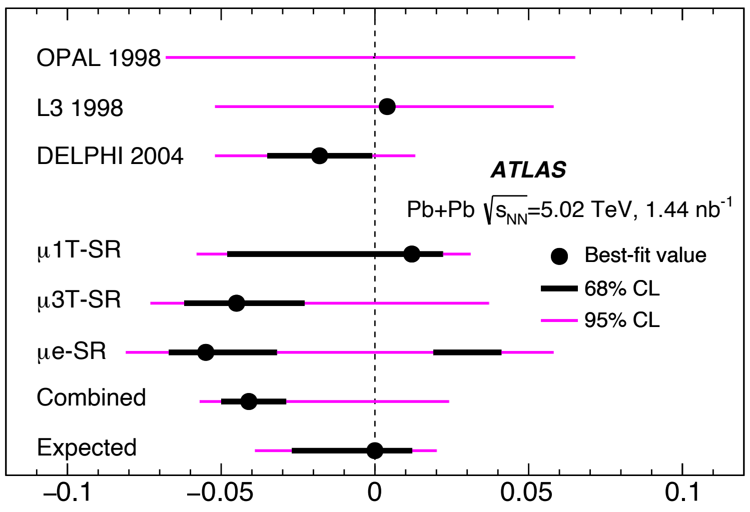

INTERPRETATION

CMS-SMP-23-005

Signal simulation

- **elastic-elastic events** are generated using gammaUPC generator with k_t smearing (arXiv:2207.03012)
- charged form factors to correct the photon flux are used (recommended by gammaUPC authors)
- a_τ & d_τ interpretation using the **EFT approach** with the SMEFTsim package, simplifying with $C_{\tau W} = 0$:

$$\delta a_\tau \propto \frac{\mathrm{Re}[C_{\tau B}]}{\Lambda^2}, \qquad \delta d_\tau \propto \frac{\mathrm{Im}[C_{\tau B}]}{\Lambda^2}$$

- scan a_τ & d_τ values through matrix element reweighting in two *independent* 1D grids of 100 points for $C_{\tau B}$:

$$\mathrm{Re}[C_{\tau B}] \in [-40,40], \quad \mathrm{Im}[C_{\tau B}] \in [-40,40]$$

- varying a_τ or d_τ changes the cross section and $m_{\tau\tau}$ distribution
- hadronized using Pythia 8.24, switching off multi-parton interaction
- result *independent* of choice of Λ, because $C_{\tau B}$ and $C_{\tau W}$ scale with Λ^2, but we fix $\Lambda = 2$ TeV in event generation

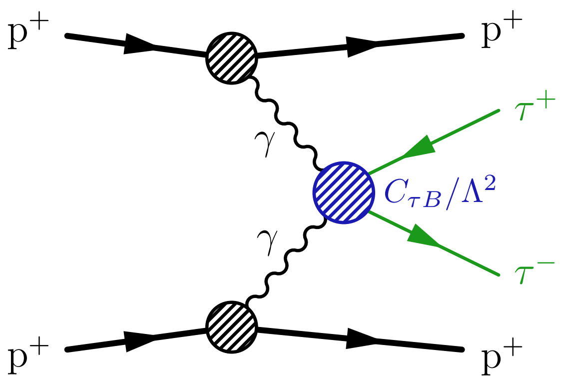

our ~ 95% CL limits

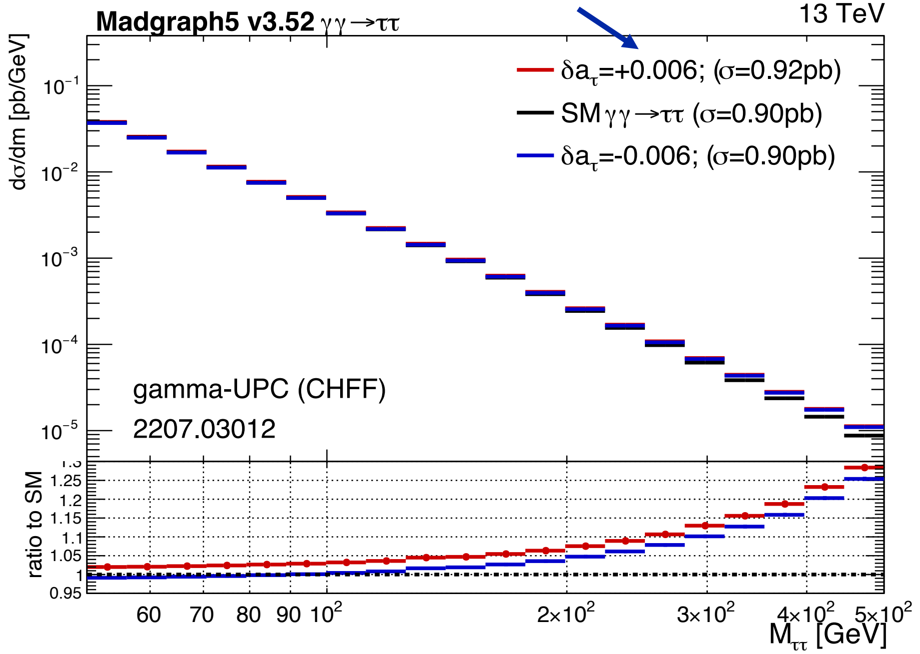

Form factors vs. EFTs

spin tensor $\sigma_{\mu\nu} = \frac{i}{2}[\gamma_\mu, \gamma_\nu]$

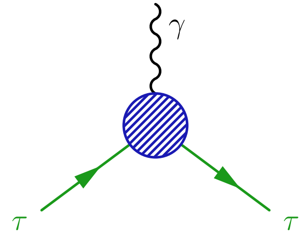

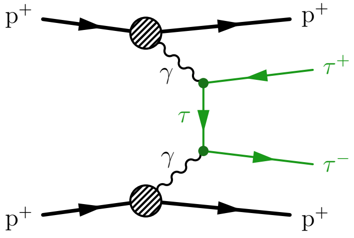

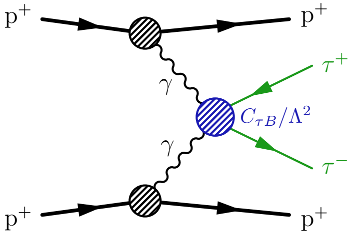

in the **SM Lagrangian** electromagnetic moments arise from:

$$\mathcal{L} \supset \mathcal{L}_{\tau\tau\gamma} = \frac{1}{2}\bar{\tau}\sigma^{\mu\nu}\left(a_\tau \frac{e}{2m_\tau} - i d_\tau \gamma_5\right)\tau_R F_{\mu\nu}$$

- previous analyses (DELPHI, ATLAS, CMS), used **form factors** to parametrize the $\gamma\tau\tau$ vertex:

$$\Gamma_\mu(q^2) = ie\left[F_1(q^2)\gamma_\mu + \frac{1}{2m_\tau}\left(iF_2(q^2) + F_3(q^2)\gamma_5\right)\sigma_{\mu\nu}q^\nu\right]$$

- $F_1(q^2)$ parametrises the vector part of the electromagnetic current and is identified at zero-momentum transfer ($q^2 = 0$) with the electric charge e, implying $F_1(0)$ = 1
- the asymptotic values of the form factors ($q^2 \to 0$) are the electromagnetic moments a_τ and d_τ:

$$a_\tau = F_2(0)$$
$$d_\tau = \frac{e}{2m_\tau}F_3(0)$$

- the virtualities of exchanged photons in $\gamma\gamma \to \ell\ell$:
  - PbPb UPC : $Q^2_{1,2} \lesssim 0.001\ \mathrm{GeV}^2$
  - pp: $Q^2_{1,2} \lesssim 0.08\ \mathrm{GeV}^2$
  - LEP e⁺e⁻: $Q^2_{1,2} < 1\ \mathrm{GeV}^2$

- we use **SMEFT model** to parametrize deviations a_τ and d_τ from the SM can be parametrized in terms of a BSM Lagrangian with dim-6 operators with NP scale Λ:

$$\mathcal{L}_{\mathrm{BSM}} = \bar{L}_\tau \sigma^{\mu\nu}\tau_R H\left[\frac{C_{\tau B}}{\Lambda^2}B_{\mu\nu} + \frac{C_{\tau W}}{\Lambda^2}W_{\mu\nu}\right]$$

- after symmetry breaking, using $C_{\tau\gamma} = \cos\theta_W\, C_{\tau B} - \sin\theta_W\, C_{\tau W}$:

$$\mathcal{L}_{\mathrm{BSM}} \supset \mathcal{L}^{\mathrm{BSM}}_{\tau\tau\gamma} = \bar{\tau}_L\sigma^{\mu\nu}\tau_R\frac{v}{\sqrt{2}\Lambda^2}C_{\tau\gamma}F_{\mu\nu}$$

- $\gamma\tau\tau$ vertex:

$$\Gamma_\mu(q^2) = ie\gamma_\mu - \frac{\sqrt{2}v}{\Lambda^2}\left[\mathrm{Re}\left[C_{\tau\gamma}\right] + i\gamma_5\mathrm{Im}\left[C_{\tau\gamma}\right]\right]\sigma_{\mu\nu}q^\nu$$

- then δa_τ & δd_τ are linearly dependent through the *complex* Wilson coefficients:

$$\delta a_\tau = \frac{2m_\tau}{e}\frac{\sqrt{2}v}{\Lambda^2}\mathrm{Re}\left[C_{\tau\gamma}\right]$$
$$\delta d_\tau = \frac{\sqrt{2}v}{\Lambda^2}\mathrm{Im}\left[C_{\tau\gamma}\right]$$

see Dynal et al. [arXiv:2002.05503], gammaUPC [arXiv:2207.03012], Haisch et al. [arXiv:2307.14133]

Fiducial cross section definition

similar to ATLAS STDM-2019-19
& CMS HIN-21-009 analyses

- measured $\gamma\gamma \to \tau\tau$ fiducial cross section $\sigma^{\mathrm{fid}}_{\mathrm{obs}} = 12.4^{+3.8}_{-3.1}$ fb
- fiducial cross section definition (using gen-level quantities and dressed leptons):

	$\mathrm{e}\mu$	$\mathrm{e}\tau_{\mathrm{h}}$	$\mu\tau_{\mathrm{h}}$	$\tau_{\mathrm{h}}\tau_{\mathrm{h}}$
$p_{\mathrm{T}}^{\mathrm{e}}$ (GeV)	$> 15/24$	> 25	—	—
$\lvert\eta^{\mathrm{e}}\rvert$	< 2.5	< 2.5	—	—
p_{T}^{μ} (GeV)	$> 24/15$	—	> 21	—
$\lvert\eta^{\mu}\rvert$	< 2.4	—	< 2.4	—
$p_{\mathrm{T}}^{\tau_{\mathrm{h}}}$ (GeV)	—	> 30	> 30	> 40
$\lvert\eta^{\tau_{\mathrm{h}}}\rvert$	—	< 2.3	< 2.3	< 2.3
$\Delta R(\ell, \ell')$	> 0.5	> 0.5	> 0.5	> 0.5
$m_{\mathrm{T}}(\mathrm{e}/\mu, \vec{p}_{\mathrm{T}}^{\mathrm{miss}})$ [GeV]	—	< 75	< 75	—
A	< 0.015	< 0.015	< 0.015	< 0.015
m_{vis} (GeV)	< 500	< 500	< 500	< 500
N_{tracks}	0	0	0	0

Table 4 from CMS-SMP-23-005

ELECTRON & MUON G – 2

Measurement of lepton g – 2

electron

- stable
- Penning traps
- Δa_{e} @ 0.13 ppt !
- agrees with SM 1 ppt

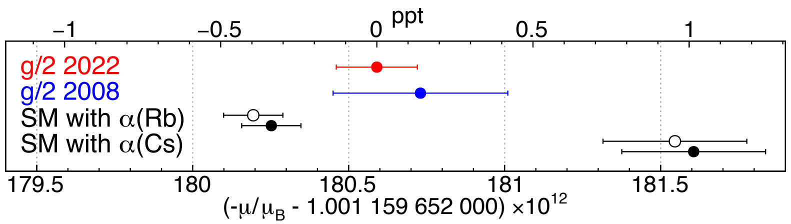

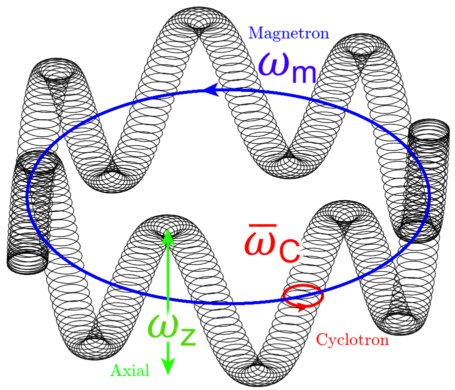

muon

- lifetime ~2.2×10^{-6} s
- cyclotrons
- Δa_{μ} @ 0.20 ppm !
- tension with theory ?

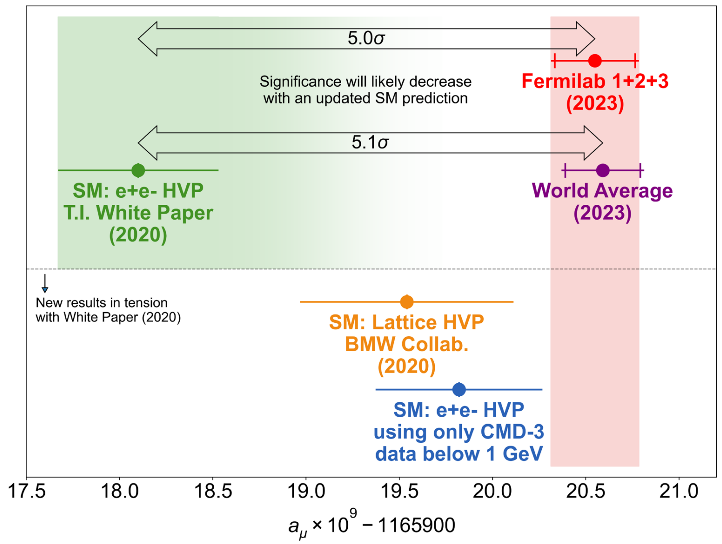

tau

- lifetime ~2.9×10^{-13} s
- $\gamma\gamma \to \tau\tau$ process in colliders !
- limit by LEP ~20 times Schwinger term
- many **BSMs** predict enhancement
  $\Rightarrow$ probe for NP ?

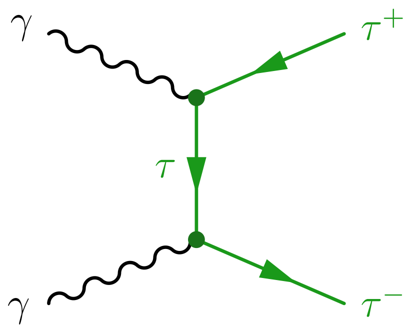

Status in 1972...

anomalous magnetic moment

$$a = \frac{g-2}{2}$$

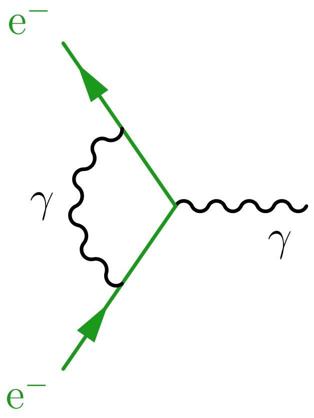

$g = 2 + 2a$

≈ 2.00232

"radiative corrections"

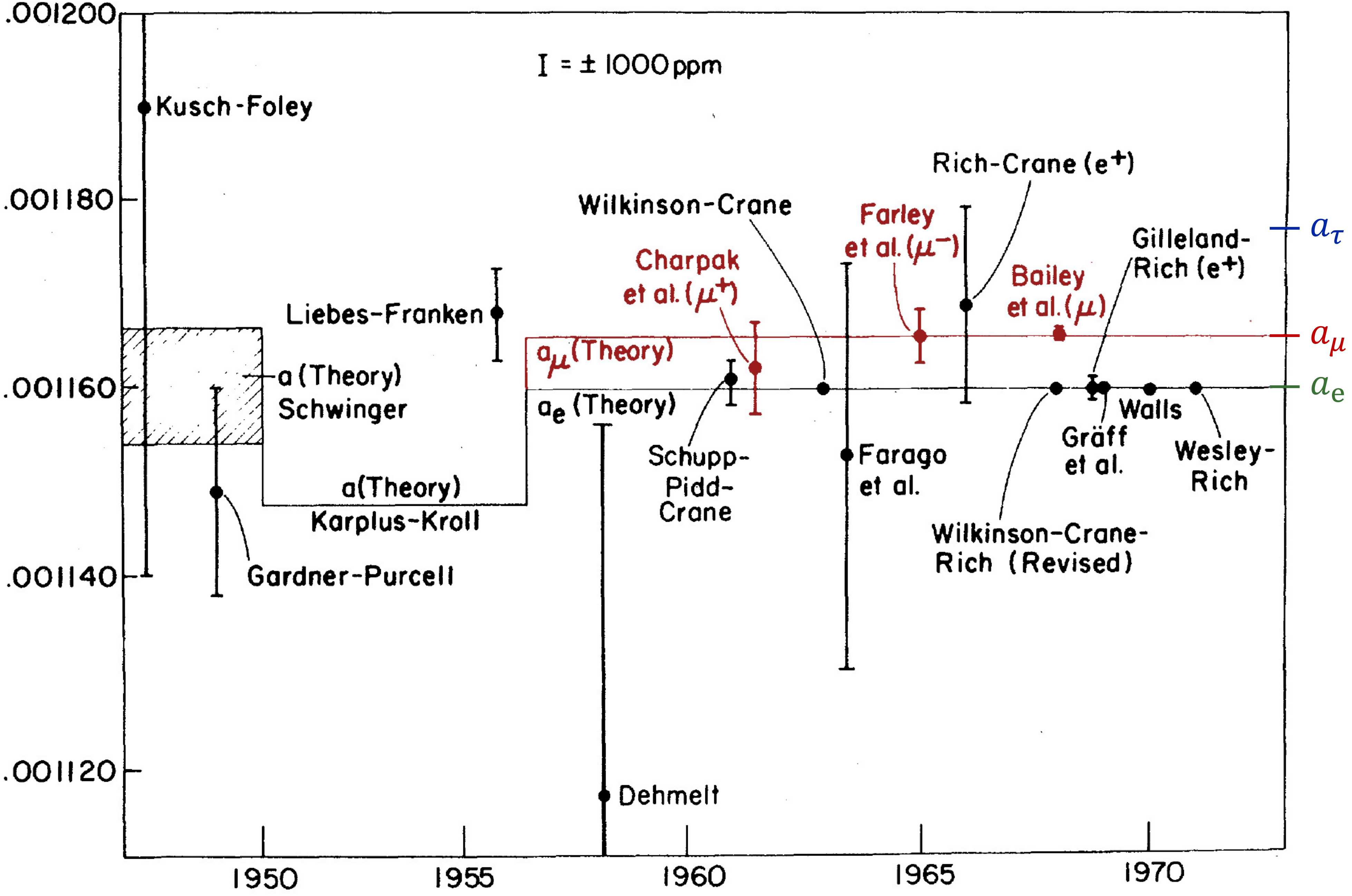

The Current Status of the Lepton g Factors, A. Rich & J.C. Wesley (1972)
https://journals.aps.org/rmp/abstract/10.1103/RevModPhys.44.250

Measurement of electron g – 2 in Penning traps

- oscillate electron in **nonuniform E field**, but **uniform B field**
- measure resonance frequencies

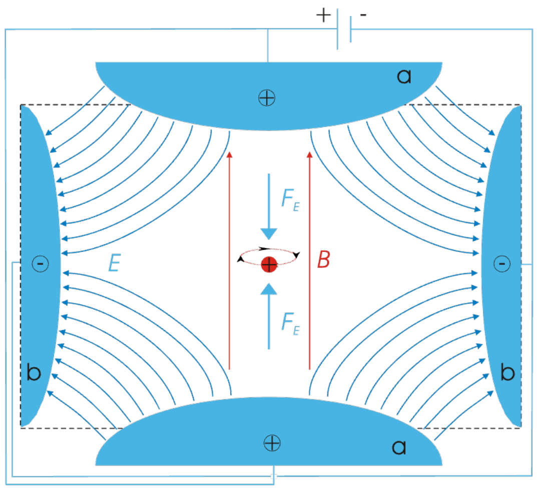

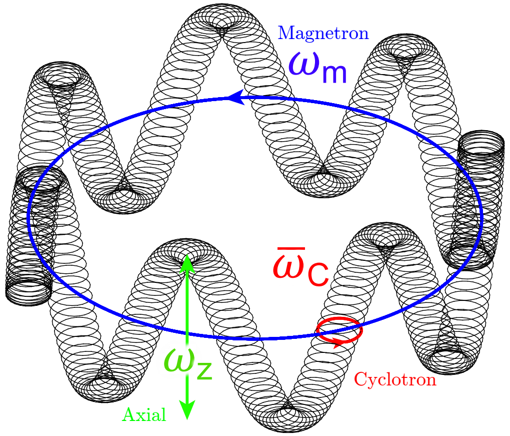

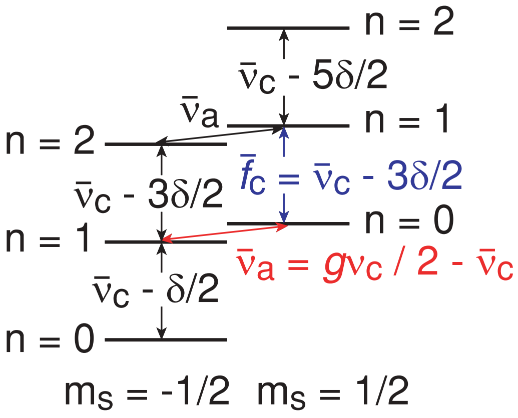

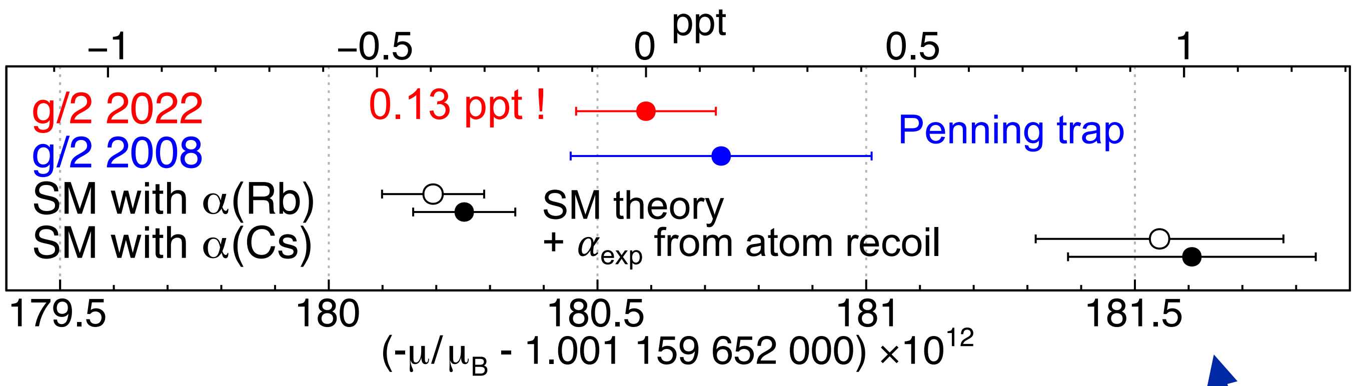

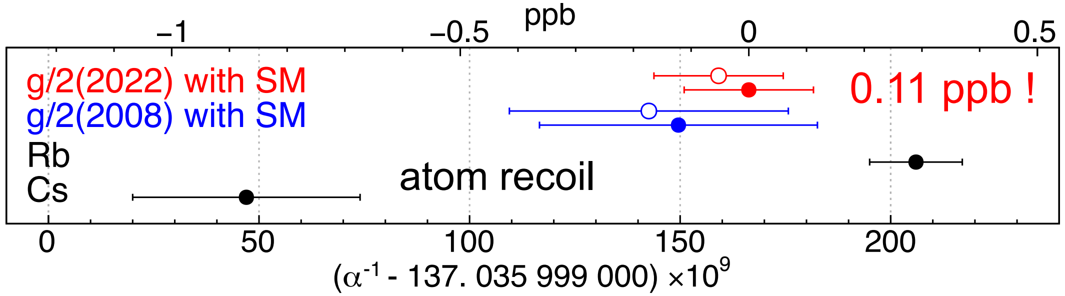

$$\frac{g}{2} = 1 + C_2\left(\frac{\alpha}{\pi}\right) + C_4\left(\frac{\alpha}{\pi}\right)^2 + C_6\left(\frac{\alpha}{\pi}\right)^3 + \ldots + a_{\mu,\tau} + a_{\text{had}} + a_{\text{weak}}$$

Measurement of muon g – 2 in cyclotrons

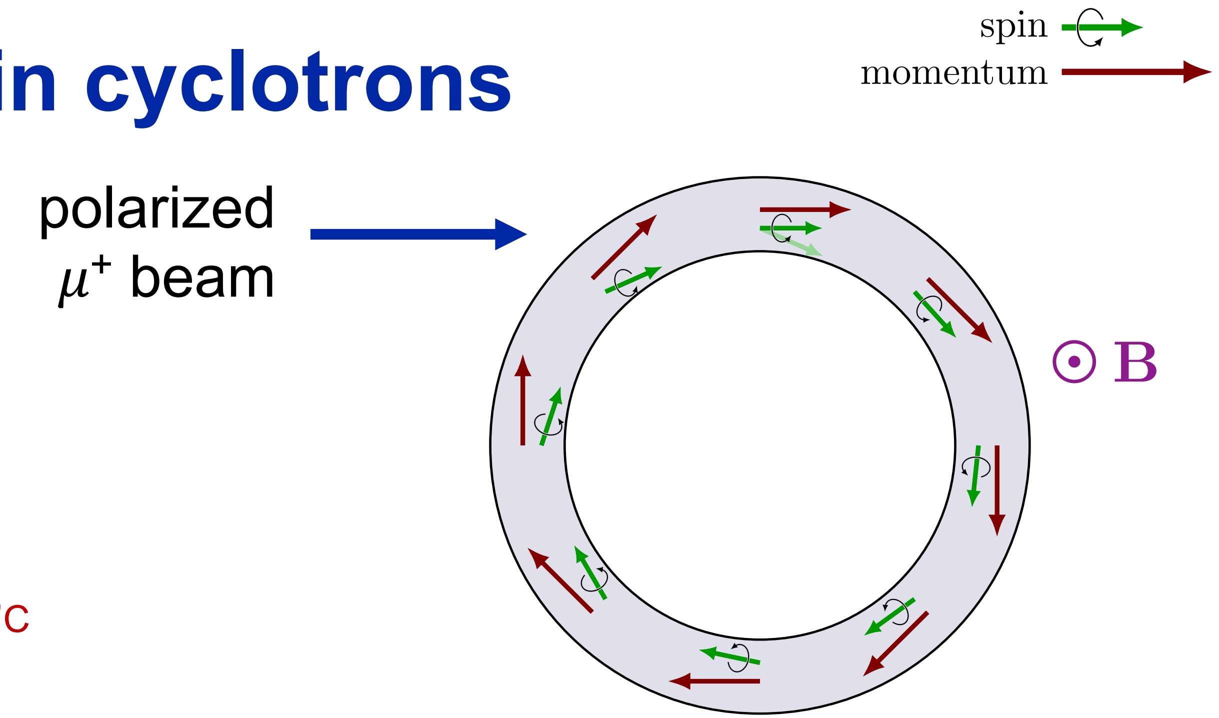

- muon lifetime ~ 2.2 μs
  ⇒ use cyclotrons
- spin precesses faster than momentum in cyclotron magnetic field:

  Larmor precession ω_S > cyclotron oscillation ω_C

$$\omega_a = \omega_S - \omega_C = \frac{g-2}{2}\frac{e}{m_\mu}B \sim 230\,\mathrm{kHz}$$

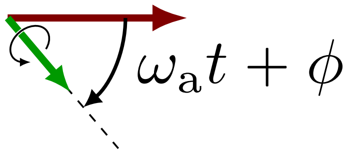

- measure oscillation in $\mu^+ \to e^+$ energy spectrum

oscillations in number of e^+ with E > 1.8 GeV

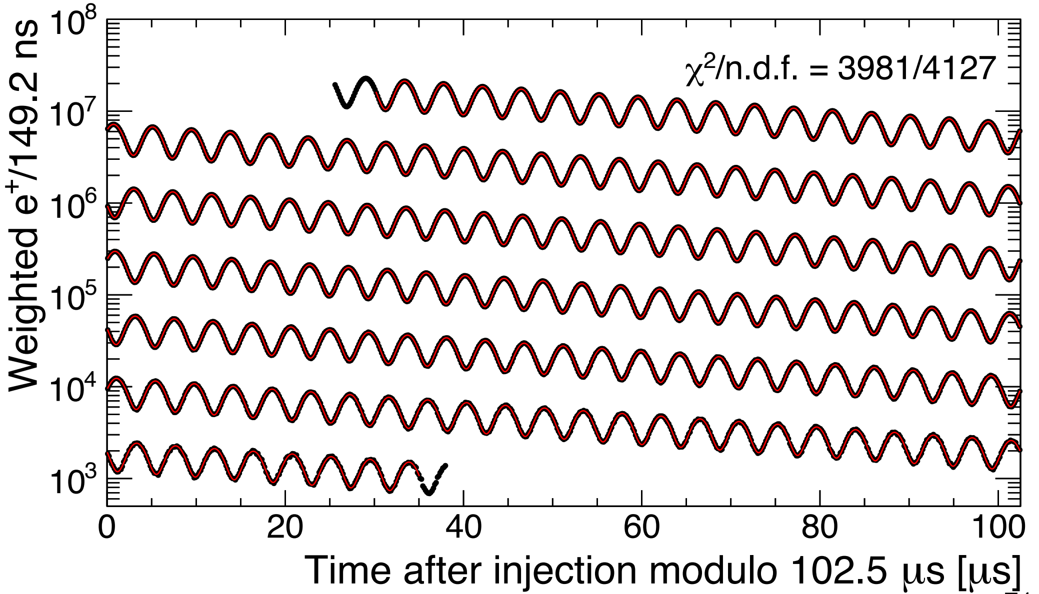

arXiv:2308.06230

Quick history: Muon g – 2

- **CERN**:
  - **1961**: ~0.2%
  - **1979**: ~7.30 ppm
- **BNL**:
  - **1999**: ~1.30 ppm
  - **2001**: ~0.54 ppm

  ⇒ discrepancy with **theory !**
- **FNAL**:
  - **2021**: ~0.46 ppm
  - **2023**: ~0.20 ppm

  ⇒ still tension